2

The Reaction Pathways of Zinc Enzymes and Related Biological Catalysts

IVANO BERTINI
Department of Chemistry
University of Florence

CLAUDIO LUCHINAT
Institute of Agricultural Chemistry
University of Bologna

I. INTRODUCTION

This chapter deals with metalloenzymes wherein the metal acts mainly as a Lewis acid; i.e., the metal does not change its oxidation state nor, generally, its protein ligands. Changes in the coordination sphere may occur on the side exposed to solvent.

The substrate interacts with protein residues inside the active cavity and/or with the metal ion in order to be activated, so that the reaction can occur. Under these circumstances the catalyzed reactions involve, as central steps with often complex reaction pathways, the following bond-breaking and/or formation processes:

peptide hydrolysis

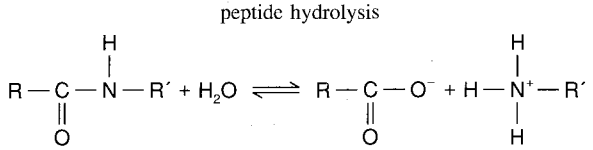

(2.1)

carboxylic ester hydrolysis

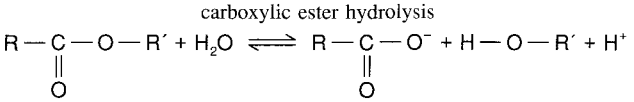

(2.2)

phosphoric ester hydrolysis

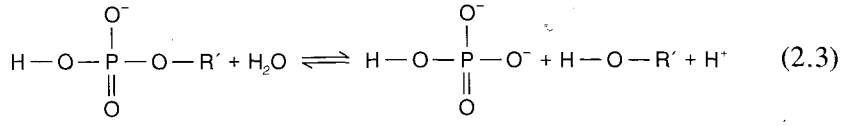

(2.3)

nucleophilic addition of OH^- and H^-

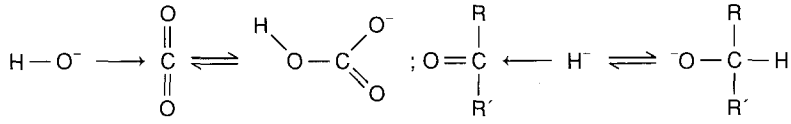

(2.4)

Scheme (2.3) also pertains to the reactions which need ATP hydrolysis to promote endoenergetic reactions.

We will also briefly deal with coenzyme B_{12}; this is a cobalt(III) complex that, by interacting with a number of proteins, produces an R—CH_2 radical by homolytic breaking of the Co—C bond as follows:

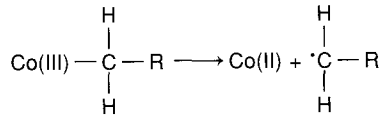

(2.5)

After an R—CH_2 radical is formed, it initiates a radical reaction. This is the only system we treat in which the oxidation state changes.

II. THE NATURAL CATALYSTS

Table 2.1 lists metalloenzymes that catalyze hydrolytic and related reactions. According to the above guidelines the hydrolysis of peptide bonds is catalyzed by enzymes called peptidases that belong to the class of hydrolases (according to the official enzyme classification). Two peptidases (carboxypeptidase and thermolysin) are known in great detail, because their structures have been elucidated by high-resolution x-ray crystallography. They share many features; e.g., their metal ions coordinate to the same kind of protein residues. A discussion of the possible mechanism of carboxypeptidase A will be given in Section V.A. Metallopeptidases are zinc enzymes: generally they are single polypeptide chains with molecular weights in the range 30 to 40 kDa. Metallohydrolases of carboxylic and phosphoric esters are also often zinc enzymes. Alkaline phosphatase will be described in Section V.B as a representative of this class. Magnesium is sometimes involved in hydrolytic reactions. This is common when phosphate groups are involved, probably because the affinity of Mg^{2+} for phosphate groups is high.[1] However, hydrolytic reactions can be performed by other systems (not treated here) like urease, which contains nickel(II),[2] or acid phosphatase, which contains two iron ions,[3] or aconitase, which contains an Fe_4S_4 cluster.[4]

Table 2.1
Representative metalloenzymes catalyzing hydrolytic and related reactions.

Enzyme	Metal(s)	Function
Carboxypeptidase	Zn^{2+}	Hydrolysis of C-terminal peptide residues
Leucine aminopeptidases	Zn^{2+}	Hydrolysis of leucine N-terminal peptide residues
Dipeptidase	Zn^{2+}	Hydrolysis of dipeptides
Neutral protease	Zn^{2+}, Ca^{2+}	Hydrolysis of peptides
Collagenase	Zn^{2+}	Hydrolysis of collagen
Phospholipase C	Zn^{2+}	Hydrolysis of phospholipids
β-Lactamase II	Zn^{2+}	Hydrolysis of β-lactam ring
Thermolysin	Zn^{2+}, Ca^{2+}	Hydrolysis of peptides
Alkaline phosphatase	Zn^{2+}, Mg^{2+}	Hydrolysis of phosphate esters
Carbonic anhydrase	Zn^{2+}	Hydration of CO_2
α-Amylase	Ca^{2+}, Zn^{2+}	Hydrolysis of glucosides
Phospholipase A_2	Ca^{2+}	Hydrolysis of phospholipids
Inorganic pyrophosphatase	Mg^{2+}	Hydrolysis of pyrophosphate
ATPase	Mg^{2+}	Hydrolysis of ATP
Na^{+}-K^{+}-ATPase	Na^{+}, K^{+}	Hydrolysis of ATP with transport of cations
Mg^{2+}-Ca^{2+}-ATPase	Mg^{2+}, Ca^{2+}	
Phosphatases	Mg^{2+}, Zn^{2+}	Hydrolysis of phosphate esters
Creatine kinase	M^{2+}	Phosphorylation of creatine
Pyruvate kinase	M^{+}, M^{2+}	Dephosphorylation of phosphoenolpyruvate
Phosphoglucomutase	Mg^{2+}	Phosphate transfer converting glucose-1-phosphate to glucose-6-phosphate
DNA polymerase	Mg^{2+} (Mn^{2+})	Polymerization of DNA with formation of phosphate esters
Alcohol dehydrogenase	Zn^{2+}	Hydride transfer from alcohols to NAD^{+}

Examples of enzymes catalyzing nucleophilic addition of OH^{-} (other than hydrolysis) and H^{-} are carbonic anhydrase and alcohol dehydrogenase. Both are zinc enzymes. In the official biochemical classification of enzymes, carbonic anhydrase belongs to the class of lyases. Lyases are enzymes that cleave C—C, C—O, C—N, or other bonds by elimination, leaving double bonds, or conversely add groups to double bonds. Carbonic anhydrase has a molecular weight around 30 kDa, and is among the most-studied metalloenzymes. It catalyzes the deceivingly simple CO_2 hydration reaction. The subtleties of its biological function, unraveled by a combination of techniques, make it an ideal example for bioinorganic chemistry. Section IV is fully dedicated to this enzyme. Alcohol dehydrogenase is a 90-kDa enzyme that catalyzes the reversible transfer of a hydride ion from alcohols to NAD^{+}. Although it is a redox enzyme (in fact, classified as an oxidoreductase) and not a hydrolytic one, it will illustrate a different use that Nature makes of zinc to catalyze nucleophilic attack at carbon (Section V.C).

Finally, the enzymatic transfer of organic radicals by enzymes involving coenzyme B_{12} will be briefly considered.

III. STRATEGIES FOR THE INVESTIGATION OF ZINC ENZYMES

A. Why Zinc?

Zinc has a specific role in bioinorganic processes because of the peculiar properties of the coordination compounds of the zinc(II) ion.

(1) Zinc(II) can easily be four-, five-, or six-coordinate, without a marked preference for six coordination. The electronic configuration of zinc(II) is $3d^{10}$ with two electrons per orbital. In coordination compounds, there is no ligand-field stabilization energy, and the coordination number is determined by a balance between bonding energies and repulsions among the ligands. Tetrahedral four-coordinate complexes have shorter metal-donor distances than five-coordinate complexes, and the latter have shorter ones than six-coordinate complexes (Table 2.2), whereas the ligand repulsion increases in the same order. The repulsion can be both steric and electronic. In enzymes, zinc(II) usually has coordination numbers smaller than six, so that they have available binding sites in their coordination spheres. Substrate can in principle bind to zinc by substituting for a coordinated water or by increasing the coordination number. This behavior would be typical of Lewis acids, and, indeed, zinc is the most common Lewis acid in bioinorganic chemistry. Zinc could thus substitute for protons in the task of polarizing a substrate bond, e.g., the carbonyl C—O bond of peptides and esters, by accepting a substrate atom (oxygen) as a ligand. This has been shown to be possible in model systems. Relative to the proton, a metal ion with an available coordination position has the advantage of being a "superacid,"[6] in the sense that it can exist at pH values where the H_3O^+ concentration is extremely low. Also, relative to the proton, the double positive charge partly compensates for the smaller electrophilicity due to the smaller charge density.

Table 2.2
Average zinc(II)-donor atom distances (Å) for some common zinc(II) ligands in four-, five-, and six-coordinate complexes.[5]

	Coordination number		
Ligand	4	5	6
H_2O	2.00	2.08	2.10
$R—COO^-$	1.95	2.02	2.07
Imidazole	2.02	—	2.08
Pyridine	2.06	2.12	2.11
$R—NH_2$	—	2.06	2.15
R, R'NH	2.19	2.27	—

(2) As a catalyst, zinc in zinc enzymes is exposed to solvent, which for enzymes is almost always water. A coordinated water molecule exchanges rap-

idly, because ligands in zinc complexes are kinetically labile. This, again, can be accounted for by zinc's lack of preference for a given coordination number. A six-coordinate complex can experience ligand dissociation, giving rise to a five-coordinate complex with little energy loss and then little energetic barrier. On the other side, four-coordinate complexes can add a fifth ligand with little energetic barrier and then another ligand dissociates.[7] The coordinated water has a pK_a sizably lower than free water. Suitable models have been synthesized and characterized in which a solvent water molecule coordinated to various dipositive metal ions has pK_a values as low as 7 (Table 2.3). This is the result of the formation of the coordination bond. The oxygen atom donates two electrons to

Table 2.3
The pK_a values of coordinated water in some metal complexes.

Complex	Note	Donor set	pK_a	Reference
$Ca(NO_3)_2(OH_2)_4^{2+}$		O_6	10.3	8
$Cr(OH_2)_6^{3+}$		O_6	4.2	8
$Cr(NH_3)_5OH_2^{3+}$		N_5O	5.1	8
$Mn(OH_2)_6^{2+}$		O_6	10.5	8
$Fe(OH_2)_6^{3+}$		O_6	1.4	8
$Co(OH_2)_6^{2+}$		O_6	9.8	8
$Co(dacoda)OH_2^{2+}$	(a)	N_2O_3	9.4	9
$Co(TPyMA)OH_2^{2+}$	(b)	N_4O	9.0	10
$Co(TMC)OH_2^{2+}$	(c)	N_4O	8.4	11
$Co(CR)OH_2^{2+}$	(d)	N_4O	8.0	12
$Co(NH_3)_5OH_2^{3+}$		N_5O	6.2	8
$Ni(OH_2)_6^{2+}$		O_6	10.0	8
$Cu(OH_2)_6^{2+}$		O_6	7.3	8
$Cu(DMAM\text{-}PMHD)OH_2^{2+}$	(e)	N_3O_2	7.1	13
$Cu(C\text{-}PMHD)OH_2^{+}$	(f)	N_2O_3	6.6	14
$Zn(OH_2)_6^{2+}$		O_6	9.0	8
$Zn(DMAM\text{-}PMHD)OH_2^{2+}$	(e)	N_3O	9.2	13
$Zn(C\text{-}PMHD)OH_2^{+}$	(f)	N_3O_2	7.1	14
$Zn(CR)OH_2^{2+}$	(d)	N_4O	8.7	12
$Zn([12]aneN_3)OH_2^{2+}$	(g)	N_3O	7.3	15,16
$Zn(HP[12]aneN_3)OH_2^{+}$	(h)	N_3O_2	10.7	16
$Zn(TImMP)OH_2^{2+}$	(i)	N_3O	<7	17
$Co(TImMP)OH_2^{2+}$	(i)	N_3O	7.8	17

(a) dacoda = 1,4-diaza-cyclooctane-1,4-diacetate. (b) TPyMA = tris(3,5-dimethyl-1-pyrazolylmethyl)amine. (c) TMC = 1,4,8,11-tetramethyl-1,4,8,11-tetraaza-cyclotetradecane. (d) CR = Schiff base between 2,6-diacetylpyridine and bis(3-aminopropyl)amine. (e) DMAM-PMHD = 1-[(6(dimethylamino)methyl)-2-pyridyl)methyl]hexahydro-1,4-diazepin-5-one. (f) C-PMHD = 1[(6-carboxy)-2-pyridyl)methyl]hexa-hydro-1,4-diazepin-5-one. (g) $[12]aneN_3$ = 1,5,9-triaza-cyclododecane. (h) $HP[12]aneN_3$ = 2-(2-hydroxyphenylate)-1,5,9-triaza-cyclododecane. (i)TImMP = tris(4,5-dimethyl-2-imidazolylmethyl)phosphinoxide.

the metal ion and formally becomes positively charged:

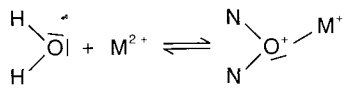

Under these conditions a proton is easily released. The nucleophilicity of coordinated water is, of course, decreased with respect to free water, owing to the decreased electronic charge on the oxygen atom, but a significant concentration of M—OH species may exist in neutral solution. In turn, the coordinated hydroxide is a slightly poorer nucleophile than the free OH^- ion, but better than water. On the basis of recent MO calculations,[18] the order of nucleophilicity for solvent-derived species can be summarized as follows:

$$H_3O^+ < H_2O{-}M^{2+} \simeq H_2O < HO{-}M^+ \simeq HO^-$$

Therefore, at neutral or slightly alkaline pH, the small decrease in efficiency of coordinated vs. free hydroxide ions is more than compensated for by the higher concentration of reactive species available (i.e., $HO{-}M^+$ vs. HO^-). Another common role for zinc enzymes is thus to provide a binding site at which the substrate can be attacked by the metal-coordinated hydroxide:

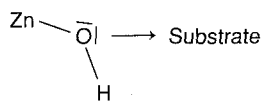

The pK_a of coordinated water in zinc complexes is controlled by the coordination number and by the total charge of the complex, in the sense that it decreases with decreasing coordination number and with increasing positive charge, because a zinc ion, bearing in effect a more positive charge, will have greater attraction for the oxygen lone pair, thus lowering the pK_a. Charged ligands affect water pK_a's more than does the number of ligands.[18] The pK_a in metalloproteins is further controlled by the presence of charged groups from protein side chains inside the cavity or by the binding of charged cofactors. The coordinated water may have a pK_a as low as 6, as in carbonic anhydrase (see later). On the other hand, the pK_a of the coordinated water is 7.6 in liver alcohol dehydrogenase (LADH) when NAD^+ is bound, 9.2 in the coenzyme-free enzyme, and 11.2 in the presence of NADH (see Section V.C).

(3) As mentioned before, Zn complexes show facile four- to five-coordinate interconversion. The low barrier between these coordination geometries is quite important, because the substrate may add to the coordination sphere in order to replace the solvent or to be coordinated together with the solvent. If the interconversion between four- and five-coordination is fast, catalysis is also fast.

Thus, to summarize, zinc is a good Lewis acid, especially in complexes with lower coordination numbers; it lowers the pK_a of coordinated water and is kinetically labile, and the interconversion among its four-, five-, and six-coordinate states is fast. All of these properties make zinc quite suitable for biological catalysis.[19]

1. The groups to which zinc(II) is bound

Zinc(II) is an ion of borderline hardness and displays high affinity for nitrogen and oxygen donor atoms as well as for sulfur. It is therefore found to be bound to histidines, glutamates or aspartates, and cysteines. When zinc has a catalytic role, it is exposed to solvent, and generally one water molecule completes the coordination, in which case the dominating ligands are histidines. It has been noted[20] recently that coordinated histidines are often hydrogen-bonded to carboxylates:

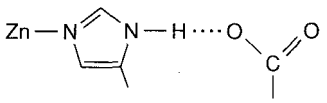

It is possible that the increase in free energy for the situation in which the hydrogen is covalently bound to the carboxylate oxygen and H-bonded to the histidine nitrogen is not large compared to k_BT. Under these circumstances the protein could determine the degree of imidazolate character of the ligand and therefore affect the charge on the metal.

The binding of zinc(II) (like that of other metal ions) is often determined by entropic factors. Water molecules are released when zinc(II) enters its binding position, thus providing a large entropy increase. Most commonly zinc is bound to three or four protein ligands. Large entropy increases are not observed, however, when zinc(II) binds to small polypeptides like the recently discovered zinc fingers, for here the binding site is not preformed (see Section III.B), and zinc(II) must be present for the protein to fold properly into the biologically active conformation.

2. The reactivity of zinc(II) in cavities

In the preceding section we discussed the properties of zinc(II) as an ion. These properties are, of course, important in understanding its role in biological catalysis, but it would be too simplistic to believe that reactivity can be understood solely on this basis. Catalysis occurs in cavities whose surfaces are constituted by protein residues. Catalytic zinc is bound to a water molecule, which often is H-bonded to other residues in the cavity and/or to other water molecules. The structure of the water molecules in the cavity cannot be the same as the structure of bulk water. Furthermore, the substrate interacts with the cavity residues through either hydrophilic (H-bonds or electric charges) or hydrophobic (London dispersive forces) interactions. As a result, the overall thermodynamics of the reaction pathway is quite different from that expected in bulk solutions. Examples of the importance of the above interactions will be given in this chapter.

3. The investigation of zinc enzymes

Direct spectroscopic investigation of zinc enzymes is difficult, because zinc(II) is colorless and diamagnetic; so it cannot be studied by means of electronic or

EPR spectroscopy. Its NMR-active isotope, ^{67}Zn, the natural abundance of which is 4.11 percent, has a small magnetic moment, and cannot (with present techniques) be examined by means of NMR spectroscopy at concentrations as low as 10^{-3} M. The enzymes could be reconstituted with ^{67}Zn. However, ^{67}Zn has a nuclear quadrupolar moment, which provides efficient relaxation times, especially in slow-rotating proteins and low-symmetry chromophores, making the line very broad.[210] Of course, ^{1}H NMR can be useful for the investigation of the native enzymes. However, often the molecular weight is such that the proteins are too large for full signal assignment given the current state of the art. At the moment the major source of information comes from x-ray data. Once the structure is resolved, it is possible to obtain reliable structural information on various derivatives by the so-called Fourier difference map. The new structure is obtained by comparing the Fourier maps of the native and of the derivative under investigation. Many x-ray data are now available on carboxypeptidase (Section V.A) and alcohol dehydrogenase (Section V.C).

The zinc ion can be replaced by other ions, and sometimes the enzymatic activity is retained fully or partially (Table 2.4). These new systems have attracted the interest of researchers who want to learn about the role of the metal and of the residues in the cavity, and to characterize the new systems per se.

Table 2.4
Representative metal-substituted zinc enzymes. Percent activities with respect to the native zinc enzyme in parentheses.[a]

Enzyme	Substituted metals
Alcohol dehydrogenase	Co(II)(70), Cu(II)(1), Cu(I)(8), Cd(II)(30), Ni(II)(12)
Superoxide dismutase	Co(II)(90), Hg(II)(90), Cd(II)(70), Cu(II)(100)
Aspartate transcarbamylase	Cd(II)(100), Mn(II)(100), Ni(II)(100)
Transcarboxylase	Co(II)(100), Cu(II)(0)
RNA polymerase	Co(II)(100)
Carboxypeptidase A	Mn(II)(30), Fe(II)(30), Co(II)(200), Ni(II)(50), Cu(II)(0),[b] Cd(II)(5), Hg(II)(0), Co(III)(0), Rh(II)(0), Pb(II)(0)
Thermolysin	Co(II)(200), Mn(II)(10), Fe(II)(60), Mg(II)(2), Cr(II)(2), Ni(II)(2), Cu(II)(2), Mo(II)(2), Pb(II)(2), Cd(II)(2), Nd(III)(2), Pr(III)(2)
Alkaline phosphatase	Co(II)(30), Cd(II)(1), Mn(II)(1), Ni(II)(0), Cu(II)(0), Hg(II)(0)
β-Lactamase II	Mn(II)(3), Co(II)(11), Ni(II)(0), Cu(II)(0), Cd(II)(11), Hg(II)(4)
Carbonic anhydrase[c]	Cd(II)(2), Hg(II)(0), Cu(II)(0), Ni(II)(2), Co(II)(50), Co(III)(0), Mn(II)(18), $V(IV)O^{2+}$(0)
Aldolase	Mn(II)(15), Fe(II)(67), Co(II)(85), Ni(II)(11), Cu(II)(0), Cd(II)(0), Hg(II)(0)
Pyruvate carboxylase	Co(II)(100)
Glyoxalase	Mg(II)(50), Mn(II)(50), Co(II)(50)

[a] Taken from Reference 21.
[b] Recent data indicate nonnegligible catalytic activity.[22]
[c] BCA II, except the value for Cd(II) obtained with HCA II.

Spectroscopic techniques can be appropriate for the new metal ions; so it is possible to quickly monitor properties of the new derivative that may be relevant for the investigation of the zinc enzyme.

B. Metal Substitution

With zinc enzymes, metallosubstitution is a convenient tool for monitoring the protein and its function by means of spectroscopic techniques. Furthermore, it is interesting to learn how reactivity depends on the nature of the metal ion and its coordination properties, because much of it depends on the protein structure, which seemingly remains constant. As discussed, zinc enzymes can be studied by replacing zinc with other spectroscopically useful metal ions, whose activities have been checked, and by transferring the information obtained to the native enzyme. The strategy of metal substitution is not limited to zinc enzymes, since it has been used for magnesium-activated enzymes and, occasionally, other metalloenzymes as well.

By dialyzing a protein solution against chelating agents, such as EDTA, 1,10-phenanthroline, or 2,6-dipicolinic acid at moderately acidic pH, or by reversibly unfolding the protein with denaturing agents (as has been done with alkaline phosphatase), one can cause zinc proteins to release their metal ions, giving rise to the corresponding but inactive apoprotein. Sometimes (e.g., by using alcohol dehydrogenase) dialysis against chelating agents can be applied to a suspension of protein microcrystals. In this way the chelating agent is still able to reach and remove the active site metal by slowly diffusing in the crystals through the hydration water, while the apoprotein is maintained in the native conformation by the crystal packing forces and denaturation is avoided. After the chelating agent is dialyzed out, often against a high-salt (e.g., ClO_4^-) buffer to reduce nonspecific binding, a new metalloprotein can obtained by addition of the appropriate metal salt.[23]

Cobalt(II)-substituted zinc proteins often show about as much activity as the native zinc enzymes (Table 2.4). This is a general characteristic of the cobalt-substituted zinc enzymes,[24] since the coordination chemistry of cobalt(II) is very similar to that of zinc(II). The two ions also show virtually identical ionic radii. Cobalt(II) derivatives generally display useful electronic spectra. High-spin cobalt(II) ions are paramagnetic, containing three unpaired electrons ($S = \frac{3}{2}$); thus they can also give rise to EPR spectra. The electronic relaxation times, i.e., the average lifetimes of the unpaired electrons in a given spin state of the S manifold ($-\frac{3}{2}$, $-\frac{1}{2}$, $\frac{1}{2}$, $\frac{3}{2}$), are very short (10^{-11} to 10^{-12} s) at room temperature. In order to detect EPR spectra, the sample temperature is usually decreased, often down to liquid helium temperature, to increase the electronic relaxation times and sharpen the EPR linewidths. On the other hand, as the paramagnetic broadening of the NMR lines in such systems is inversely proportional to the electronic relaxation times (see Section IV.C.3), room-temperature ^1H NMR spectra of cobalt(II) complexes can be easily detected, even in the absence of chemical exchange. Therefore cobalt(II) is an exceptional probe to monitor the structure

and reactivity of zinc enzymes. Of course, the transfer of information from the artificial to the native enzyme must be done with caution. However, if we can understand the functioning of the cobalt enzyme, we then have a reference frame by which to understand the kinetic properties of the native enzyme. The spectroscopic properties of cobalt(II) in cobalt-substituted proteins have been reviewed.[25]

Copper(II)-substituted zinc proteins are generally inactive with respect to the natural and most artificial substrates (Table 2.4). In model compounds copper(II) is often principally four-coordinate, with at most two more ligands present at metal-ligand distances that are longer than normal coordination bonds. As a consequence, the ability of zinc to switch between four- and five-coordinate species without any appreciable barrier and with usual metal-donor distances is not mimicked by copper. Furthermore, binding at the four principal coordination positions is generally stronger for copper than for zinc. It follows that substrates may have slow detachment kinetics. These properties are unfavorable for catalysis.

Copper(II) can be easily and meaningfully studied by means of electronic spectroscopy. Moreover, the EPR spectra can be recorded even at room temperature because of the long electronic relaxation times, which are of the order of 10^{-9} s. Because a protein is a macromolecule, it rotates slowly, and the EPR spectra in solution at room temperature look like those of crystalline powders or frozen solutions (powder-like spectra). ENDOR spectra are also easily obtained for copper proteins at low temperatures, because at low temperature the electronic relaxation times are even longer, and saturation of the EPR lines (which is a requirement to obtain ENDOR spectra) is easy to accomplish. The long electronic relaxation times make the broadening effects on the NMR lines of nuclei sensing the metal ion too severe; so these lines, unlike those of cobalt(II) complexes, generally escape detection. However, if the nucleus under investigation is in fast exchange between a free species in large excess and a bound species, the line may be observed, because the broadening effects are scaled down by a factor equal to the molar fraction of bound species. The nuclear relaxation parameters contain precious structural and/or dynamic information (see Section IV.C.3). The spectroscopic properties of copper(II) in proteins have been extensively reviewed.[26,27]

Cadmium-substituted zinc proteins may also be active (Table 2.4), although usually at higher pH. This observation is readily explained in terms of the pK_a of a coordinated water, which is expected to be higher than that of analogous zinc complexes because the cadmium ion is larger and polarizes the Cd—OH_2 bond less.

^{113}Cd and ^{111}Cd are nuclei with relatively high sensitivity for NMR spectroscopic study. The ^{113}Cd chemical shift spans from -200 to 800 ppm relative to $CdSO_4$ in H_2O, depending on the number and nature of donor atoms.[24,28] Sulfur donor atoms cause larger downfield shifts than oxygens or nitrogens, and the downfield shift increases with decreasing number of donor atoms. Therefore, ^{113}Cd NMR probes have been used extensively to study zinc enzymes, metal-storage proteins like thioneins, and other proteins with cysteine ligands, and

chemical shifts in various cadmium proteins, together with the proposed ligand donor set, have been obtained (Figure 2.1).

Manganese(II)-containing proteins give rise to detectable EPR signals; however, their interpretation in terms of structure and dynamics is not always informative. The electronic relaxation times of Mn^{2+} are the longest among metal ions, of the order of 10^{-8} s at room temperature and at the magnetic fields of interest. This property and the large $S = \frac{5}{2}$ value account for a large NMR linewidth, even larger than in copper(II) systems. Manganese(II)- and nickel(II)-substituted zinc proteins have often been reported to have fractional activity (Table 2.4).[24] Several efforts have been devoted to Mn(II) derivatives, especially by studying the NMR signals of nuclei in molecules that exchange rapidly with the metalloprotein.

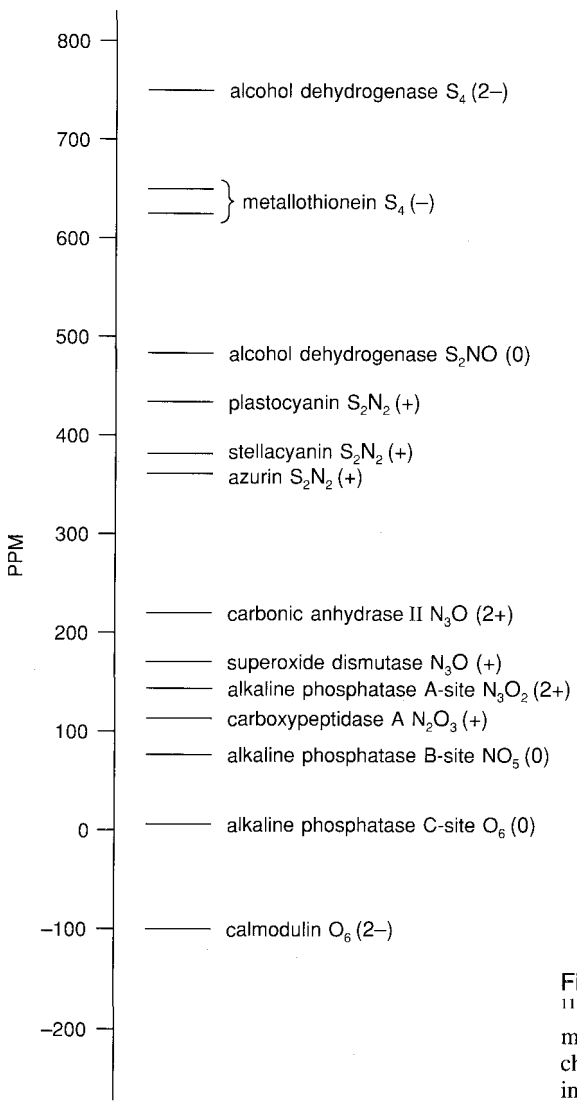

Figure 2.1
^{113}Cd chemical shifts in cadmium(II)-substituted metalloproteins.[24,28] Donor sets and overall charges (in parentheses) of the complexes are indicated.

Finally, several other metal-substituted zinc metalloprotein derivatives have been prepared, including those of VO^{2+}, Fe(II), Co(III), Pt(II), and $HgCl_2$. Although these systems add little directly to our understanding of the relationship between structure and function of the enzymes, nonetheless they represent new bioinorganic compounds and are of interest in themselves, or can add information on the coordinating capabilities, and reactivity in general, of the residues present in the active cavity.

Under the heading *zinc enzymes* there are several enzymes in which zinc is essential for the biological function, but is not present in the catalytic site. Among the most-studied enzymes, zinc has a structural role in superoxide dismutase, where the ligands are three histidines and one aspartate. In alcohol dehydrogenase there is a zinc ion that has a structural role, besides the catalytically active one. The former zinc has four cysteine ligands. Cysteine ligands are also present in zinc thioneins, which are zinc-storage proteins. The recently discovered class of genetic factors containing "zinc fingers" are zinc proteins in which the metal has an essentially structural role.[29] Such a role may consist of lowering the folding enthalpy of a protein to induce an active conformation or to stabilize a particular quaternary structure.

Zinc may also have a regulatory role; i.e., it does not participate in the various catalytic steps, but its presence increases the catalytic rate. This is a rather loose but common definition. Typically, zinc in the B site of alkaline phosphatase (Section V.B) has such a role, and the ligands are histidines, aspartates, and water molecules.

The enzymes in which zinc plays a structural or regulatory role will not be further discussed here, because they do not participate in the catalytic mechanisms; see the broader review articles.[23,29,30] Rather, we will describe in some detail the enzyme carbonic anhydrase, in order to show how researchers have investigated such complicated systems as enzymes. We will discover as we look at the details of the structures and mechanisms of enzymes that there are large differences between reactivities in solution and in enzymatic cavities. The fundamental properties underlying these differences are still not fully understood.

IV. ELUCIDATION OF STRUCTURE–FUNCTION RELATIONSHIPS: CARBONIC ANHYDRASE AS AN EXAMPLE

A. About the Enzyme

Carbon-dioxide hydration and its mechanism in living systems are of fundamental importance for bioinorganic chemistry. In 1932 the existence of an enzyme catalyzing CO_2 hydration in red blood cells was established.[31] The enzyme was named carbonic anhydrase (abbreviated CA). In 1939 the enzyme was recognized to contain zinc.[32] Because CO_2 is either the starting point for photosynthesis or the endpoint of substrate oxidation, carbonic anhydrases are now known to be ubiquitous, occurring in animals, plants, and several bacteria. Different

enzymes from different sources, catalyzing the same reaction and usually having homologous structures, are termed isoenzymes. Sometimes the same organism has more than one isoenzyme for a particular function, as is true for human carbonic anhydrase.

CO_2 gas is relatively soluble in water (3×10^{-2} M at room temperature under $p_{CO_2} = 1$ atm), equilibrating with hydrogen carbonate at pK_a 6.1:

$$CO_2 + H_2O \rightleftharpoons HCO_3^- + H^+ \tag{2.6}$$

The uncatalyzed reaction is kinetically slow around physiological pH ($k \simeq 10^{-1}\ s^{-1}$), whereas, in the presence of the most efficient isoenzyme of CA, the maximal CO_2 turnover number (i.e., the number of substrate molecules transformed per unit time by each molecule of enzyme)[33] is $\simeq 10^6\ s^{-1}$. The uncatalyzed attack by water on CO_2 may be facilitated by two hydrogen-bonded water molecules, one of which activates the carbon by means of a hydrogen bond to a terminal CO_2 oxygen, the other of which binds the carbon atom via oxygen:[34,35]

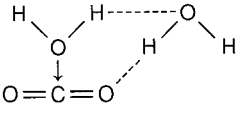

(2.7)

Only above pH 9 does the uncatalyzed reaction become fast, owing to direct attack of OH^-, which is a much better nucleophile than H_2O ($k \simeq 10^4\ M^{-1}s^{-1}$, where M^{-1} refers to the OH^- concentration):

$$CO_2 + OH^- \rightleftharpoons HCO_3^- \tag{2.8}$$

On the other hand, the rate constant in the presence of the enzyme, called k_{cat}, is pH-independent above pH 8 in every CA isoenzyme (Figure 2.2).[33,36]

In vitro, carbonic anhydrase is quite versatile, catalyzing several reactions that involve both OH^- and H^+, such as the hydrolysis of esters and the hydration of aldehydes. The various isoenzymes have been characterized to different degrees of sophistication. High-activity forms are labeled II ($k_{cat} \simeq 10^6\ s^{-1}$ at 25°C); low-activity forms I ($k_{cat} \simeq 10^5\ s^{-1}$), and the very-low-activity forms III ($k_{cat} \simeq 10^3\ s^{-1}$).[37] X-ray structural information at nominal 2 Å resolution is available for HCA I[38] and HCA II,[39] where H indicates human. The structure of HCA II has been refined recently.[40] High-resolution structures of mutants and of their substrate and inhibitor derivatives are being reported.[211] All isoenzymes are single-chain polypeptides, with M.W. about 30 kDa and one zinc ion per molecule. They have the shape of a rugby ball with a crevice 16 Å deep running through the south pole (Figure 2.3 *See color plate section, page C-2.*). At the bottom of the crevice, the zinc ion is anchored to the protein by three histidine nitrogen atoms and is exposed to solvent. Two histidines (His-94 and His-96, HCA I numbering) are bound to zinc via their Nϵ2 atoms, whereas one (His-

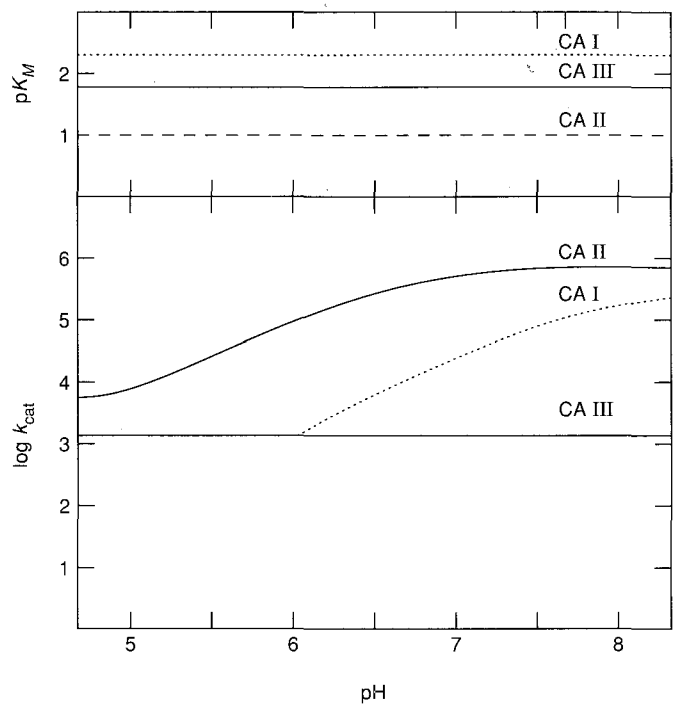

Figure 2.2
pH dependence of k_{cat} and K_m values for CO_2 hydration catalyzed by carbonic anhydrase I, II, and III isoenzymes.[33,36]

119) is bound via its Nδ1 atom (Figure 2.4). It is quite general that histidines bind zinc equally well by either of the two histidine nitrogens, the preference being probably dictated by the steric constraints imposed by the protein folding. The three histidine NH protons are all engaged in H-bonding (Figure 2.4). Histidine-119 is involved in H-bonding with a glutamate residue. As mentioned, this could be a way of controlling the basicity of the metal ligands. A solvent molecule bound to zinc is involved in an H-bond with Thr-199, which in turn is H-bonded to Glu-106. This H-bonding network is important for understanding the subtle structural changes that occur with pH changes; these could, in principle, account for the pH-dependent properties. Although the structure of crystals grown at pH 8 in sulfate-containing buffer gives some indication of a single solvent molecule bound to zinc (Figures 2.3 and 2.5 *See color plate section, pages C2, C3.*), theoretical studies indicate that two water molecules can be at bonding distances.[42] Such a finding is consistent with spectroscopic studies on other derivatives and with the concept that attachment and detachment of substrates occur through five coordination.

Just as is true for every zinc enzyme in which zinc is at the catalytic site, activity is lost if the metal is removed, and is restored by zinc uptake. The tertiary structure of carbonic anhydrase is maintained in the absence of zinc; even the denatured apoprotein can refold spontaneously from a random coil to a native-like conformation. Although such a process is accelerated by zinc,[43,44]

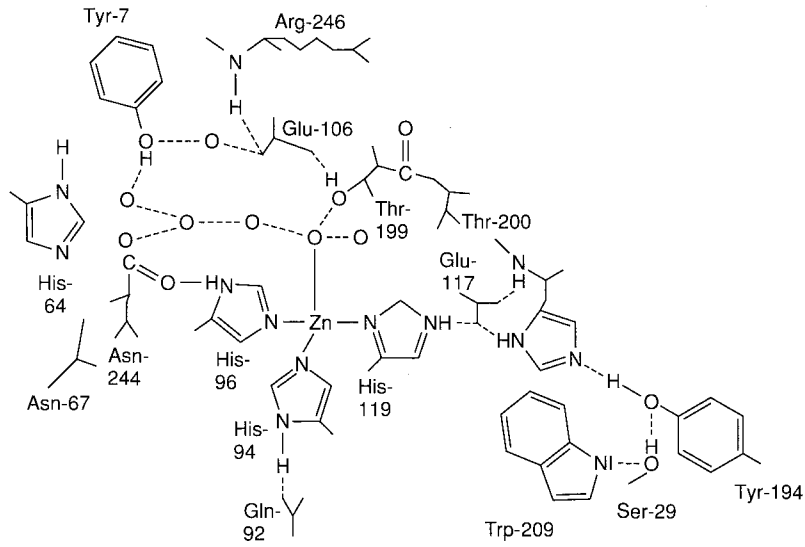

Figure 2.4
Schematic representation of the active site of human carbonic anhydrase II. Hydrogen bonds (---) and ordered water molecules (o) are indicated.[41]

the presence of the metal does not seem to be an absolute requirement for the correct folding of CA, whereas it is an absolute requirement for several other metalloproteins.[23,29,30]

Anions are attracted in the metal cavity by the positive $Zn(N_3OH_2)^{2+}$ moiety, and are believed to bind to zinc in carbonic anhydrase very effectively; so their use should be avoided as much as possible if the goal is to study the enzyme as it is. When the protein is dialyzed against freshly doubly distilled or carefully deionized water under an inert atmosphere, the pH of the sample approaches the isoelectric point, which is below 6 for HCA I and bovine (BCA II) enzymes. The pH can then be adjusted by appropriate additions of NaOH. All the measurements reported in the literature performed in acetate, phosphate, imidazole, or tris sulfate buffers are affected by the interference of the anion with the metal ion. However, buffer species containing large anions like Hepes (4[(2-hydroxyethyl)-1-piperazinyl]ethanesulfonic acid) can be used,[45] since these anions do not enter the cavity.

There are many indications that zinc in the high-pH form of CA is four-coordinate with an OH group in the fourth coordination site. At low pH the enzyme exists in a form that contains coordinated water; the coordination number can be four (one water molecule) or five (two water molecules). Of course, the occurrence of the low-pH species depends on the pK_a's of the complex acid-base equilibria.

B. Steady-State and Equilibrium Kinetics of Carbonic Anhydrase-Catalyzed CO_2/HCO_3^- Interconversion

The $CO_2 \rightleftharpoons HCO_3^-$ interconversion catalyzed by CA is extremely fast. The usual kinetic parameters describing an enzymatic reaction are the turnover number or kinetic constant for the reaction, k_{cat}, and the Michaelis constant K_m. In the simple catalytic scheme

$$E + S \underset{k_{-1}}{\overset{k_1}{\rightleftharpoons}} ES \xrightarrow{k_2} E + P,$$

where E stands for enzyme, S for substrate, and P for product, K_m^{-1} is given by $k_1/(k_{-1} + k_2)$. If k_2 is small, $k_{cat} = k_2$ and $K_m^{-1} = k_1/k_{-1}$, the latter corresponding to the thermodynamic affinity constant of the substrate for the enzyme. The pH dependences[46] of k_{cat} and K_m for CO_2 hydration for the high- and low-activity isoenzymes have been determined (Figure 2.2).[33,36] It appears that K_m is pH-independent, whereas k_{cat} increases with pH, reaching a plateau above pH 8. For bicarbonate dehydration (the reverse of Equation 2.6), H^+ is a cosubstrate of the enzyme. The pH dependence of k_{cat}/K_m for HCO_3^- dehydration is also mainly due to k_{cat}, which shows the same pH profile as that for CO_2 if the experimental kinetic data are divided by the available concentration of the H^+ cosubstrate.[47,48] Further measurements have shown that the pH dependence of k_{cat} reflects at least two ionizations if the measurements are performed in the absence of anions.[49] The value of k_{cat} reaches its maximum at alkaline pH only when buffer concentrations exceed 10^{-2} M.[50] In other words, the exchange of the proton with the solvent is the rate-limiting step along the catalytic pathway if relatively high concentrations of proton acceptors and proton donors are not provided by a buffer system. This limit results from the high turnover of the enzyme, which functions at the limit imposed by the diffusion rate of the H^+ cosubstrate. At high buffer concentration, k_{cat} shows an isotope effect consistent with the occurrence of an internal proton transfer as the new rate-limiting step.[51]

Measurements of the catalyzed reaction performed at chemical equilibrium starting from mixtures of ^{12}C-^{18}O-labeled HCO_3^- and ^{13}C-^{16}O-labeled CO_2 have shown the transient formation of ^{13}C-^{18}O-labeled species (both CO_2 and HCO_3^-) before ^{18}O-labeled water appears in solution.[52] These experiments provided evidence that, at chemical equilibrium, an oxygen atom can pass from HCO_3^- to CO_2 and vice versa several times before being released to water. Furthermore, maximal exchange rates are observed even in the absence of buffers.

Under chemical equilibrium conditions, ^{13}C NMR spectroscopy is particularly useful in investigating substrate interconversion rates, since the rates pass from a slow-exchange regime in the absence of enzyme to fast exchange at sufficient enzyme concentration. In the absence of enzyme two ^{13}C signals are observed, one for CO_2 and the other for HCO_3^-. In the presence of enzyme only one averaged signal is observed (Figure 2.6). Starting from the slow exchange situation, in the absence of enzyme, the increase in linewidth ($\Delta\nu$) of the substrate (A) and product (B) signals (caused by exchange broadening that is caused

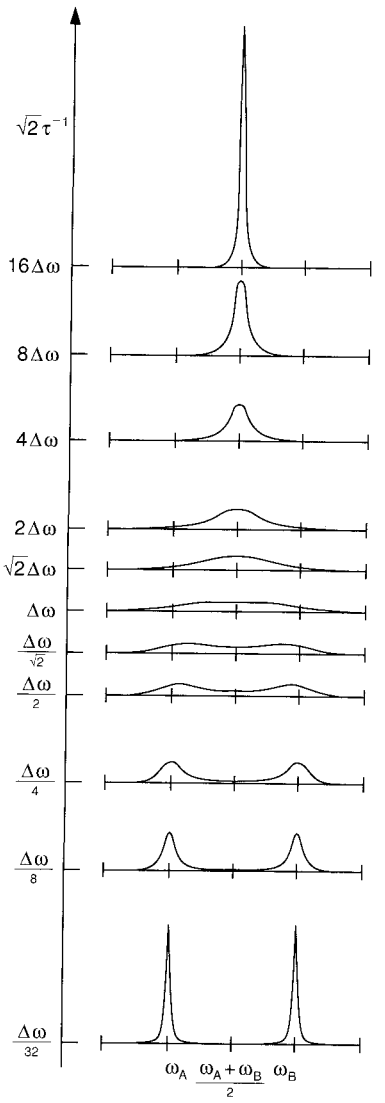

Figure 2.6
Calculated lineshape for the NMR signals of nuclei equally distributed between two sites ([A] = [B]), as a function of the exchange rate τ^{-1}. $\Delta\omega$ is the peak separation in rad s^{-1}.

in turn by the presence of a small amount of catalyst) depends on the exchange rate and on the concentration of each species, according to the following relation:

$$\Delta\nu_A[A] = \Delta\nu_B[B] = \tau_{exch}^{-1}. \tag{2.9}$$

Therefore, the exchange rate τ_{exch}^{-1} can be calculated.[53] The appearance of the NMR spectrum for different τ_{exch} values is illustrated in Figure 2.6 under the condition [A] = [B]. For the high-activity enzyme it was found that the maximal exchange rates are larger than the maximal turnover rates under steady-state conditions; the ratio between k_{exch} of the high-activity (type II) and low-activity (type I) forms is 50, i.e., larger than the ratio in $k_{cat.}$[49,54] This result is consistent with the idea that the rate-limiting step in the steady-state process is an intra-

molecular proton transfer in the presence of buffer for type II enzymes, whereas it may not be so for the type I enzymes. The exchange is pH-independent in the pH range 5.7–8, and does not show a proton-deuteron isotope effect. The apparent substrate binding (HCO_3^-) is weaker than steady-state K_m values, indicating that these values are not true dissociation constants. Chloride is a competitive inhibitor of the exchange.[49]

A similar investigation was conducted for type I CoHCA at pH 6.3, where the concentrations of CO_2 and HCO_3^- are equal.[55] The two lines for the two substrates were found to have different linewidths but equal T_1 values. Measurements at two magnetic fields indicate that the line broadening of the HCO_3^- resonance is caused by substrate exchange and by a paramagnetic contribution due to bonding. The temperature dependence of the linewidth shows that the latter is determined by the dissociation rate. Such a value is only about 2.5 times larger than the overall $CO_2 \rightleftharpoons HCO_3^-$ exchange-rate constant. Therefore the exchange rate between bound and free HCO_3^- is close to the threshold for the rate-limiting step. Such an exchange rate is related to the higher affinity of the substrate and anions in general for type I isoenzymes than for type II isoenzymes. This behavior can be accounted for in terms of the pK_a of coordinated water (see below).

C. What Do We Learn from Cobalt Substitution?

1. Acid-base equilibria

It is convenient to discuss the cobalt-substituted carbonic anhydrase enzyme, since its electronic spectra are markedly pH-dependent and easy to measure (Figures 2.7 and 2.8).[56,57] The spectra are well-shaped, and a sharp absorption at 640 nm is present at high pH and absent at low pH. Whereas CoHCA I is almost entirely in the low-pH form at pH 5.7, this is not true for the CoBCA II isoenzyme. The acid-base equilibrium for Co-substituted carbonic anhydrase (deprotonation of the metal-coordinated water) involves three species:

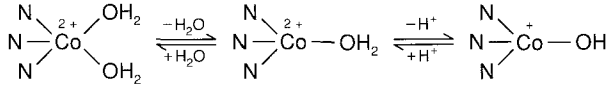

(2.10)

The first equilibrium has never been directly monitored, and the conditions that determine it are quite vague. However, the five-coordinate species has been proposed in HCA I at low pH values.[48] Figure 2.7 at first seems to show isosbestic points* between 16,000 and 18,000 cm^{-1}, so that a single acidic group could

* An isosbestic point is a value of frequency where the two species in an A $\rightleftharpoons$ B equilibrium have the same absorption. As a consequence, all mixtures of A and B also show the same absorption at that frequency, and all the spectra along, e.g., a pH titration from A to B, plotted one on top of the other, cross at the isosbestic point. The presence of isosbestic points thus indicates the presence of only two species in equilibrium.

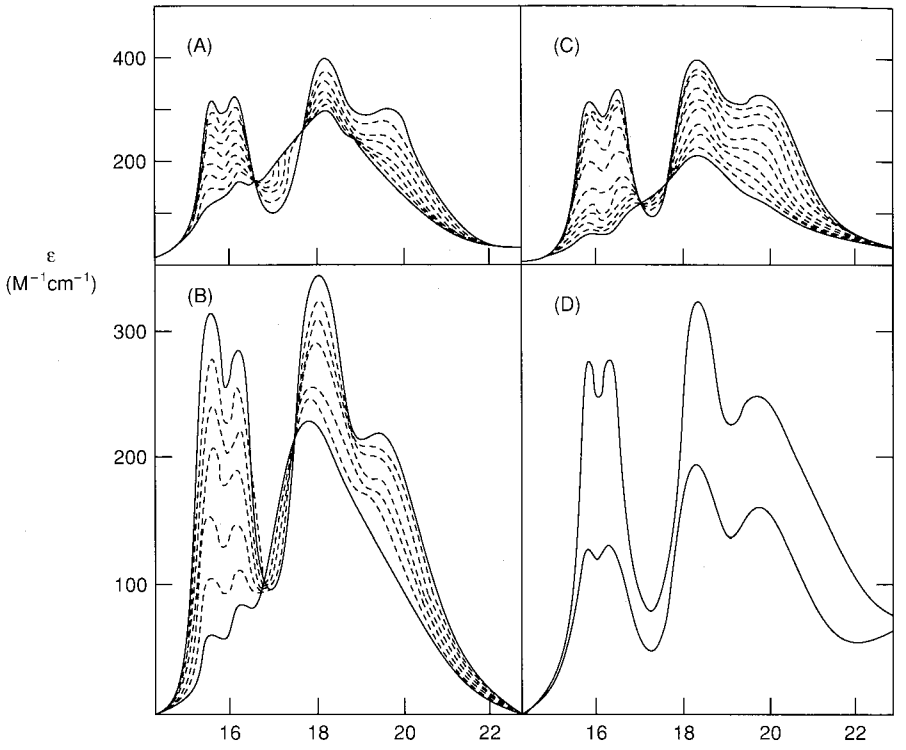

Figure 2.7
pH-variation of the electronic spectra of cobalt(II)-substituted BCA II (A), HCA II (B), HCA I (C), and BCA III (D). The pH values, in order of increasing $\epsilon_{15\cdot6}$, are (A) 5.8, 6.0, 6.3, 6.7, 7.3, 7.7, 7.9, 8.2, 8.8; (B) 6.1, 6.6, 7.1, 7.8, 8.3, 8.6, 9.5; (C) 5.3, 6.1, 6.6, 7.0, 7.3, 7.5, 7.9, 8.4, 8.6, 9.1, 9.6.[56]

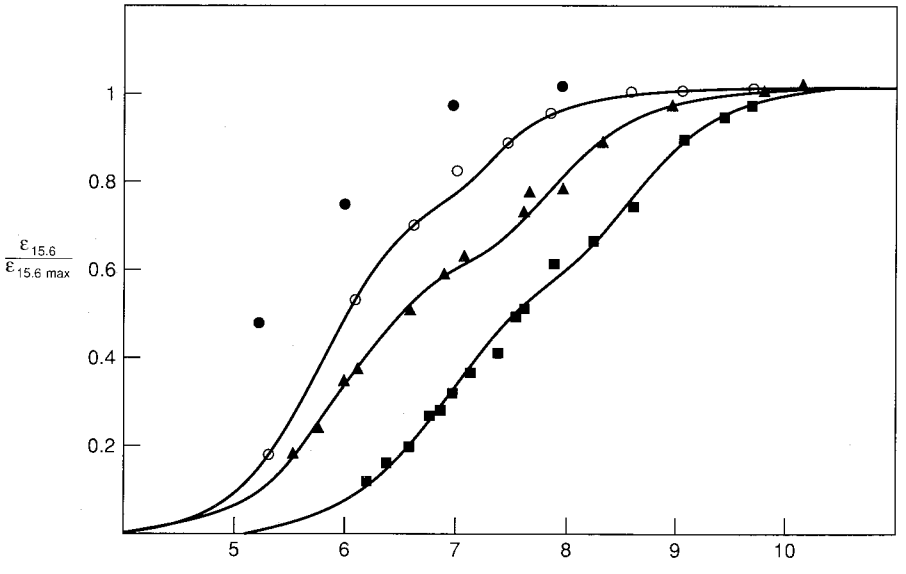

Figure 2.8
pH dependence of $\epsilon_{15\cdot6}$ for cobalt(II)-substituted BCA III (●), HCA II (o), BCA II (▲), and HCA I (■) isoenzymes. The high pH limit value of $\epsilon_{15\cdot6}$ is normalized to 1 for each isoenzyme.[57]

account for the experimental data. Therefore, CoHCA I would have a pK_a of about 8, CoBCA II and CoHCA II a pK_a of about 6.5, and CoBCA III a pK_a around 5.5. The analysis of the dependence of the absorbance on pH, however, clearly shows that two apparent pK_a's can be extracted from the electronic spectra of at least CoCA I and II (Figure 2.8). These kinds of isoenzymes contain at least another histidine in the cavity, which represents another acidic group, with a pK_a of about 6.5 in its free state. The interaction between such an acidic group and metal-coordinated water, for example, via a network of hydrogen bonds, provides a physical picture that can account for the observed experimental data.[49] Two apparent acid dissociation constants K_a can be obtained from the fitting of the curves of Figure 2.8. They are called apparent, because they do not represent actual acid dissociations at the microscopic level. When there are two acidic groups interacting with each other, the system must be described in terms of four constants, also called microconstants, because the dissociation of each of the two groups is described by two different pK_a's, depending on the ionization state of the other group (Figure 2.9); so the two apparent constants

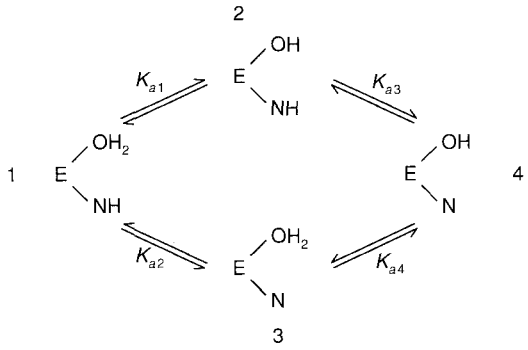

Figure 2.9
General scheme for two coupled acid-base equilibria applied to carbonic anhydrase. The two acid-base groups are the metal-coordinated water molecule and a histidine residue present in the active-site cavity.[58]

can be expressed in terms of four microconstants describing two interacting acidic groups. It is again a general feature of these systems that the four microconstants can be obtained only by making some assumptions. In one analysis the molar absorbances of species (1) and (3), and of species (2) and (4), were assumed to be equal.[58] In other words, it is assumed that the changes in the electronic spectra of cobalt(II) (Figure 2.7) are due entirely to the ionization of the coordinated water, not at all to the ionization state of the other group. This assumption accounts for the observation of approximate isosbestic points, even though there is an equilibrium between more than two species. With this assumption the four microconstants could be obtained (Table 2.5). Recall that the activity and spectroscopic profiles follow one another (see Figure 2.2 and Section IV.B). Furthermore, similar microconstant values had been obtained on

Table 2.5
Values of microconstants associated with acid-base equilibria[a] in cobalt(II)-substituted carbonic anhydrases.[58]

	pK_{a1}	pK_{a2}	pK_{a3}	pK_{a4}
CoHCA I	7.14	7.21	8.45	8.38
CoHCA II	5.95	5.62	6.62	6.95
CoBCA II	6.12	6.28	7.75	7.59

[a] As defined in Figure 2.9.

ZnHCA II by analyzing the pH dependence of the maximum velocity of the hydration reaction, V_{max}, assuming that the two hydroxo-containing species had the same activity.[49] The present analysis implies that species (2) and (3) of Figure 2.9 are distinguishable, although their interconversion may be fast.

Metal coordination lowers the pK_a of coordinated water. Factors affecting the acidity of the coordinated water are many, and their effects are probably overlapping, making the analysis quite complex (see also Section III.A). Nonetheless, the following factors probably contribute to the lowering of the pK_a:

(1) the charge of the chromophore, which in this case is 2+, although it may be somewhat lowered by the H-bonding between a coordinated histidine and a negative glutamate residue;
(2) the coordination number (which is four), since a higher value leads to a larger electron density on the metal ion ligands;
(3) the presence of other acidic groups with which the coordinated water interacts;
(4) the presence of positively charged residues inside the metal binding cavity that favors the removal of a proton from the cavity.

This last factor is presumably operating for CA III, which contains several arginine residues in the cavity; the same factor may also induce changes in the microscopic properties of the solvent inside the active cavity. These considerations account for the observation that most model complexes have a significantly higher pK_a value than the protein itself.

2. Coordination Geometries

The binding of inhibitors is also pH-dependent. It is possible, however, to obtain fully inhibited systems by adjusting the inhibitor concentration and pH. In this manner the so-called limit spectra of CoCA derivatives are obtained. Many systems have been characterized, providing a variety of spectral characteristics[59] (Figure 2.10). The differences in molar absorbance are larger than expected for changing only one coordinated atom. A rationalization of the

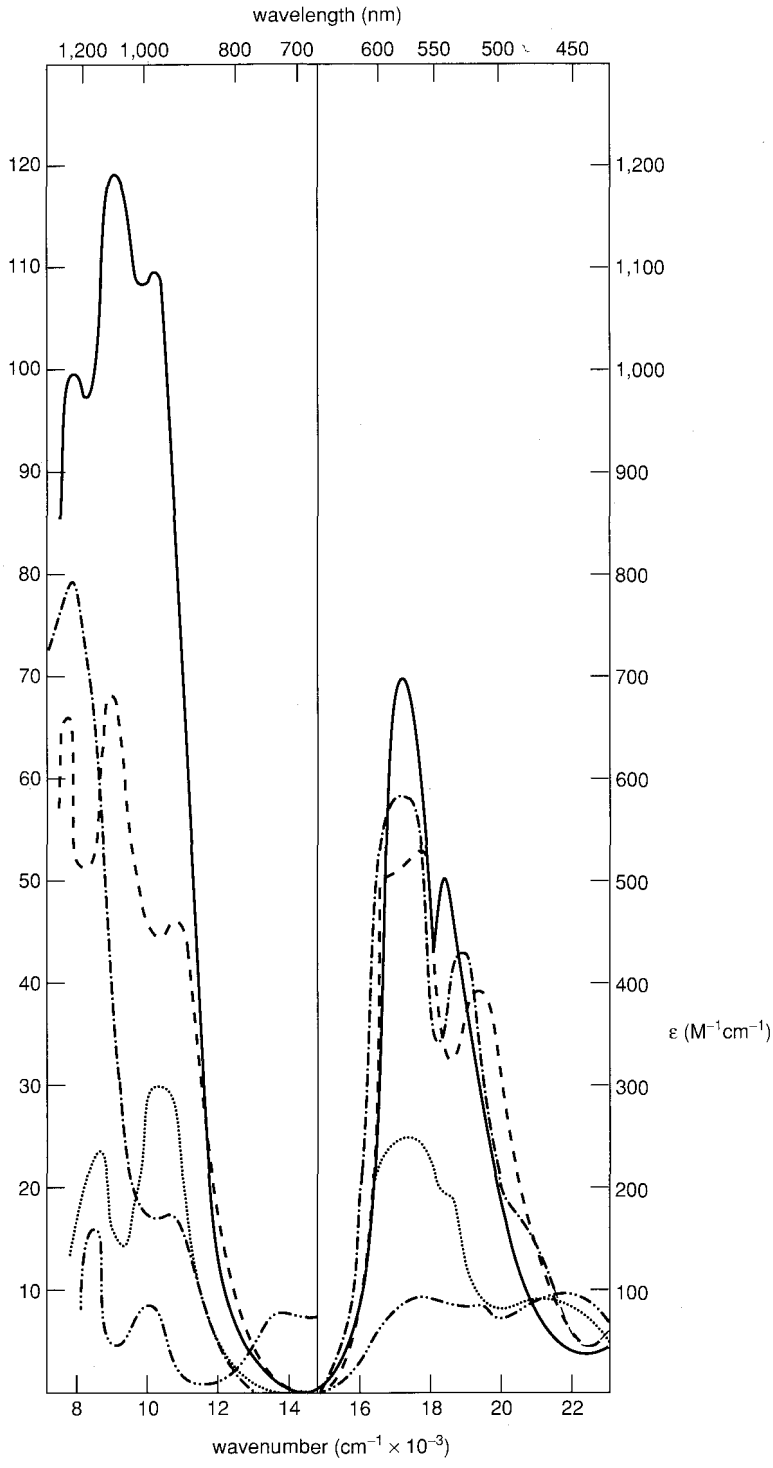

Figure 2.10
Electronic spectra of cyanide (————), cyanate (–·–·–), acetazolamide (– – –), azide (· · · · ·), and thiocyanate (–··–) adducts of cobalt(II)-substituted bovine carbonic anhydrase II.[59]

experimental data came by applying a criterion, first suggested by Gray,[60] according to which four-coordinate species have larger maximal absorption than five-coordinate species. This property theoretically arises from greater mixing of p and d metal orbitals in the four-coordinate case, which makes the d-d transitions partially allowed, neglecting other factors such as the covalency of the coordination bond, nephelauxetic effects,* or vicinity of charge transfer bands. Subsequent extension of the measurements to the near-infrared region was instructive:[59] the low-intensity spectra exhibited a weak absorption between 13,000 and 15,000 cm^{-1}. The latter band was assigned to the highest in energy of the F $\rightarrow$ F transitions, which increases in energy with the coordination number.† Therefore both the low intensity of the bands ($\epsilon_{max} < 200\ M^{-1}\ cm^{-1}$) and the presence of the F $\rightarrow$ F transition at high energy were taken as evidence for five coordination. Spectra showing high maximal absorption ($\epsilon_{max} > 300\ M^{-1}\ cm^{-1}$) were assigned as arising from four-coordinate species. The corresponding chromophores are $CoN_3In(OH_2)$ and CoN_3In, where In denotes inhibitor. Intermediate maximal absorptions may indicate an equilibrium between four- and five-coordinate species. In Table 2.6 some inhibitors are classified according to their behavior. Bicarbonate, which is a substrate of the enzyme, gives rise to an equilibrium between four- and five-coordinate species.[48,59]

The differences in the electronic spectra outlined above also have been detected in both CD and MCD spectra. In the latter, pseudotetrahedral species

Table 2.6
Classification of inhibitors of bovine carbonic anhydrase II according to the electronic spectral properties of the adducts with cobalt(II) derivatives.[a] [48,59]

Four-coordinate	Equilibria between four- and five-coordinate species	Five-coordinate
Sulphonamides (N_4)	Bicarbonate (N_3O—N_3O_2)	Carboxylates (N_3O_2)
Cyanide (N_3C)	Chloride (N_3Cl—N_3OCl)	Thiocyanate (N_4O)
Cyanate (N_4)	Bromide (N_3Br—N_3OBr)	Nitrate (N_3O_2)
Aniline (N_4)	Azide (N_4—N_4O)	Iodide (N_3OI)
Phenol (N_3O)		
Chlorate (N_3O)		

[a] Donor sets in parentheses.

* Nephelauxetic (literally, cloud-expanding) effects are due to partial donation of electrons by the ligand to the metal, and are stronger for less electronegative and more reducing ligands.

† By F $\rightarrow$ F transition we mean here a transition between two electronic states originating from the same F term (the ground term) in the free ion and split by the ligand field; the stronger the ligand field, the larger the splitting. For high-spin cobalt(II), the free-ion ground state ^4F (quartet F) is split in octahedral symmetry into $^4T_{2g}$, $^4T_{1g}$, and $^4A_{2g}$ states, the $^4T_{2g}$ lying lowest; in lower symmetries the T states are further split. The highest F $\rightarrow$ F transition is, therefore, that from the ground state $^4T_{2g}$, or the lowest of its substates in low symmetry, to the $^4A_{2g}$ state. For the same type of ligands, e.g., nitrogens or oxygens, the ligand field strength, and therefore the energy of the F $\rightarrow$ F transition, increases with the number of ligands.

give a sizably positive band in the high-energy region, whereas five-coordinate species show a much weaker positive band and six-coordinate complexes have only weak negative bands (Figure 2.11).[21,61] This additional empirical criterion may be helpful in assigning the coordination number. A further criterion is based on how much of the splitting of the $S = \frac{3}{2}$ ground state is caused by spin-orbit coupling (zero-field splitting). This splitting can be indirectly measured from the temperature dependence of the electronic relaxation times of the cobalt complexes, in turn estimated from their ability to saturate the EPR lines of the complexes at low temperatures.[62] There are theoretical reasons to predict that the above splitting increases in the order four coordination < five coordination < six coordination.[63]

Three binding sites have been identified in the cavity of CA[40,64–66] (Figure 2.12). The OH^- binding site, which provides a tetrahedral structure around the metal ion, is called the A site. The hydrogen interacts via hydrogen bonding with the oxygen of Thr-199. Thr-199 and Thr-200, together with their protein backbone, identify a hydrophilic region that probably plays a fundamental role in the energetic balance of ligand binding. On the back of the cavity there is a hydrophobic region formed by Val-143, Leu-198, and Trp-209. Although this cavity is hydrophobic, the x-ray structure shows evidence of a water molecule, H-bonded to the coordinated water. Ligands with a hydrophobic end could easily be located in this binding position, which is called B. The coordinated water

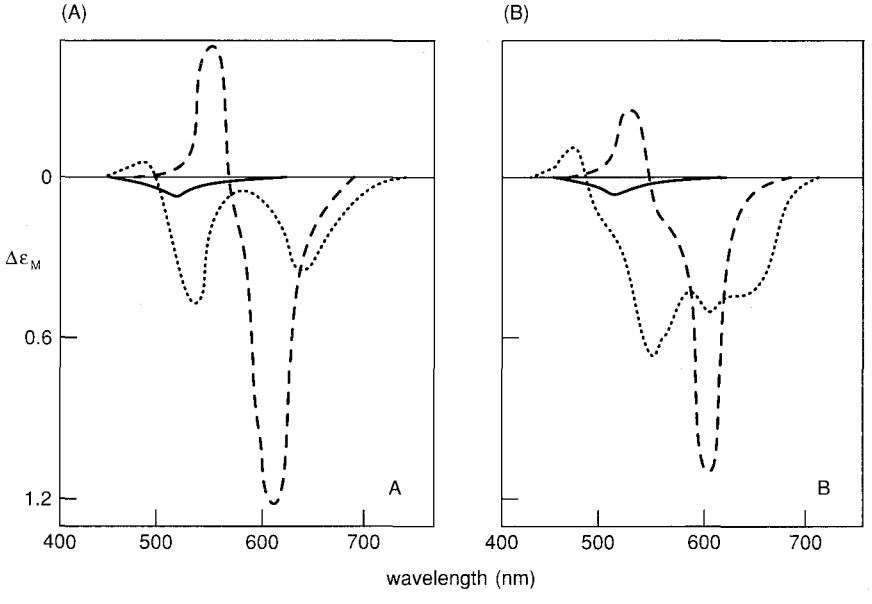

Figure 2.11
(A) MCD spectra of model six-coordinate ($Co(Gly\text{-}Gly)_2$, ———), five-coordinate ($(Co\text{-}Me_6tren)Br_2$, ... , and four-coordinate ($Co(py)_2Br_2$, – – –) cobalt(II) complexes and (B) MCD spectra of the cobalt(II) derivatives of pyruvate kinase (———), alkaline phosphatase (· · · · ·), and carbonic anhydrase in the presence of acetazolamide (– – –).[21,61]

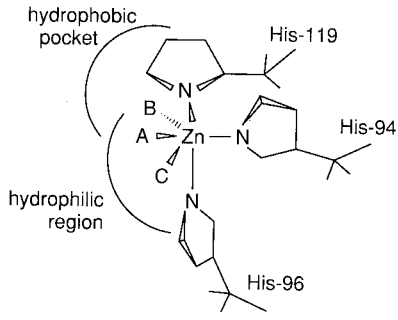

Figure 2.12
Schematic drawing of the active cavity of HCA II showing the three possible ligand binding sites.[64–66] Site A is the site of the OH^- ligand in the active form; site B is the binding site of NCS^-, which gives rise to a five-coordinate adduct with a water molecule in the C site.[64–66]

molecule would change its position in order to make reasonable angles between coordinated groups. The new position is labeled C. The x-ray structure of the thiocyanate derivative of HCA II[40,64] illustrates the latter case (see Figure 2.5). The NCS^- ion is in van der Waals contact with Val-143, Leu-198, and Trp-209. The water interacts with the hydroxyl group of Thr-199. The geometry of the five-coordinate derivative can be roughly described as a distorted square pyramid with His-94 in the apical position (Figure 2.13A). This could be a typical structure for those derivatives that have spectra typical of five-coordinate adducts, like the carboxylate derivatives.

In aromatic sulfonamide ($Ar—SO_2—NH_2$) derivatives, which probably bind as anions (see Section IV.C.4), the NH^- group binds zinc in the A position,[64–66] giving rise to an H-bond with Thr-199. The oxygens do not interact with the metal; one of them sits in the hydrophobic pocket. The chromophore around zinc is pseudotetrahedral (Figure 2.13B). The energy involved in the coordination includes the coordination bond, the hydrophobic interactions of the aromatic sulfonamide ring, and the maintainance of the Zn-X-H-Thr-199 hydrogen bonding (X=N,O). It is interesting to note that cyanate, according to spectroscopic studies,[48,59] gives rise to tetrahedral derivatives, probably because the terminal oxygen can enter into H-bonds with the hydrophilic region of the cavity. ^{13}C NMR data on $N^{13}CO^-$ interacting with CoBCA indicate that the anion interacts directly with the metal ion.[67] We do not have direct information on where it binds.[212]

The fine balance between hydrophobic and hydrophilic interactions, as well as major steric requirements, play important roles in the binding of inhibitors. Cyanide is the only ligand that may bind in a 2:1 ratio.[68] It is likely that the bis-cyanide adduct has the same arrangement as the $NCS^-—H_2O$ derivative. The spin state of the bis-cyanide adduct is $S = \frac{1}{2}$.[68]

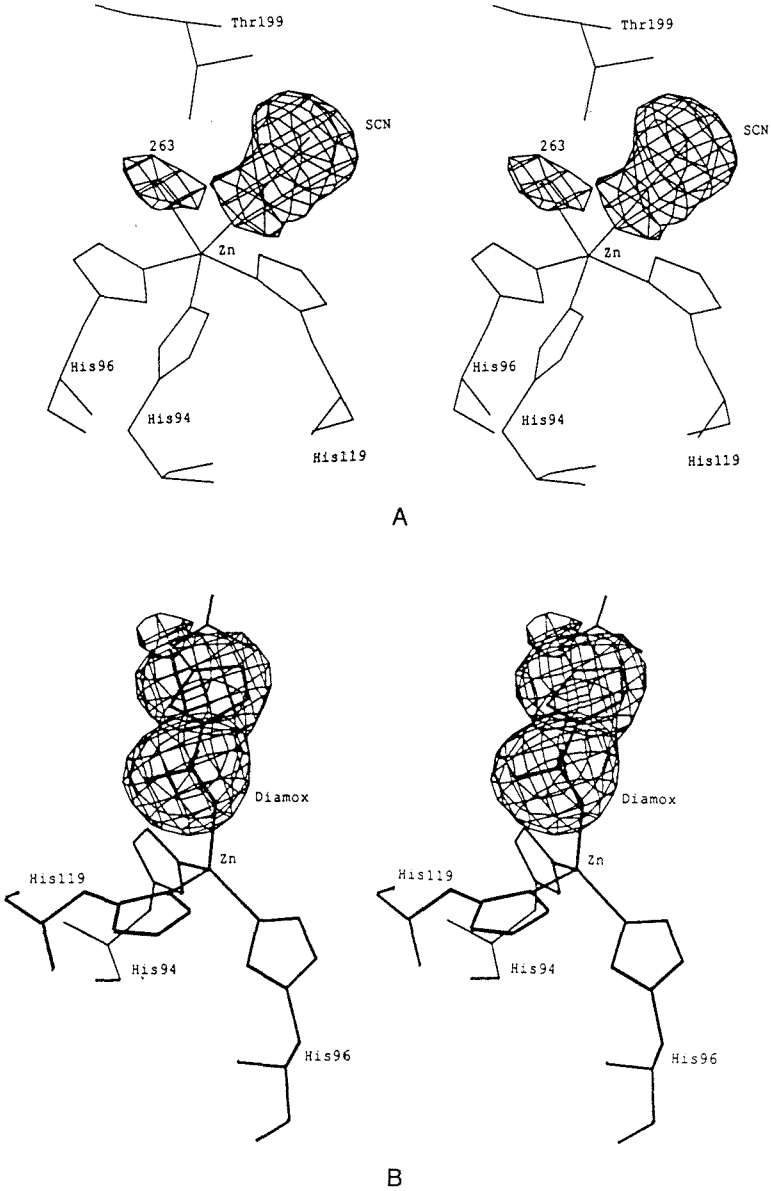

Figure 2.13
Stereo views of the NCS^- (A) and acetazolamide (B) adducts of HCA II.[40]

3. Coordinated water and NMR

It is quite relevant to know whether a water molecule is coordinated to the metal ion in a metalloenzyme, and whether it is still coordinated in the presence of substrates and inhibitors. The presence or absence of H_2O coordinated to a paramagnetic center can in principle be monitored by solvent water ^1H NMR,[69] by exploiting the occurrence of a magnetic interaction between the magnetic moments of the unpaired electrons and the nuclear magnetic moments of the

water protons. When this interaction fluctuates with time, it causes a shortening of the water-proton relaxation times.*

The longitudinal relaxation rate values, T_1^{-1}, of all the solvent water protons increase when even a single water molecule interacts with a paramagnetic center, provided that this bound water exchanges rapidly with free water molecules. To obtain the necessary experimental data, a methodology has been developed based on the measurement of water ^1H T_1^{-1} values at various magnetic fields (Nuclear Magnetic Relaxation Dispersion, NMRD).[69–71] The experimental data contain information on the correlation time, i.e., the time constant for the dynamic process that causes the proton-unpaired electron interaction to fluctuate with time; furthermore, under certain conditions, they may provide quantitative information on the number of interacting protons and their distance to the metal. The enhancement of T_1^{-1}, called T_{1p}^{-1}, is caused by the paramagnetic effect on bound water molecules and by the exchange time τ_m, according to the relationship

$$(T_{1p})^{-1} = f_M(T_{1M} + \tau_M)^{-1}, \tag{2.11}$$

where f_M is the molar fraction of bound water and T_{1M} is the relaxation time of a bound water proton. Therefore we measure the water ^1H T_1^{-1}, subtract the diamagnetic effect (i.e., the water-proton relaxation rate measured in a solution of a diamagnetic analogue), obtain T_{1p}^{-1}, then check that τ_m is negligible with respect to T_{1M}. For high-spin cobalt(II), T_{1M} is of the order of 10^{-3} s, whereas τ_m is about 10^{-5} s. Then the experimental T_{1p} can be safely related to T_{1M}. It is now important, in order to proceed with the analysis, to define the correlation time for the interaction between proton nuclei and unpaired electrons, τ_c. Its definition is important in order to obtain a physical picture of the system, and to quantitatively analyze the obtained T_{1M} values.[69] τ_c is defined by

$$\tau_c^{-1} = \tau_r^{-1} + \tau_s^{-1} + \tau_m^{-1}, \tag{2.12}$$

where τ_r is the rotational correlation time, τ_s is the electronic relaxation time, and τ_m has been previously defined. τ_r depends on the size of the molecule, which can be calculated rigorously if the molecule is spherical, or approximately if it is not. The appropriate expression is

$$\tau_r = \frac{4\pi\eta a^3}{3k_BT}, \tag{2.13}$$

* The nuclear longitudinal relaxation time, T_1, can be defined as the rate constant by which the populations of the $M_I = \frac{1}{2}$ and $M_I = -\frac{1}{2}$ (for protons) levels reach their equilibrium value after an external perturbation (e.g., a radiofrequency pulse in an NMR experiment). The transverse relaxation time, T_2, can be defined as the average lifetime of a hydrogen nucleus in a given spin state. The NMR linewidth is inversely proportional to T_2. The relation $T_2 \leq T_1$ always holds.

where η is the microviscosity of the solution, a is the radius (or approximate radius) of the molecule, k_B is the Boltzmann constant, and T is the absolute temperature. For CA, τ_r can be safely calculated to be $\simeq 10^{-8}$ s at room temperature. Since the correlation time τ_c in high-spin cobalt proteins varies between 10^{-11} and 10^{-12} s, it must therefore be determined by the electronic relaxation time.

Water ^{1}H NMRD profiles are often analyzed by using the classical dipolar interaction approach, as first described by Solomon:[72]

$$T_{1M}^{-1} = \frac{2}{15}\left(\frac{\mu_0}{4\pi}\right)^2 \frac{\gamma_I^2 g_e^2 \mu_B^2 S(S+1)}{r^6}\left(\frac{7\tau_c}{1+\omega_S^2\tau_c^2} + \frac{3\tau_c}{1+\omega_I^2\tau_c^2}\right), \quad (2.14)$$

where μ_0 is the permeability of vacuum, γ_I is the nuclear magnetogyric ratio, g_e is the electron g-factor, S is the electron spin quantum number, r is the electron-nucleus distance, and ω_S and ω_I are the electron and nuclear Larmor frequencies, respectively. This equation describes the dipolar interaction between the magnetic moment of nucleus I ($\hbar\gamma_I\sqrt{I(I+1)}$) and the magnetic moment of the electrons S ($g_e\mu_B\sqrt{S(S+1)}$) as a function of the correlation time (τ_c) and of the magnetic field (expressed as ω_I and ω_S). Neglect of the zero-field splitting of the $S = \frac{3}{2}$ manifold may introduce an error in the quantitative estimates within a factor of two.[73]

Fitting of the data for pseudotetrahedral complexes shows that they have τ_s of 10^{-11} s, whereas five-coordinate complexes have a shorter τ_s, on the order of 10^{-12} s. The latter derivatives also have exchangeable protons that could correspond to a water molecule in the coordination sphere, whereas the former do not.[25] The τ_s values are thus proposed as indicators of the coordination number in low-symmetry, four- and five-coordinate cobalt complexes. The shorter electronic relaxation times are related to low-lying excited states, which, independently of the particular mechanism, favor electron relaxation.[74]

Short electronic relaxation times in paramagnetic compounds cause only minor broadening of ^{1}H NMR lines, whereas the isotropic shifts (i.e., the shifts due to the presence of unpaired electron(s), usually very large) are independent of the value of the electronic relaxation times. For cobalt-substituted carbonic anhydrase, the ^{1}H NMR spectra have been recorded for several derivatives, and the proton signals of histidines coordinated to the metal were found to be shifted well outside the diamagnetic region (Figure 2.14).[75] Five-coordinate species give sharper signals than four-coordinate ones. The spectra in D_2O for both kinds of derivatives show three fewer isotropically shifted signals than in H_2O. These signals are assigned to histidine NH protons, which are replaced by deuterons in D_2O. Five-coordinate species provide ^{1}H NMR spectra with many signals slightly shifted from the diamagnetic position. It is believed that such complexes have relatively large magnetic anisotropy, which, summed up to the external magnetic field, provides further differentiation in shifts of the protons. Such shift contributions are called pseudocontact shifts. These shifts depend on the third power of the distance from the metal and on the position of the proton

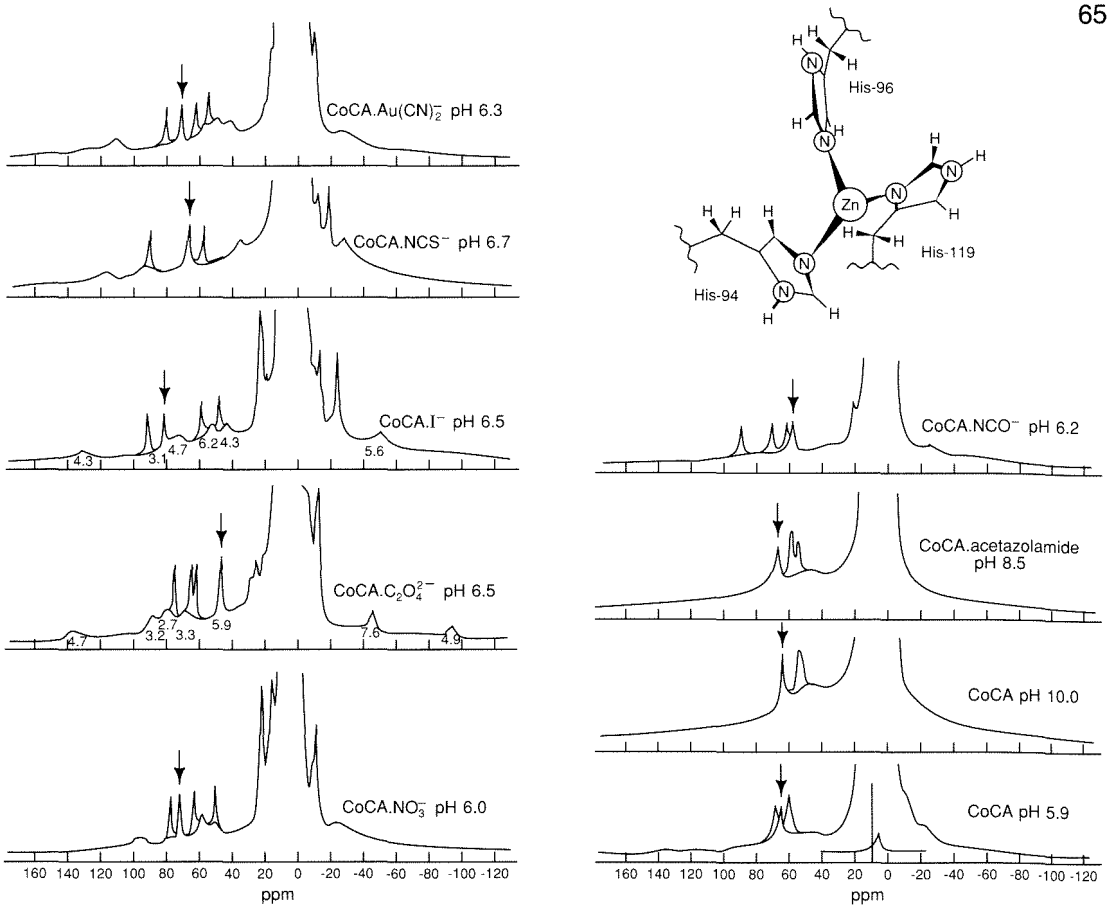

Figure 2.14
^{1}H NMR spectra of cobalt(II)-substituted bovine carbonic anhydrase II and some inhibitor derivatives. The three sharp downfield signals in each spectrum disappear in D_2O and are assigned to the exchangeable ring NH protons of the three coordinated histidines. The sharp signal labeled with an arrow is assigned to the Hδ2 proton of His-119, which is the only non-exchangeable ring proton in a meta-like rather than in an ortho-like position with respect to the coordinating nitrogen. The T_1 values (ms) of the signals for the I^- and $C_2O_4^{2-}$ derivatives are also shown.[25,75]

with respect to the molecular axes. These signals belong to protons of noncoordinated residues from 5 to 10 Å from the metal. Their assignment in principle provides further information on the structure in the vicinity of the metal ion. The ^{1}H NMR spectra of cobalt(II) enzymes thus afford a powerful method for monitoring structure and reactivity of the metal-bound residues. This is one task for future investigations of the enzyme.

4. pH dependence of inhibitor binding

The ease with which electronic spectra can be obtained provides a simple way of determining the affinity constants of inhibitors for the cobalt-substituted enzymes. An aliquot of enzyme is diluted in a spectrophotometric cell up to a

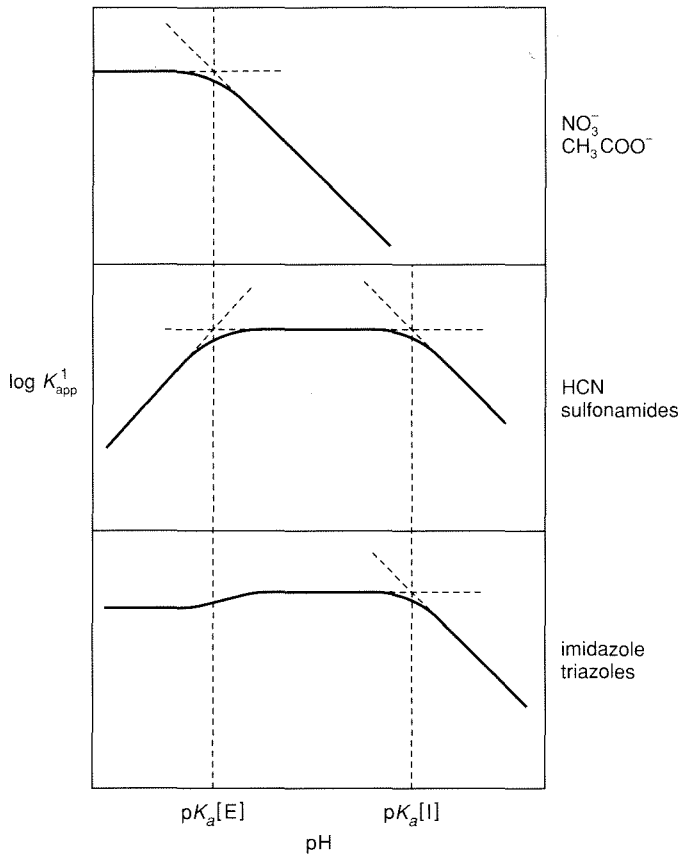

Figure 2.15
Types of pH dependences observed for the affinity constants of inhibitors for cobalt(II)-substituted carbonic anhydrases. pK_a[E] represents the main pK_a value of the enzyme, pK_a[I] that of the inhibitor, if present.[48]

fixed volume, and the spectrum is measured. Then the spectra are remeasured on samples containing the same amount of enzyme plus increasing amounts of inhibitor in the same cell volume. The pH is rigorously controlled. If solutions of enzyme and inhibitor have the same pH, the pH should be verified after the spectral measurements, in order to avoid contamination from the electrode salt medium. Both absolute values and pH dependences of affinity constants obtained from electronic spectra are the same as those obtained from inhibition measurements, where known, and are comparable to those obtained on the native enzyme.

Although affinity constant values reported in the literature were measured under different experimental conditions of, e.g., pH, buffer type, and buffer concentration, several pH-dependent trends are apparent. According to such dependences, three classes of inhibitors can be identified[48] (Figure 2.15). In the

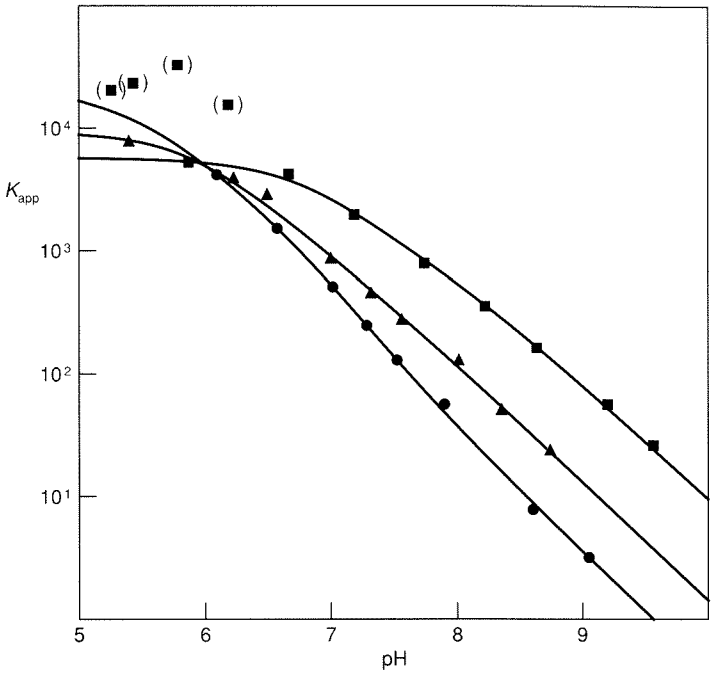

Figure 2.16
pH dependence of the apparent affinity constants of nitrate for human I (■), bovine II (▲), and human II (●) carbonic anhydrases. The curves are best-fit curves obtained assuming non-zero affinity of the anion for species 1 and 3 of Figure 2.9. The best-fit parameters are reported in Table 2.6. Points in parentheses for HCA I reflect possible binding of a second nitrate ion and have been excluded from the fit.[57]

first class, the affinity constant, expressed as log K, decreases linearly with increasing pH. Anions that are weak Lewis bases (Cl^-, N_3^-, CH_3COO^-, NO_3^-, etc.) behave in this manner, as do neutral ligands like CH_3OH and aniline. An example is shown in Figure 2.16. A qualitative fit to such curves can be obtained using a single pK_a. This behavior could be accounted for by assuming that the ligand binds only the low-pH form of the enzyme, in a simplified scheme in which only one pK_a value determines the species distribution in CA. We know, however, that the picture is more complex. If the species distribution calculated according to the scheme of Figure 2.9 is assumed to hold, and if it is assumed that only the two water-containing species (1) and (3) can be bound by the ligand, then actual affinity constants can be evaluated for both species (1) and (3)[57] (see Table 2.7). Such constants are similar for the three isoenzymes, whereas the apparent affinity constants at pH 7, for example, mainly depend on the pK_a's of the coordinated water according to the values of Table 2.5. Therefore, the low-activity species CA I has larger affinity for anions like nitrate (and bicarbonate) than do the high-activity forms at pH 7.

Table 2.7
Affinity constants of nitrate for species 1 and 3[a] of cobalt(II)-substituted carbonic anhydrases.[57]

	HCA I	BCA II	HCA II
$\log K_1$	3.74 ± 0.04	4.01 ± 0.02	4.34 ± 0.04
$\log K_3$	2.62 ± 0.06	2.56 ± 0.04	2.61 ± 0.05

[a] As defined in Figure 2.9.

A second type of behavior occurs for weak acids like HCN, H_2S, and aromatic sulfonamides ($ArSO_2NH_2$).[76,77] Assuming that the anions (conjugated bases) bind the low-pH species of the enzyme, the bell-shaped plot of log K versus pH (Figure 2.15) can be accounted for. In fact, at low pH, the inhibitors are in the protonated form, which is not suitable for metal binding. At high pH the concentration of the low-pH species of the enzyme decreases. The maximal apparent affinity is experimentally halfway between the pK_a of the inhibitor and the "pK_a" of the enzyme, treated as if it were only one. The same type of curve is also expected if the high-pH species of the enzyme binds the weak acid. Indeed, kinetic measurements seem to favor this hypothesis for sulfonamides.[78]

A third type of behavior obtains for inhibitors like imidazole and triazoles,

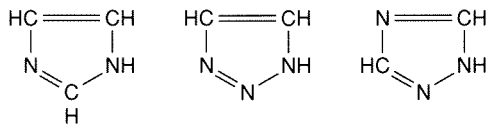

which bind the enzyme with similar affinities over a large range of pH (Figure 2.15),[79,80] because both the imidazolate anion and the neutral imidazole can bind to the aquo forms of the enzyme with essentially the same affinity,[48,80,81] and the reaction of imidazole with the Zn—OH species cannot be distinguished thermodynamically from the reaction of imidazolate with the aquo forms:

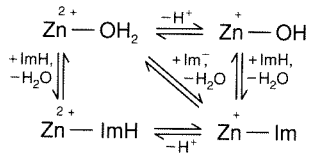

It is possible that the noncoordinated nitrogen can interact with a group in the protein via a hydrogen bond. A candidate could be the NH group of His-200 in HCA I or the hydroxyl group of Thr-200 in HCA II. Indeed, only imidazole and triazoles, which have two nitrogens in 1,3-positions, seem to have this ability.[213]

In summary, from cobalt substitution we have learned:

(1) the coordination geometry of the high- and low-pH forms by means of electronic spectroscopy;

(2) the values of the pK_a's from the pH dependence of the electronic spectra;

(3) the four and five coordination of the various derivatives with exogenous ligands;

(4) the affinity constants of exogenous ligands and their pH dependence;

(5) a fingerprint in the ^{1}H NMR spectra that can be used to monitor structural variations.

Most of these conclusions can be safely transferred to the native zinc enzyme, although minor differences can occur, for example, in the position of the equilibrium between four- and five-coordinate species.

D. What Do We Learn from Copper Substitution?

The coordination chemistry of CuCA is not yet fully understood, since the electronic spectra are not very pH-sensitive. Nevertheless, the affinity of anions is pH-dependent, as it is for CoCA.[82] As could be anticipated from Section III.B, the affinity of anions, including HCO_3^-, is higher than that of CoCA. Water is usually present in the coordination sphere, along with the anion, as checked by water ^{1}H NMRD.[83,84] The steric requirements of the three histidines and of the cavity allow the anion and the water molecule to arrange in an essentially square pyramidal geometry (Figure 2.17). This is consistent with the electronic and

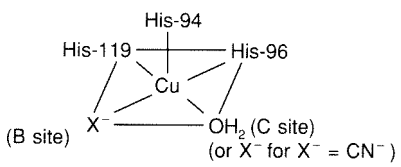

Figure 2.17
Schematic representation of the suggested coordination geometry for the anion adducts of CuCA.

EPR spectra. In particular, the EPR spectra are all axial, with g-values decreasing from 2.31 in the nonligated enzyme to 2.24 in the various anion adducts.[84] The water molecule would be in the C site or hydrophilic binding site, and the anion would be in the B site or hydrophobic pocket. His-94 would be in the apical position of the square pyramid. It has been shown by EPR spectroscopy that at low temperature two cyanide anions bind to copper. The donor atoms are two cyanide carbon and two histidine nitrogen atoms in the basal plane, and the third histidine nitrogen in the axial position.[85] The hyperfine splitting is observed only with nuclei in the basal plane. It is observed both with ^{13}C nuclei of ^{13}C-enriched CN^- and with the two ^{14}N of two histidines. The second cyanide may thus displace the coordinated water (Figure 2.17). Oxalate and sulfonamides displace water from the coordination sphere.[85,86] For the oxalate ion this may occur through bidentate behavior. Coordination to an oxygen of the sulfon-

amide cannot be ruled out, although the electronic and EPR spectra of the sulfonamide complex are more consistent with a pseudotetrahedral chromophore. The SO_2 moiety would in any case point toward the B binding site. It is likely that sulfonamides bind as in ZnCA. Bicarbonate also shows less water relaxivity than other monodentate anions.[83,84,86]

^{13}C NMR spectroscopy has been used to investigate the location of the two substrates, CO_2 and HCO_3^-, with respect to the metal ion in CuCA.[86–88] As was pointed out in Section IV.B, the interconversion between the two species is slow on the NMR timescale in the absence of catalysts. Therefore, two signals are observed (Figures 2.6 and 2.18). In the presence of the catalytically active CoCA, only one signal is observed at suitable enzyme concentrations, and individual information on CO_2 binding cannot be obtained.[89,90] In the presence of inactive CuCA, two signals are again observed, which are broadened to different extents.

For the HCO_3^- signal the T_2^{-1} values as estimated from the linewidth are much larger than T_1^{-1}. Since the equation for T_2^{-1}, analogous to Equation (2.14), would predict similar T_1 and T_2 values,[69,72] a sizeable broadening due to chemical exchange must be present. Indeed, unlike T_{1p}^{-1} (Equation 2.11), T_{2p}^{-1} may be a complicated function of the exchange time τ_M and of the isotropic shift, $\Delta\omega_M$,

$$T_{2p}^{-1} = \frac{f_M}{\tau_M} \frac{T_{2M}^{-2} + T_{2M}^{-1}\tau_M^{-1} + (\Delta\omega_M)^2}{(T_{2M}^{-1} + \tau_M^{-1})^2 + (\Delta\omega_M)^2}. \tag{2.15}$$

In the slow-exchange region, i.e., when two separate signals are observed and the broadening is due to exchange, $T_{2p}^{-1} = f_M\tau_M^{-1}$. This region is characterized

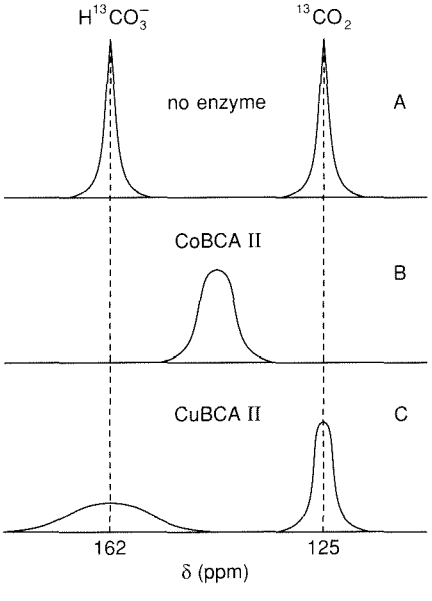

Figure 2.18
Schematic representation of the ^{13}C NMR spectra of the CO_2/HCO_3^- system (A) in pure water, (B) in the presence of CoCA, and (C) in the presence of CuCA.[56]

by a marked increase in linewidth with increasing temperature, as confirmed by measurements at 4 and 25°C. Therefore, T_{2p} gives a direct measure of τ_M.[56] The ^{13}C T_1^{-1} values of HCO_3^- are consistent with bicarbonate bound to the metal. The Cu—C distance would be 2.5 Å if the unpaired electron were completely on the copper ion, as estimated by using Equation (2.1) and a value of $\tau_c = 2.1 \times 10^{-9}$ s independently obtained from water ^1H NMRD.[83] This distance is much too short for a coordinated bicarbonate; however, electron delocalization on the bicarbonate ligand may account for such a short calculated distance; the possibility of a bidentate type of ligation cannot be discarded. The dissociation rate, which is very low, by itself accounts for the lack of activity of the derivative.

For CO_2, a carbon-copper distance could be calculated if the affinity constants of the substrate for the protein were known. When the binding site, if any, starts being saturated, fast exchange with excess ligand (in this case, CO_2) decreases the observed paramagnetic effect. From this behavior, the affinity constant may be estimated. For CO_2 the paramagnetic effect remained constant up to 1 M CO_2; i.e., the affinity constant is smaller than 1 M^{-1}. This means that practically there is no affinity for copper; yet the paramagnetic effect is paradoxically high.[88]

Another picture comes by analyzing the NMR data in terms of a pure diffusive model.[88] Here Hubbard's equation[91] has been used:

$$T_{2p}^{-1} = N_M \left(\frac{\mu_0}{4\pi}\right)^2 \frac{8\pi}{225} \frac{\gamma_I^2 n_c^2 \mu_B^2 S(S+1)}{d(D_N + D_M)} \left(13f(\omega_S, \tau_D) + 3f(\omega_S, \tau_D)\right), \quad (2.16)$$

where

$$f(\omega, \tau_D) = \frac{15}{2} I(u);$$

$$u = [\omega\tau_D]^{1/2};$$

$$I(u) = u^{-5}\{u^2 - 2 + e^{-u}[(u^2 - 2)\sin u + (u^2 + 4u + 2)\cos u]\};$$

d is the distance of closest approach, D_N and D_M are the diffusion coefficients of the molecules containing the nucleus under investigation, and $\tau_D = 2d^2/(D_N + D_M)$. The experimental paramagnetic effect can be reproduced with a CO_2 concentration inside the cavity much larger than the one in the bulk solution. This result indicates that substrate does not bind to a specific site, but probably binds in the hydrophobic region. Note that CO_2 is more soluble in organic solvents than in water.

The effect of the cavity is to attract CO_2 by interaction either with the metal ion or with a hydrophobic part of the cavity itself. But the affinity constant is in any case lower than expected from the Michaelis constant (see Section IV.B) measured under steady-state conditions, indicating that the latter does not represent the dissociation constant of the enzyme-CO_2 system.

In summary, the main information concerning the catalytic cycle obtained from the copper derivative is the structural and kinetic characterization of both

CO_2 and HCO_3^- species when they are not interconverting but present within the cavity. In this way we have further proof that HCO_3^- is bound to the metal and that CO_2 is attracted inside the cavity either by hydrophobic interactions or by the metal ion or both. The data obtained on the geometry around copper are consistent with those obtained on cobalt.

E. What Do We Learn from Manganese and Cadmium Substitution?

Several studies have been performed on MnCA. Although CA is not the protein for which Mn(II) has been most extensively used as a paramagnetic probe to map substrates and inhibitors within the metal cavity, by measuring the T_{2M}^{-1} values of protons of the inhibitor N-acetyl-sulfanilamide, and by assuming that dipolar contributions are dominant, researchers have mapped the orientation of the inhibitor inside the active cavity (Figure 2.19).[92] This orientation is consistent with x-ray data on stronger binding sulfonamides.[64–66] MnCA is not completely inactive. ^{13}C NMR studies of the $CO_2 \rightleftharpoons HCO_3^-$ interconversion at pH 8.5 showed that the interconversion rate is about 4 percent that of the native enzyme.[93] The T_1^{-1} and T_2^{-1} values of $H^{13}CO_3^-$ suggest that bicarbonate might be bidentate in the central step of the catalytic cycle.[93]

Data from ^{113}Cd studies that have been performed on CdBCA II and CdHCA I are consistent with the general picture presented here.[94] The ^{113}Cd chemical shifts are indeed consistent with a donor set of three nitrogens and two oxygens. The cadmium(II) derivative could thus be five-coordinate with two water mole-

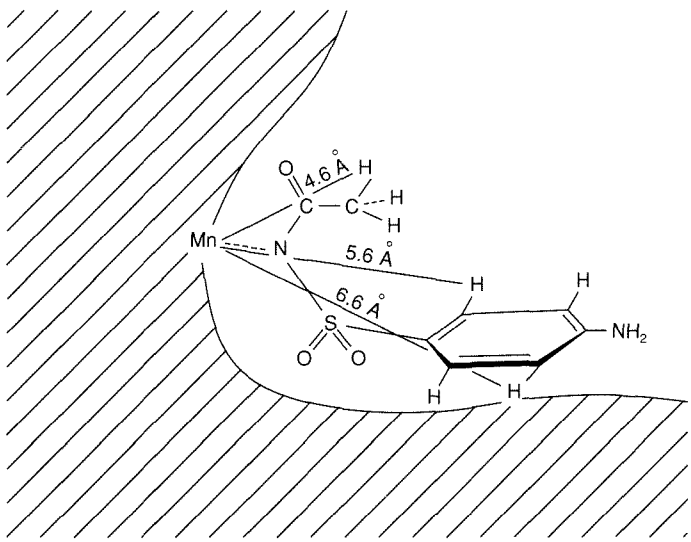

Figure 2.19
Schematic drawing of the geometric arrangement of the inhibitor N-acetyl-sulfanilamide in the active cavity of manganese(II)-substituted CA, as revealed by ^1H NMR spectroscopy.[92]

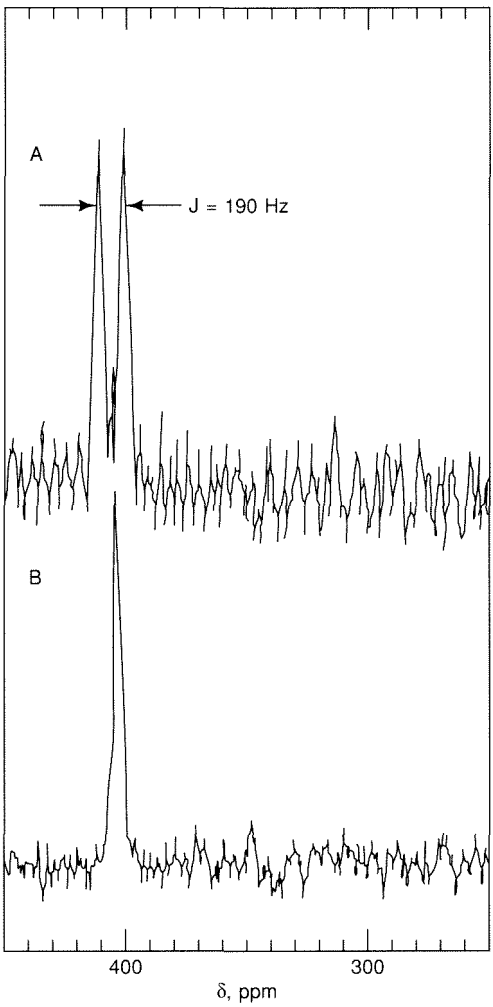

Figure 2.20
^{113}Cd NMR spectra of Cd-substituted bovine carbonic anhydrase II in the presence of ^{15}N-enriched (A) or ^{14}N-enriched (B) benzenesulfonamide inhibitor.[95]

cules, in agreement with the expectation based on its ionic radius being larger than that of zinc(II). The ^{113}Cd signal of CdBCA II in the presence of benzenesulfonamide enriched in ^{15}N is split into a doublet because of the nitrogen-cadmium coupling (Figure 2.20).[95] This result provides direct evidence for metal-nitrogen bonding in sulfonamides, which has been confirmed by x-ray data.[65]

F. Catalytic Mechanism

All the above structural and kinetic information obtained under a variety of conditions with different metal ions can be used to propose a catalytic cycle for carbonic anhydrase (Figure 2.21). As shown by studies on the pH-dependent properties of native and metal-substituted CAs, both type-I and type-II proteins have two acidic groups, the zinc-coordinated water and a free histidine. At

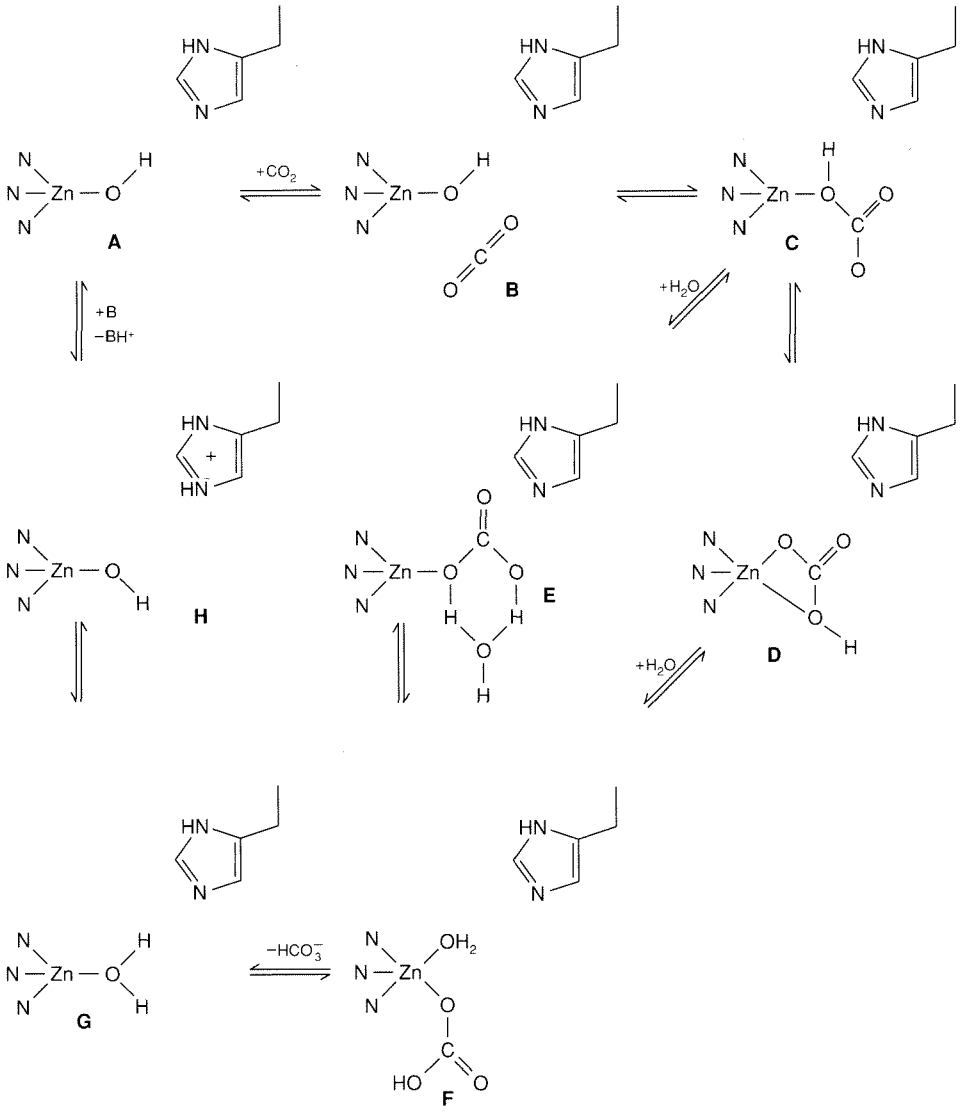

Figure 2.21
Proposed catalytic cycle of CA.

physiological pH the enzyme is essentially in the Zn—OH form (step A in Figure 2.21). A Zn—OH moiety is a relatively good nucleophile, poised for nucleophilic attack on carbon dioxide. It is possible that the hydrogen bond with Thr-199, which seems to be consistent with an sp^3 oxygen, orients the OH for attack at the substrate CO_2. Studies of the copper derivative indicated that the concentration of CO_2 in the cavity is higher than in bulk solution (step B).

Molecular dynamics calculations have shown that there are either three[96] or two[97] potential wells for CO_2 in the hydrophobic pocket. It was shown[98] that when Val-143 is replaced by the much larger Phe, the activity decreases by a factor of 10^3. Apparently the large Phe residue does not leave space within the cavity to accomodate CO_2.

It would also be nice if the enzyme were able to activate CO_2. There is no evidence that it does, even though the positive charge around zinc and the NH of Thr-199 would represent two electrostatic attraction points that could activate CO_2. It is well-known that CO_2's interactions with positive charges activate the carbon for nucleophilic attack.[99,100] The positioning of CO_2 between zinc and the peptide NH of Thr-199 would be ideal for the OH attack. Merz[97] locates it as shown in Figure 2.22.

It was believed that, once bicarbonate is formed (C), the proton has to transfer to a terminal oxygen atom, either via an intermediate in which bicarbonate is bidentate (D) or via a hydrogen-bond network (E). Indeed, in model compounds one would expect HCO_3^- to bind through a nonprotonated oxygen. However, the possibility of restoring the hydrogen bond with Thr-199 as in sulfonamide adducts could justify the presence of the hydrogen on the coordinating oxygen.[214] The bicarbonate derivative is presumably in equilibrium between four- and five-coordinate species (F), as shown by the electronic spectra of the cobalt derivative.[59] The five-coordinate species provides a low barrier for the substrate detachment step via an associative mechanism involving coordination of a water molecule (G). A possible five-coordinate species would contain bicarbonate in the B site and water in the C site (Figure 2.12). It is reasonable that the measured K_m for the reaction of bicarbonate dehydration is the thermodynamic dissociation constant of the M—HCO_3^- species. Anionic or neutral

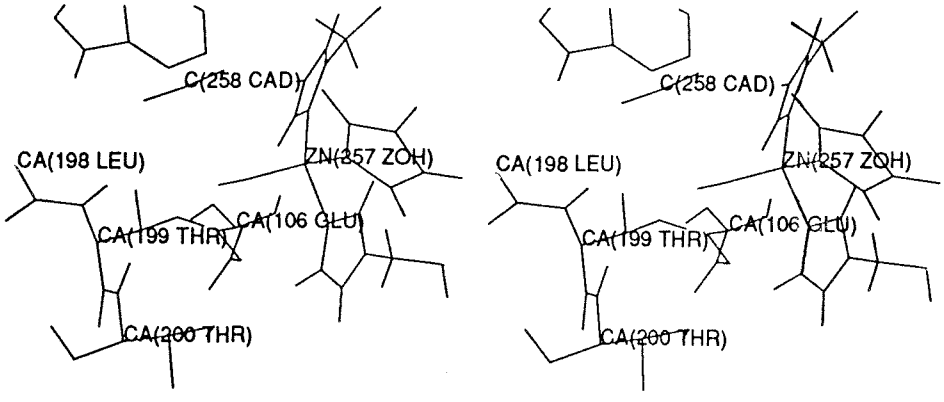

Figure 2.22
Stereo view of the site of activation of CO_2 in the cavity of CA as proposed by Merz.[97]

inhibitors are competitive with bicarbonate because they tend to bind at the same site. At this stage the second substrate, which is H^+, has to be released (H). It is reasonable that the water proton transfers to a group inside the cavity, e.g., the free histidine mentioned above, and subsequently to the solvent. In the absence of buffers the latter step is rate-limiting for the high-activity isoenzymes, since the diffusion rate cannot exceed the product of the concentration times the diffusion coefficient, i.e., 10^{-7} M $\times$ 10^{11} M^{-1} s^{-1}. Such a limit is then 10^4 s^{-1}, whereas the turnover rate is 10^6 s^{-1}. The presence of buffer can assist in proton transfer at this stage, in such a way that the rate-limiting step becomes the internal proton transfer. The release of H^+ from the Zn—OH_2 moiety is also the rate-limiting step for the low-activity CA III, as nicely shown by the electronic spectra of CoCA III. These spectra change from the basic form at the beginning of the reaction to the acidic form upon CO_2 addition (Figure 2.23).[101] After the interconversion of CO_2 into bicarbonate, there is an accumulation of the $CoOH_2$ species, the deprotonation of which is slower than the release of HCO_3^-.

G. Model Chemistry

Some efforts have been reported in the literature to simulate the activity of CA and therefore to obtain further information on the mechanism. The pK_a of Zn—OH_2 moieties in various complexes has been studied as discussed in Sec-

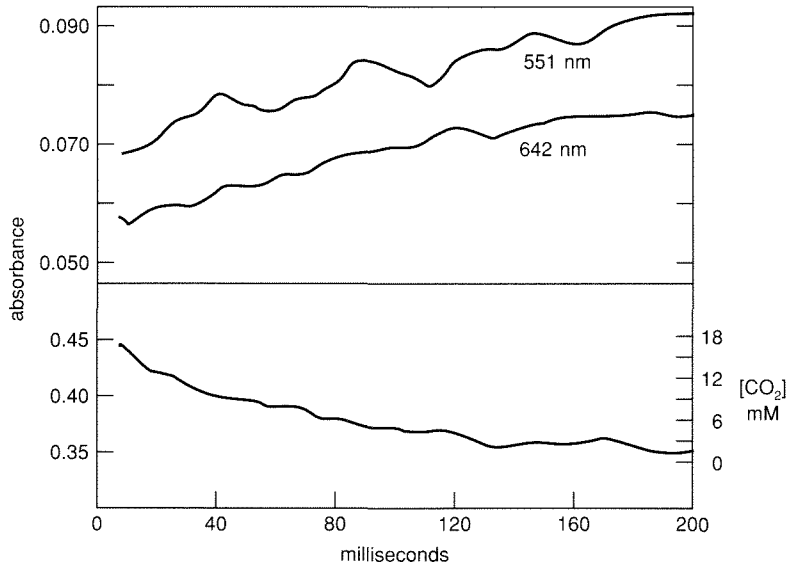

Figure 2.23
Time dependence of $\epsilon_{15.6}$ and $\epsilon_{18.1}$ of cobalt(II)-substituted CA III after addition of CO_2 to a buffered enzyme solution at pH 8. The initial drop of absorbance reflects the accumulation of a $CoOH_2$ intermediate.[101]

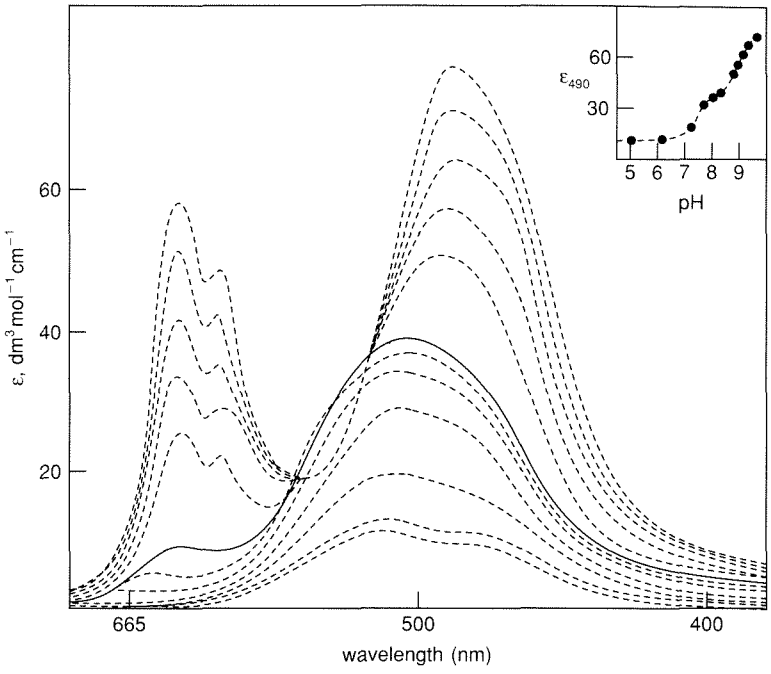

Figure 2.24
Electronic spectra of $Co(TPyMA)OH_2^{2+}$ (Table 2.3) at various pH values.[10] Note the similarity to the electronic spectra of cobalt-substituted carbonic anhydrase at various pH values as reported in Figure 2.7.[56]

tion III.A. The electronic spectra of some cobalt analogues have been found to be similar. One such example is shown in Figure 2.24; the complex $Co(TPyMA)OH_2^{2+}$ (Table 2.3)[10] provides a five-coordinate adduct with a weakly bound axial nitrogen (Figure 2.25A).

The interconversion between $Co(TPyMA)OH_2^{2+}$ and $Co(TPyMA)OH^{+}$ was studied by electronic spectroscopy (Figure 2.24). Despite the difference in the number of coordinated nitrogens, the difference between the high- and low-pH forms resembles that of the cobalt enzyme (cf. Figure 2.7).[10]

Table 2.3 shows that only one compound, with zinc(II) as the metal ion, seems to have three nitrogens and a water, whereas all the other models have a higher coordination number.[15–17] The simple $[Co^{III}(NH_3)_5OH]^{2+}$ complex has been shown to accelerate the formation of bicarbonate ($k = 2 \times 10^2\ M^{-1}\ s^{-1}$), but, of course, bicarbonate remains coordinated to the metal because of the kinetic inertness of cobalt(III).[102,103] Some relatively ill-defined systems have been reported to have some kind of activity. The ligand shown in Figure 2.25B, with zinc(II) as the metal ion in H_2O, accelerates the attainment of the equilibrium[104]

$$CO_2 + H_2O \underset{k_{-1}}{\overset{k_1}{\rightleftharpoons}} HCO_3^- + H^+ \qquad (2.17)$$

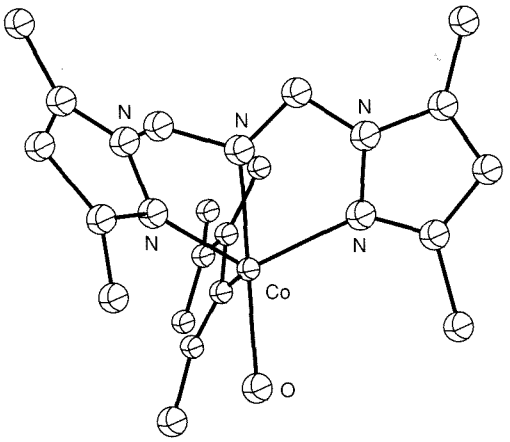

(A)

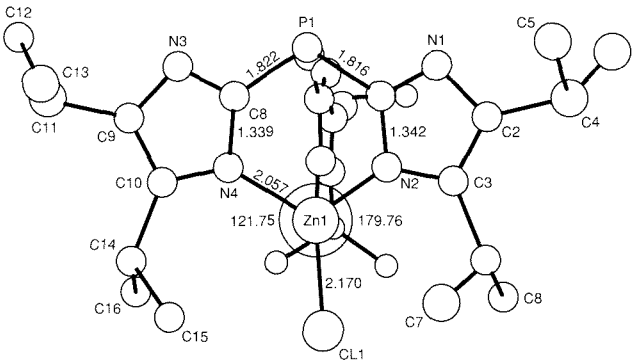

(B)

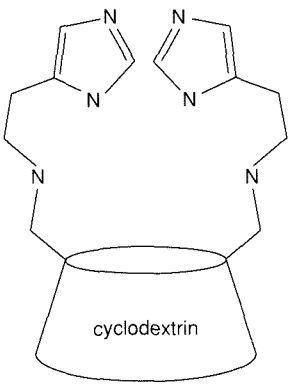

(C)

Figure 2.25
Some multidentate ligands as models of CA: (A) tris-(3,5-dimethyl-l-pyrazolylmethyl) amine[4] (cobalt[II] complex); (B) tris (4,5-diisopropylimidozal-2yl)phosphine[104] (zinc[II] complex); (C) bis(histamino) β-cyclodextrin.

with $k_{obs} = k_1 + k_{-1} \simeq 10^3\ M^{-1}\ s^{-1}$. The system in Figure 2.25C, with Zn^{2+} and excess imidazole, promotes CO_2 hydration, though not the back reaction.[105] The cobalt(II) analogue shows no activity.[106]

It can be concluded that the M—OH group can indeed be involved in one step of the enzymatic pathway. The sophistication of the whole enzymatic function has not yet been fully achieved with the present generation of models, even though the functionalization of both hydrophilic and hydrophobic molecules like cyclodextrins (Figure 2.25C) has also been used.[105]

V. OTHER ENZYMATIC MECHANISMS AND MODEL CHEMISTRY

A. Peptide Hydrolysis

At neutral pH the uncatalyzed hydrolysis of amides or peptides

$$R—CO—NH—R' + H_2O \rightleftharpoons R—COO^- + R'—NH_3^+ \qquad (2.18)$$

is a slow process, with rate constants as low as 10^{-11} s^{-1}. Peptide hydrolysis catalyzed by carboxypeptidase or thermolysin can attain k_{cat} values of 10^4 s^{-1}. Organic chemistry teaches us that amide hydrolysis is relatively efficiently catalyzed by acids and bases. The general mechanisms involve protonation of the carbonyl oxygen (or amide nitrogen), and addition of OH^- (or of a general nucleophile) to the carbonyl carbon atom. Several organic and inorganic bases have been found to be reasonably efficient catalysts. On the other hand, transition metal aquo-ions or small metal-ion complexes also display catalytic efficiency (Table 2.8).[107–114] A metal ion is a Lewis acid, capable of effectively polarizing the carbonyl bond by metal-oxygen coordination. Furthermore, the metal ion can coordinate a hydroxide group in such a way that there is a high OH^- concentration at neutral or slightly alkaline pH. It is thus conceivable that a metalloenzyme may combine some or all of these features and provide a very efficient catalyst.

Much experimental work has been done on mimicking ester and especially peptide hydrolysis with model coordination compounds. Most of the work car-

Table 2.8
Rate constants for amide and ester hydrolysis catalyzed by acids, bases, or metal ions.

Compound	Catalyst and conditions	Rate constant	Reference
Glycine amide	pH 9.35	1.9×10^{-5} s^{-1}	107
	Cu^{2+}, pH 9.35	2.6×10^{-3} M^{-1} s^{-1}	107
$[Co(en)_2(glycine\ amide)]^{3+}$	pH 9.0[a]	2.6×10^{-4} s^{-1}	108
D,L-phenylalanine ethylester	pH 7.3	5.8×10^{-9} s^{-1}	109
	Cu^{2+}, pH 7.3	3.4×10^{-2} M^{-1} s^{-1}	109
$(tn)_2O_3PO—C_6H_4NO_2$	OH^-	5.1 M^{-1} s^{-1}	110
$Co^{III}—(tn)_2O_3PO—C_6H_4NO_2$	—[a]	7×10^{-5} s^{-1}	110
Ethyl-β-phenylpropionate	H^+	5×10^{-3} M^{-1} s^{-1}	111
	OH^-	1.3×10^{-6} M^{-1} s^{-1}	111
Adenosine triphosphate	pH 5.3	5.6×10^{-6} s^{-1}	112
	Cu^{2+}, pH 5.3	1.1×10^{-2} M^{-1} s^{-1}	112
Glycine methylester	Co^{2+}(1:1), pH 7.9	1.6×10^{-2} s^{-1}	113
	Cu^{2+}(1:1), pH 7.3	4.2×10^{-2} s^{-1}	113
Glycine propylester	Co^{3+}(1:1), pH 0	1.1×10^{-3} s^{-1}	114
	Co^{3+}(1:1), pH 8.5	$>1 \times 10^{-2}$ s^{-1}	114

[a] autohydrolysis.

ried out has involved[108,110,115,116] cobalt(III). Although such an ion may not be the best conceivable model for zinc-promoted hydrolytic reactions (see Section IV.G), it has the great advantage of being substitutionally inert, thus removing mechanistic ambiguities due to equilibration among isomeric structures in the course of the reaction. Interesting amide hydrolysis reactions also have been described using complexes with other metal ions, such as copper(II)[117] and zinc(II)[118] itself. In recent years efforts have focused on the construction of bifunctional catalysts to better mimic or test the enzymatic function. For instance, phenolic and carboxylic groups can be placed within reach of Co(III)-chelated amides in peptidase models.[116] The presence of the phenolic group clearly accelerates amide hydrolysis, but carboxyl groups are ineffective. This model chemistry is too simple to provide insights into the actual enzymatic mechanism, which must start with recognizing the substrate through several steps, orienting it, activating it, performing the reaction, and finally releasing the products. See the more specialized reviews dealing with nonenzymatic reactivity.[119–121]

From basic knowledge of the chemistry of hydrolytic reactions, the x-ray structures of carboxypeptidase A and a variety of its derivatives with inhibitors as substrate analogues, product analogues, and transition-state analogues have revealed several features of the active site that are potentially relevant for the catalytic mechanism (Figures 2.26–2.28 *See color plate section, pages C4, C5.*).[122] The metal ion is coordinated to two histidine residues (His-69 and His-196), to a glutamate residue that acts as a bidentate ligand (Glu-72), and to a water molecule. The metal is thus solvent-accessible and, as such, can activate the deprotonation of a water molecule to form a hydroxide ion, or polarize the carbonyl oxygen of the substrate by coordinating it in the place of the solvent

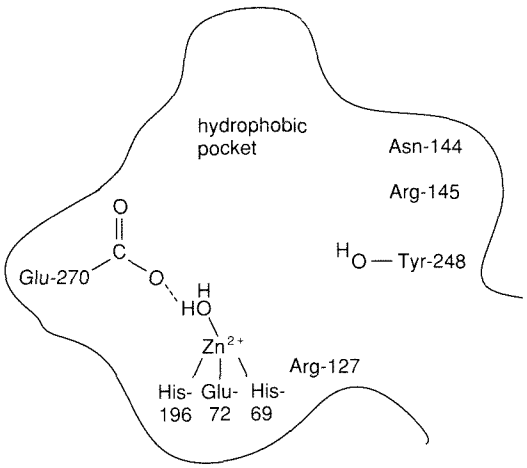

Figure 2.26
Schematic drawing of the active-site cavity of carboxypeptidase A.[122] Only the residues believed to play a role in the catalytic mechanism are shown.

molecule, or both, if some flexibility of the coordination sphere is allowed. Another glutamic-acid residue (Glu-270) is in close proximity to the metal center. If the role of the metal were mainly to polarize the carbonyl carbon, Glu-270 in its deprotonated form could be positioned to perform a nucleophilic attack on the carbonyl carbon, yielding an anhydride intermediate. Alternatively, the metal could mainly serve to provide a coordinated hydroxide ion that, in turn, could attack the carbonyl carbon; here Glu-270 would help form ZnOH by transferring the proton to the carboxylate group:

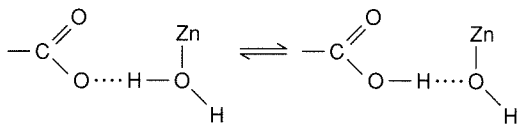

On the opposite side of the cavity is a tyrosine residue that has been shown to be quite mobile and therefore able to approach the site where the catalytic events occur. The cavity has a hydrophobic pocket that can accommodate the residue, R, of nonpolar C-terminal amino acids of the peptide undergoing hydrolysis (Figures 2.26 and 2.28), thereby accounting for the higher efficiency with which hydrophobic C-terminal peptides are cleaved. Finally, an Asn and three Arg residues are distributed in the peptide-binding domain; Asn-144 and Arg-145 can interact via hydrogen bonds with the terminal carboxyl group. Arg-127 can hydrogen-bond the carbonyl oxygen of the substrate.

All these features have enabled detailed interpretation of many chemical and physico-chemical data at the molecular level. The essential data are as follows:

(1) *Metal substitution.* Table 2.9 lists the divalent metals that have been substituted for zinc(II) in CPA, together with their relative peptidase (and esterase) activities.[22] For some of them, the available x-ray data

Table 2.9
Catalytic activities of metal-substituted carboxypeptidases.[a 22]

	Peptidase	Esterase
Apo	0	0
Cobalt	200	110
Nickel	50	40
Manganese	30	160
Cadmium	5	140
Mercury	0	90
Rhodium	0	70
Lead	0	60
Copper	—[b]	—[b]

[a] Activities are relative to the native enzyme, taken as 100%.

[b] Some activity toward both peptides and esters has recently been observed.[22]

show[123] that the active-site structure is essentially maintained. Even the copper derivative is slightly active. The apoenzyme is completely inactive, however.

(2) *Active-site modifications.* Chemical modification and site-directed mutagenesis experiments suggest that Glu-270 is essential for catalysis.[124,125] Tyr-248,[126] Tyr-198,[127] and one or more of the arginines[124] are involved but not essential.

(3) *Kinetics.* k_{cat}/K_m pH profiles are bell-shaped, characterized by an acid pK_a limb around 6 and an alkaline pK_a limb around 9: k_{cat} increases with the pK_a of 6 and then levels off, and K_m increases with a pK_a of 9. Several lines of evidence suggest that the $pK_a \approx 6$ corresponds to the ionization of the Glu-270-coordinated H_2O moiety:

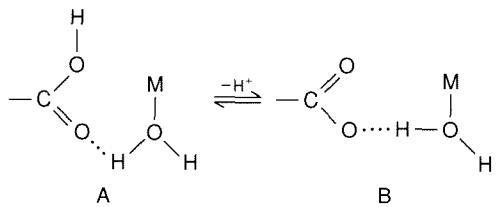

(2.19)

Site-directed mutagenesis has ruled out Tyr-248 as the group with the pK_a of 9 in the rat enzyme.[125,126] Unfortunately, in this enzyme the pK_a of 9 is observed in k_{cat} rather than K_m; so the situation for the most-studied bovine enzyme is still unclear. Tyr-248 favors substrate binding three to five times more than the mutagenized Phe-248 derivative.[126] The three possible candidates for this pK_a are the coordinated water, Tyr-248, and the metal-coordinated His-196, whose ring NH is not hydrogen-bonded to any protein residue.[128] The x-ray data at different pH values show a shortening of the Zn—O bond upon increasing pH.[129] This favors the ZnOH hypothesis.

(4) *Anion binding.* The metal binds anionic ligands only below pH 6, i.e., when Glu-270 is protonated, when Glu-270 is chemically[130] or genetically[125] modified, or when aromatic amino acids or related molecules are bound in the C-terminal binding domain (Arg-145 + hydrophobic pocket).[131–134]

(5) *Intermediates.* An anhydride intermediate involving Glu-270 for a slowly hydrolyzed substrate may have been identified.[135] Some other intermediates have been observed spectroscopically at subzero temperatures with the cobalt(II) derivative.[22,136] Peptides bind in a fast step without altering the spectroscopic properties of cobalt(II), following which a metal adduct forms and accumulates.[22] Thus, if an anhydride intermediate is formed, it is further along the catalytic path.

On the basis of these data, and many related experiments, a detailed mechanism can be formulated (Figure 2.29). The incoming peptide interacts with

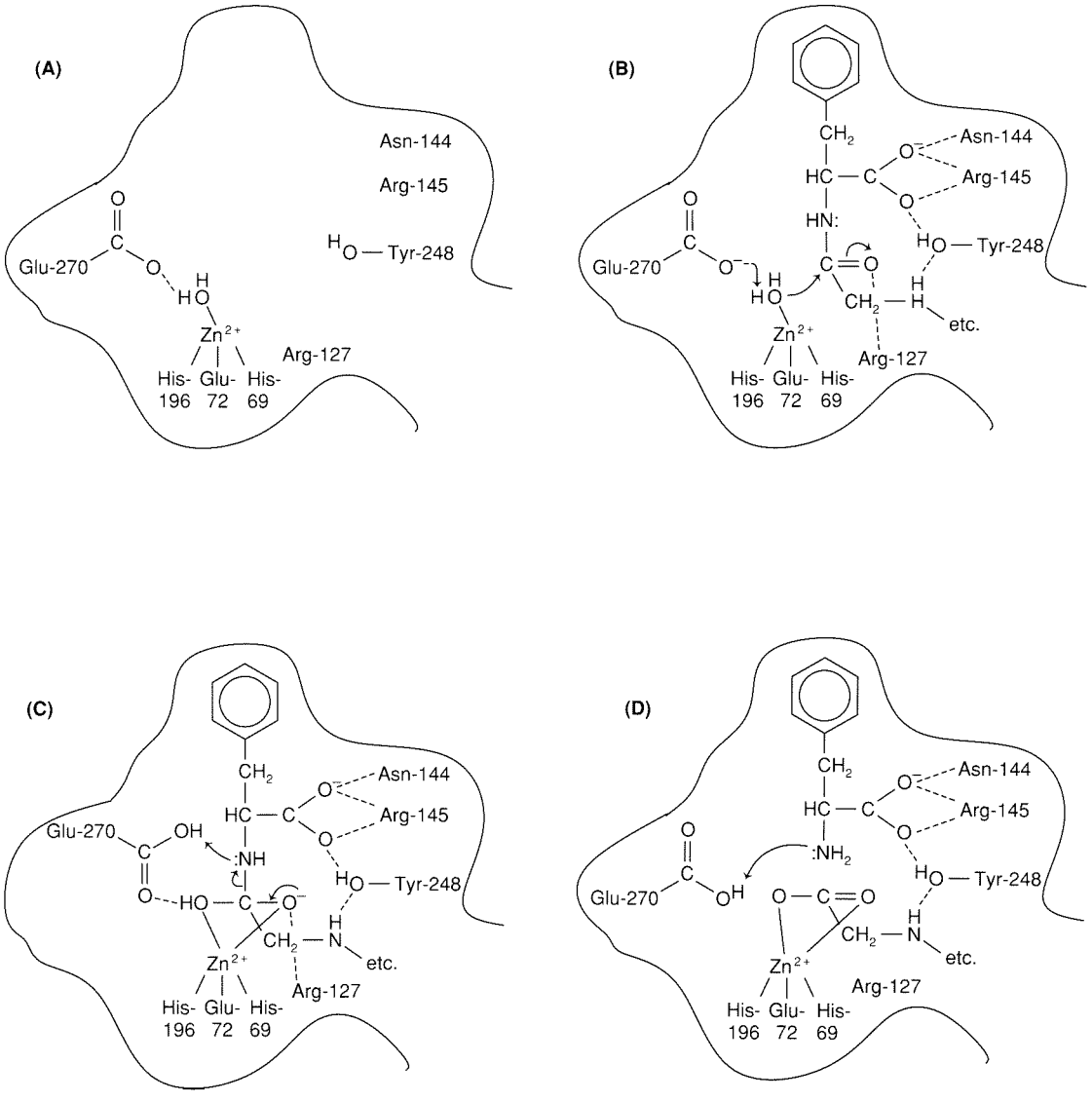

Figure 2.29
Possible catalytic cycle of CPA.

arginine residues through its terminal carboxylate group. The interaction could initially involve Arg-71 (not shown); then the peptide would smoothly slide to its final docking position at Arg-145, while the R residue, if hydrophobic, moves to the hydrophobic pocket (Figure 2.29B). The carbonyl oxygen forms a strong hydrogen bond with Arg-127. Additional stabilization could come from hydrogen bonding of Tyr-248 to the penultimate peptide NH. This adduct might be the first intermediate suggested by cryospectroscopy[22,136] (Figure 2.24).

At this point the metal-bound hydroxide, whose formation is assisted by Glu-270, could perform a nucleophilic attack on the carbonyl carbon activated by Arg-127 and possibly, but not necessarily, by a further electrostatic interaction of the carbonyl oxygen with the metal ion. The structure of the substrate analogue α-R-β-phenylpropionate shows that the carbonyl binds in a bidentate fashion:

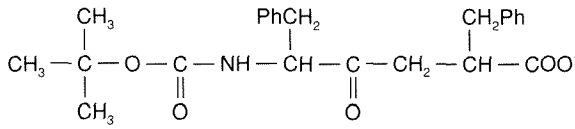

(Figure 2.30).[137] Five coordination is maintained by switching the Glu-72 metal

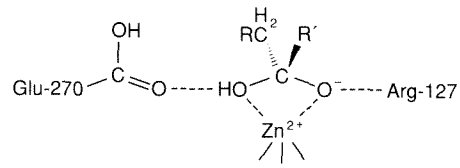

Figure 2.30
Binding mode of α-R-β-phenylpropionate to the zinc(II) ion in CPA.[137]

ligand from bidentate to monodentate, because the metal moves toward Arg-127. It is likely that this situation mimics an intermediate of the catalytic cycle. The resulting adduct might be the second spectroscopic intermediate (Figure 2.29C).

The system then evolves toward breaking of the C—N bond, caused by addition of a proton to the amino nitrogen. This proton could come from Glu-270, which thereby returns to the ionized state. The breaking of the peptide bond could be the rate-limiting step.[22] The second proton required to transform the amino nitrogen into an NH_3^+ group could come from the coordinated carboxylic group of the substrate, which now bears one excess proton, again through Glu-270 (Figure 2.29D). The system shown in Figure 2.29D can, in fact, be seen as a ternary complex with a carboxylate ligand and an amino-acid zwitterion, bound synergistically.[131–134] Finally, the metal moves back to regain a bidentate Glu-72 ligand, and the cleaved peptide leaves, while a further water molecule adds to the metal ion and shares its proton with the free carboxylate group of Glu-270.

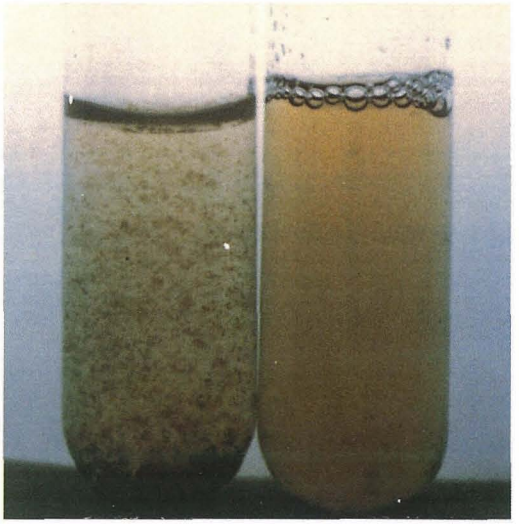

Figure 1.1
The stabilization of Fe in aqueous solution by the protein coat of ferritin. In the absence of protein, at neutral pH, in air, flocculent precipitates of ferric hydrous oxide form. The equivalent concentration of Fe(III) in the solution of ferritin is about 10^{14} times greater than in the inorganic solution. *Left*: a solution of Fe(II)SO_4, pH 7, in air after 15 min. *Right*: the same solution in the presence of apoferritin, the protein coat of ferritin (reprinted from Reference 6).

A

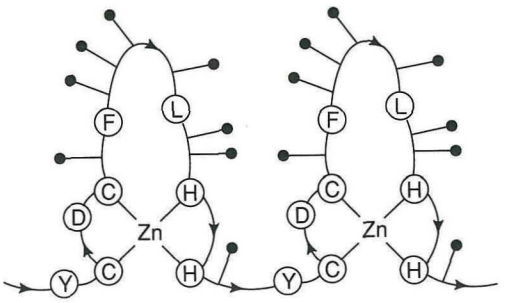

B

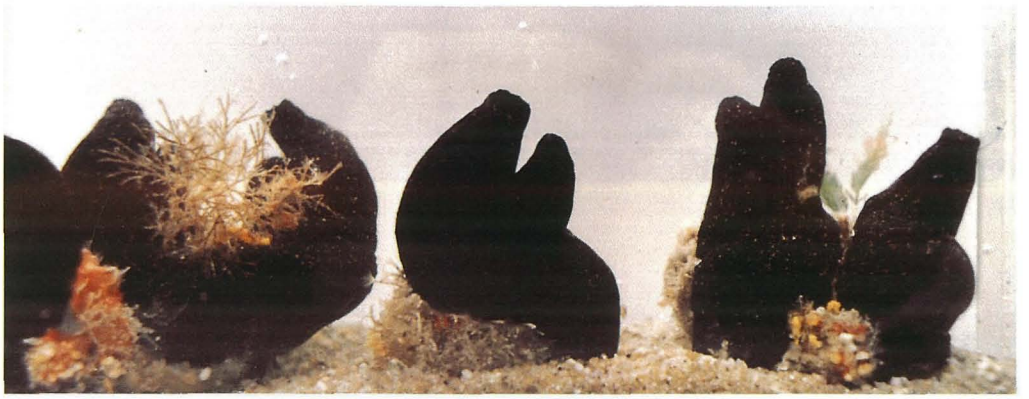

Figure 1.2
(A) Zinc-binding domains of a DNA-binding protein from frog eggs. Two of the nine repeating units of polypeptide with Zn-binding ligands are displayed, with two of the 7–11 zinc atoms per molecule in the configuration originally proposed by Klug and coworkers for "zinc fingers." The protein studied regulates the transcription of DNA to RNA and also binds to RNA, forming a storage particle.[9] Recently, the putative zinc-binding sequence has been shown to occur in many nucleic acid-binding proteins.[10] Each finger binds to a site on the double helix. However, other zinc-finger proteins function with fewer fingers, related apparently to the structure of the nucleic acid site. (B) Examples of the sea squirt (tunicate) *Ascidia nigra* (reproduced with permission from Reference 18a).

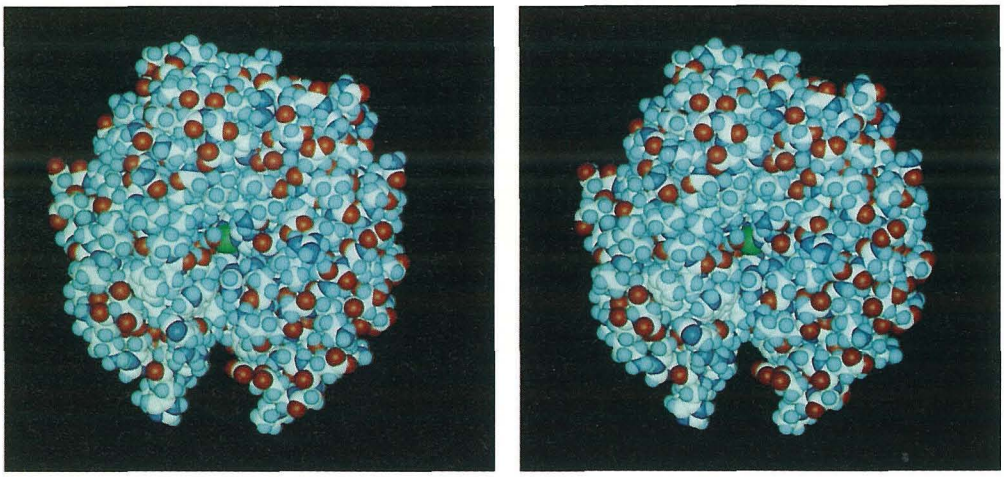

Figure 2.3
Human carbonic anhydrase II viewed as a CPK model. The zinc ion is the green sphere at the bottom of the active site. The color codes for the other atoms are: C = white, H = cyan, N = blue, O = red, S = yellow. Among the zinc ligands, the His-94 ring and the water molecule are clearly visible at the right- and left-hand side of the zinc ion, respectively. The presence of a hydrophobic region above the zinc ion can also be discerned. The crevice that runs longitudinally below the active site is obstructed by the histidine ring of His-64, one of the invariant active-site residues.

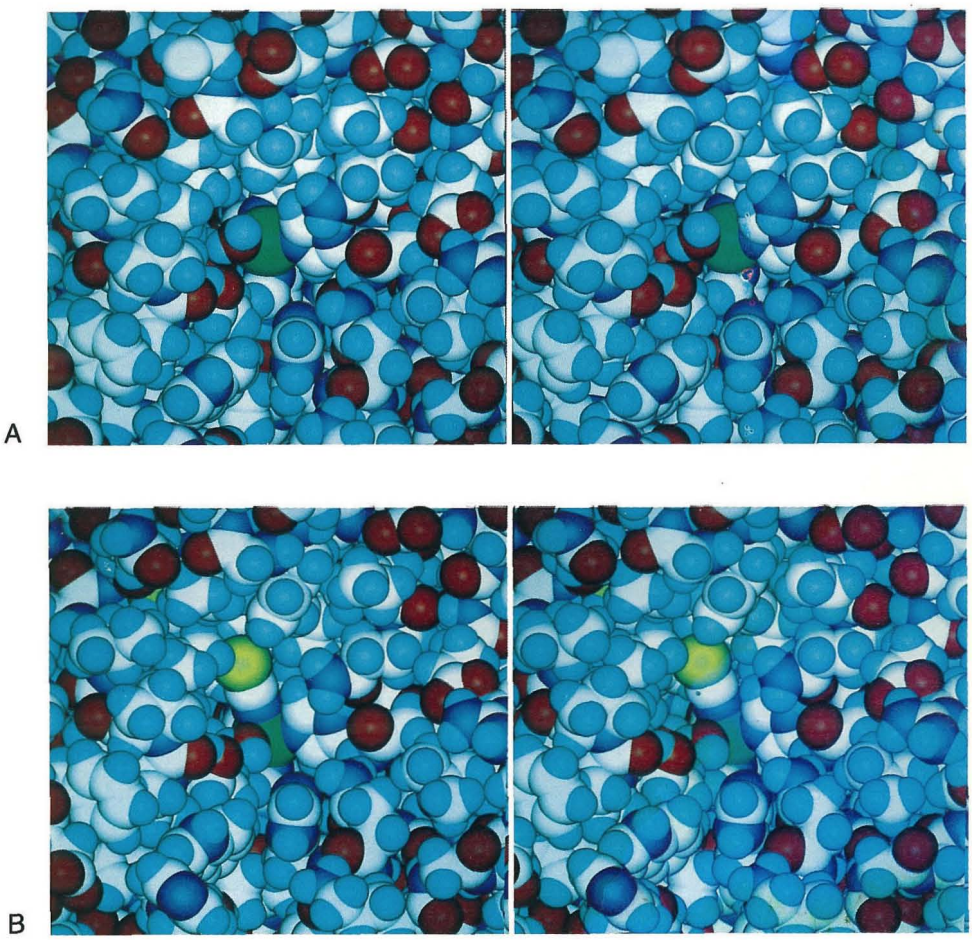

Figure 2.5
Active site of human carbonic anhydrase II (A) and its NCS^- adduct (B) viewed as CPK models. It is apparent from the comparison that the NCS^- ion occupies a binding site (B site) that is more buried than the binding site of the OH^- ion in the active form (A site). The water molecule in the NCS^- adduct occupies the C site, which is pointing more toward the entrance of the cavity.[64]

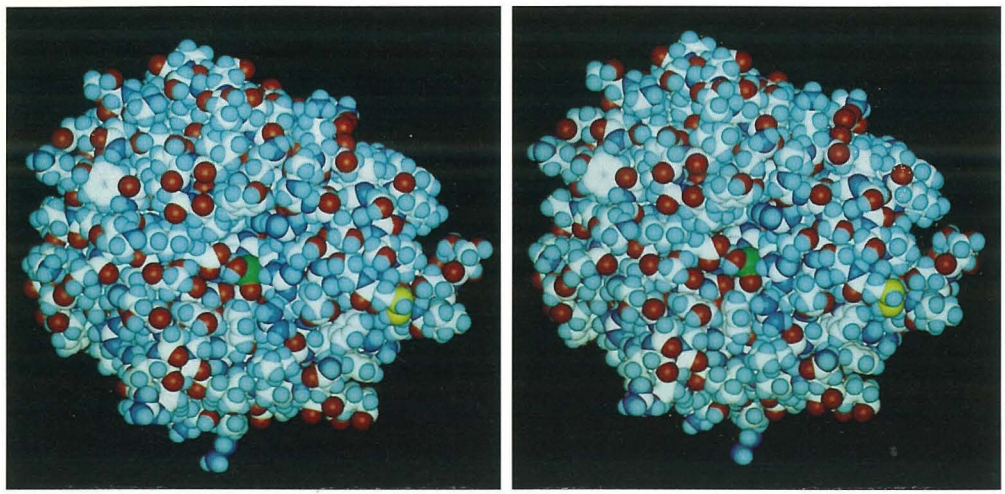

Figure 2.27
Carboxypeptidase A viewed as a CPK model. The color codes are as in carbonic anhydrase. Note the shallower active-site cavity with respect to carbonic anhydrase.

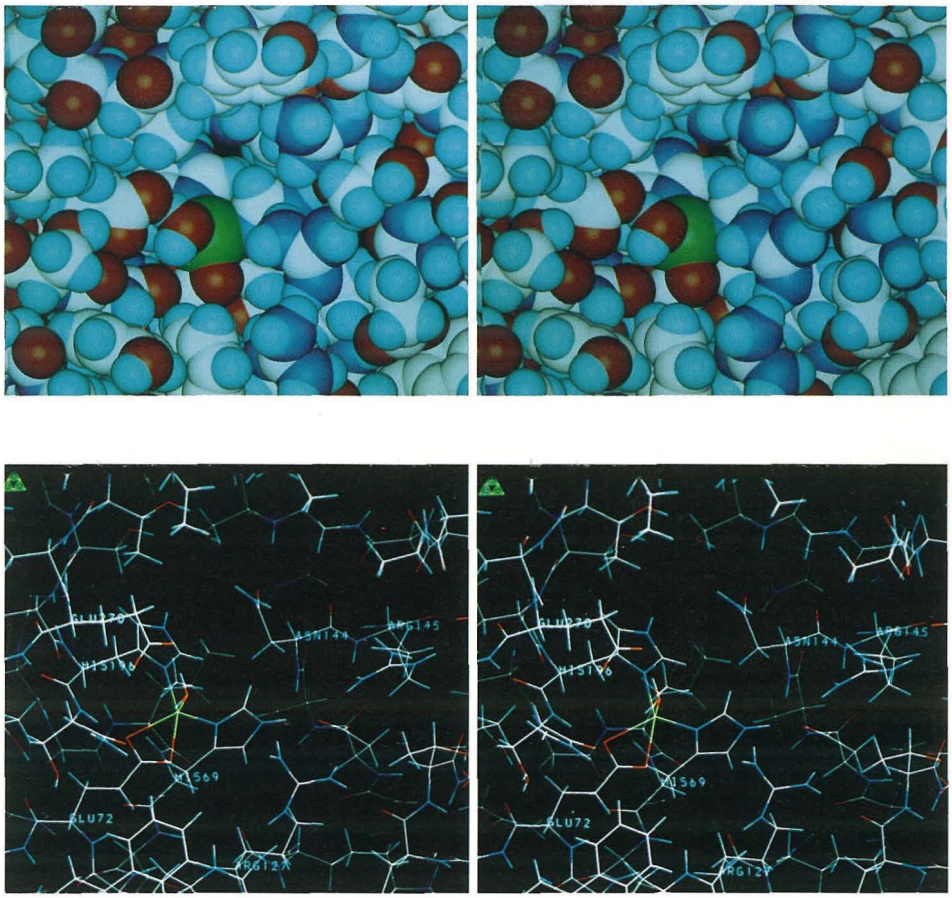

Figure 2.28
Active site of carboxypeptidase A viewed as CPK (A) and stick (B) models. The two views are taken from about the same perspective, i.e., from the entrance of the cavity. View B is self-explanatory. In view A, the zinc ion is the green sphere; its ligands are His-69 (on the right), His-196 (in the back), and Glu-72 (one of the two coordinated oxygens is clearly visible below the zinc ion). The coordinated water molecule (pointing outward) is hydrogen-bonded to Glu-270. On the opposite side of Glu-270 the three arginines (Arg-145, Arg-127, and Arg-71) can be seen, more or less on a vertical line, running from top to bottom of the figure. In the upper part of the figure, pointing outward, is the aromatic ring of Tyr-248. Behind it is the hydrophobic pocket.

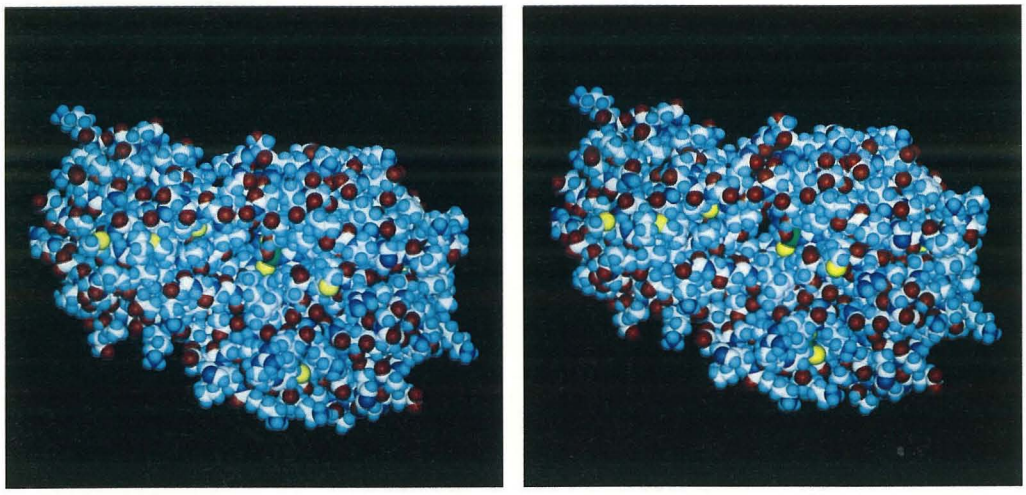

Figure 2.34
Liver alcohol dehydrogenase subunit viewed as a CPK model. The left-hand side of the molecule is the coenzyme binding domain and the right-hand side is the catalytic domain. The catalytic zinc ion is accessible from two channels located above (not visible) and below the coenzyme binding domain. The upper channel permits approach of the nicotinamide ring of the coenzyme. The lower channel permits approach of the substrate. The substrate channel closes up, trapping the substrate inside the molecule, when both coenzyme and substrate are present.

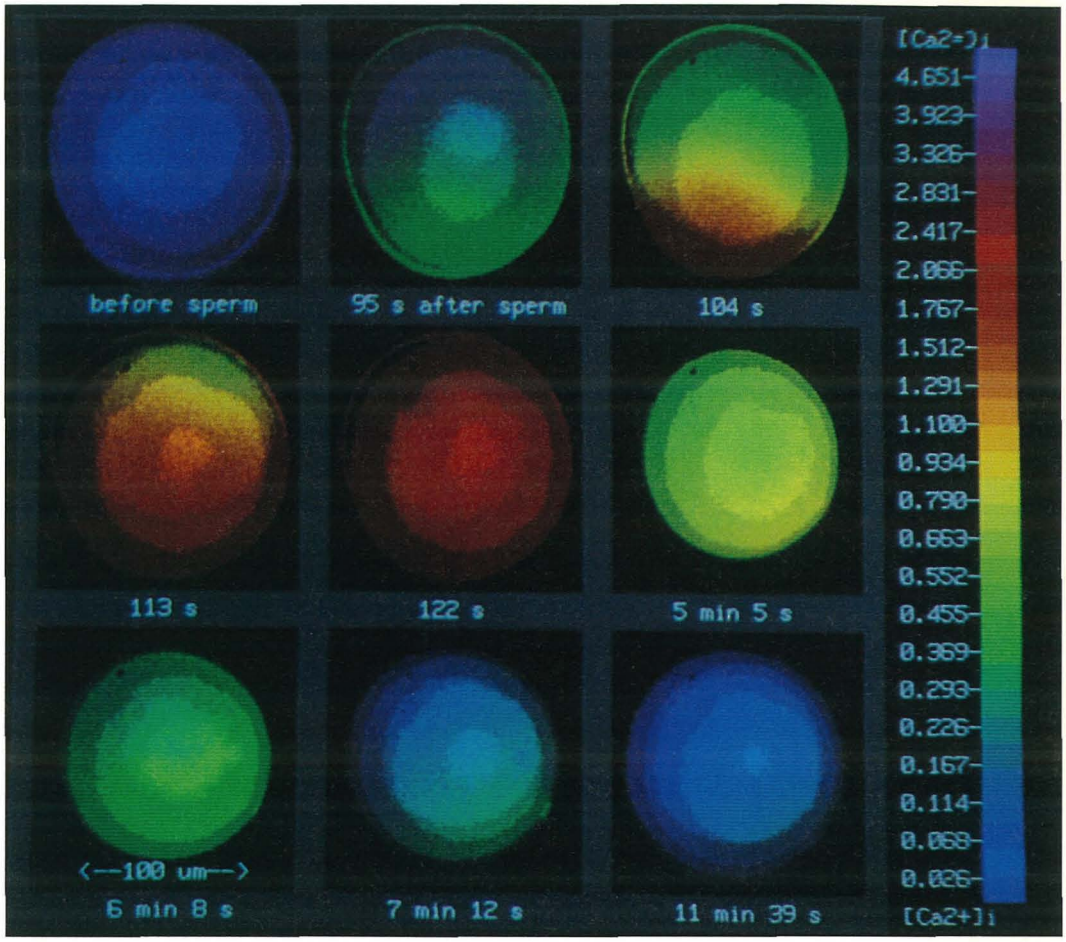

Figure 3.4
A Fura-2 study of the transient Ca^{2+} fluxes in an egg of the sea urchin (*Lutechinus pictus*). The diameter of this egg is about 120 μM. The fluorescent dye was injected into the egg, and the fluorescence intensity with excitation at 350 and 385 nm was measured with a lower-light-level television camera feeding a digital image processor (512 $\times$ 486 pixels). The image finally displayed in pseudocolor is the ratio of intensities at the two excitation wavelengths. The series of images shows a wave of high Ca^{2+} concentration that traverses the egg after it is fertilized by a sperm. Resting Ca^{2+} concentration is typically 100 nM and uniform through the cell. The fertilizing sperm sets off a transient wave of high Ca^{2+} that begins as a local elevation and thereafter spreads rapidly. After 20–30 seconds, the Ca^{2+} concentration of the entire egg is uniformly high ($\sim$2 μM). The figure is from an experiment by M. Poenie, J. Alderton, R. Steinhardt, and R. Tsien; see also Reference 26.

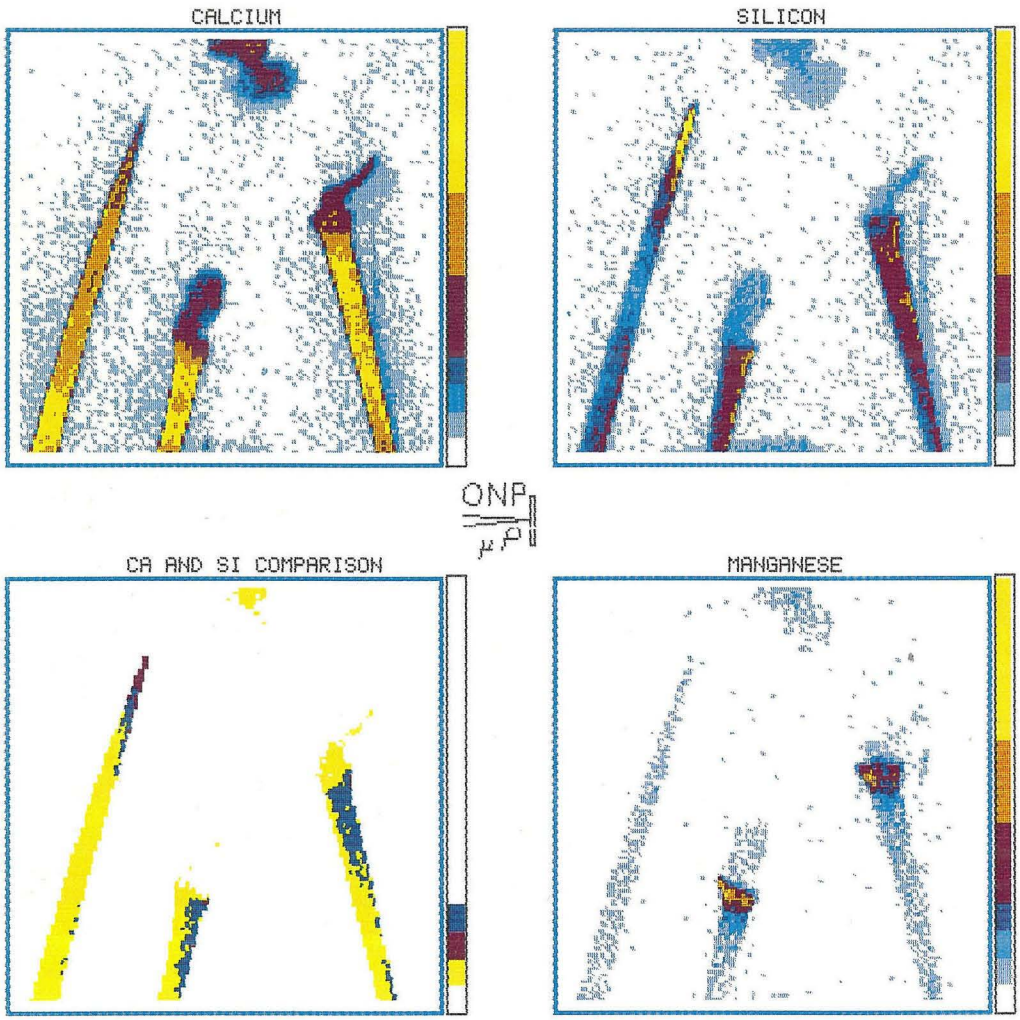

Figure 3.7
The elemental distribution of Ca, Si, and Mn in the hair of the common stinging nettle (*Urtica dioica*) obtained using the Oxford University PIXE microprobe. The color code for Ca is: yellow, >3.4 M; orange, 2.0–3.4 M; red, 1.5–2.0 M; dark blue, 1–1.5 M; blue, 0.5–1.0 M; light blue, 0.1–0.5 M; white, <0.1 M. The color codes of Si and Mn are similar. The PIXE data show that the tip mainly is made up of Si (presumably amorphous silica), but the region behind is largely made up of Ca (calcium oxalate crystals). The base of the hair contains substantial amounts of Mn. The pictures were kindly provided by R. J. P. Williams.

Figure 3.17
Space-filling stereo model of bovine brain calmodulin. Residues 5 to 147 are included, N-terminal half at the top. Positively charged side chains (Arg, Lys, His) are dark blue, negatively charged (Asp, Glu) red, hydrophobic (Ala, Val, Leu, Ile, Phe) green, Met yellow, Asn and Gln purple, Ser, Thr, and Tyr orange, and Pro, Gly, and main-chain atoms light blue. The figure was kindly provided by Y. S. Babu *et al.*[85]

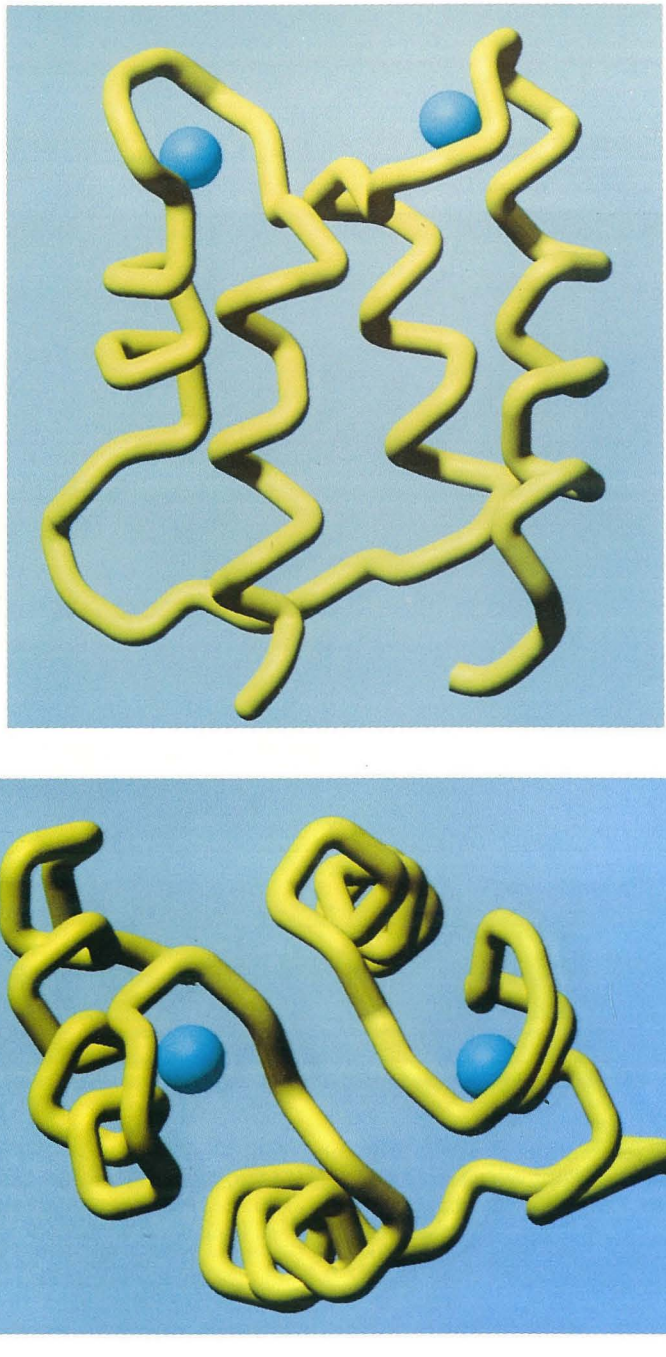

Figure 3.25
The backbone trace of the solution structure of porcine calbindin D_{9k} calculated from NMR data[124] shown in two different views. The position of the calcium ions (blue spheres) is modeled after the crystal structure[123] of bovine calbindin D_{9k}. Figure kindly provided by M. Pique, M. Akke, and W. J. Chazin.

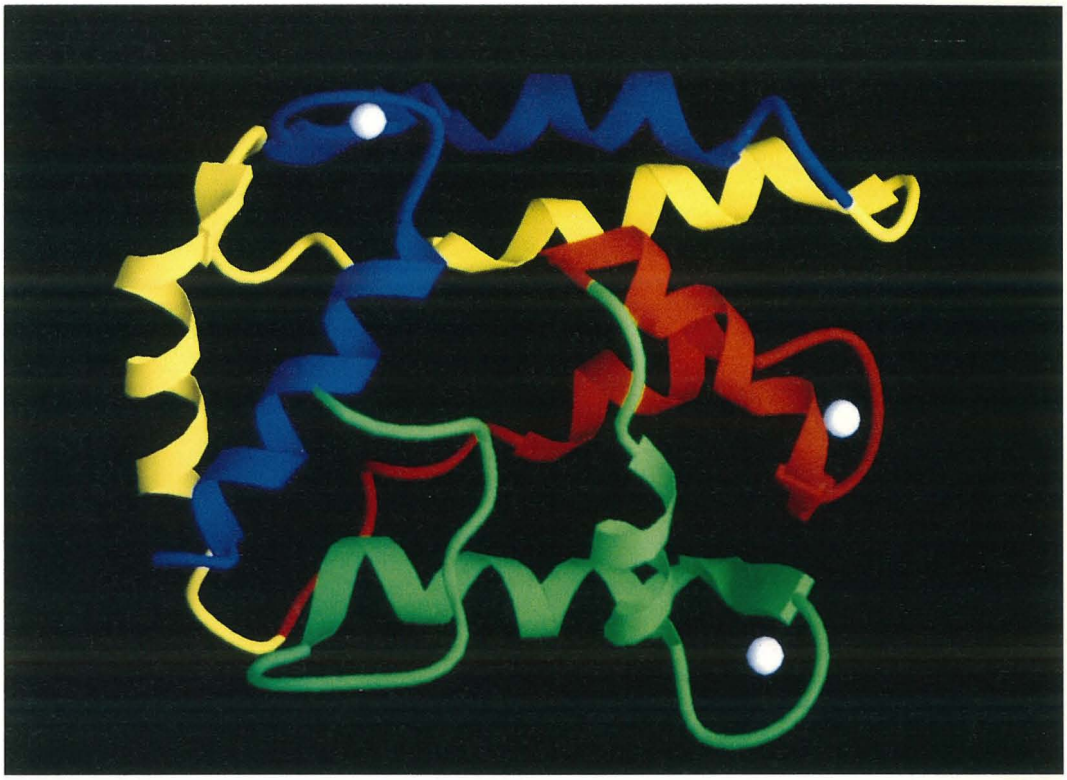

Figure 3.26
Drawing of the crystal structure of the sarcoplasmic calcium-binding protein from *Nereis diversicolor*.[130] The drawing is based on the α-carbon positions; helices are represented by thin ribbons, β-strands by thick ribbons, and Ca^{2+} ions by white spheres. Domain I (residues 1–40) is colored blue, domain II (41–86) yellow, domain III (87–126) red, and domain IV (127–174) green. Figure kindly provided by W. J. Cook.

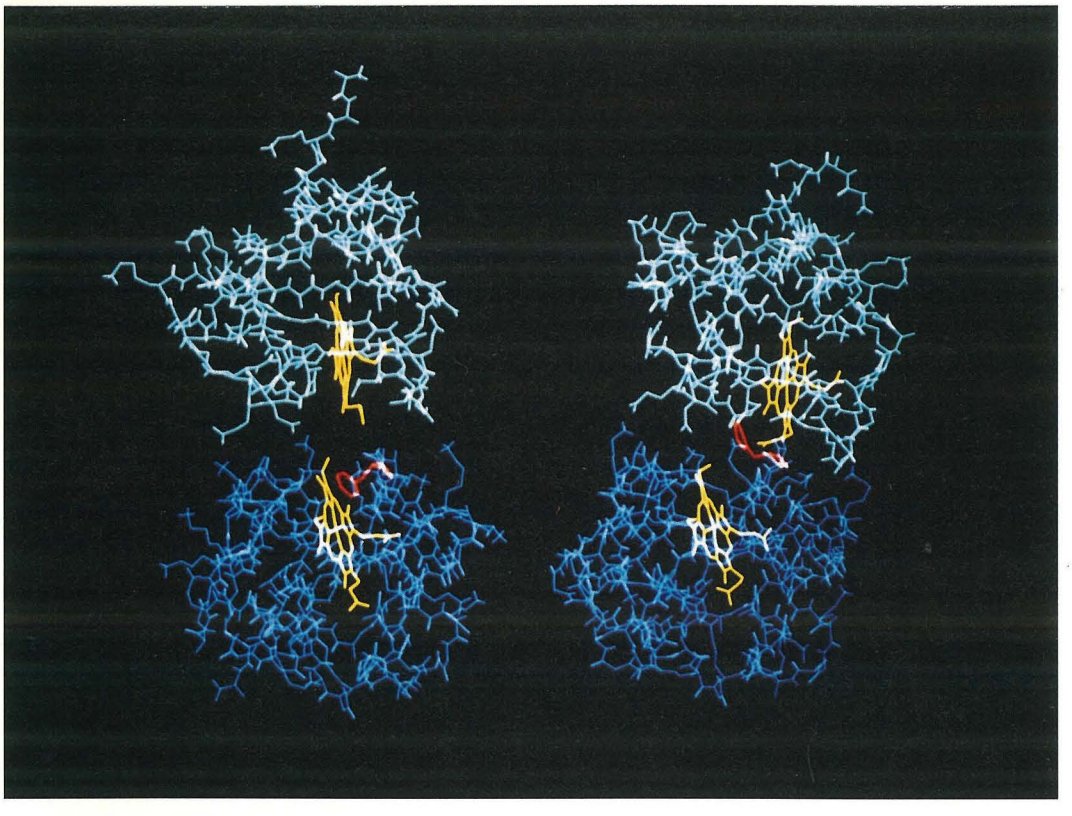

Figure 6.29
Computer-graphics models of the cytochrome b_5/cytochrome c complex: (left) static model produced by docking the x-ray structures of the individual proteins; (right) after extension by molecular dynamics simulations.[112] Reproduced with permission from Reference 112.

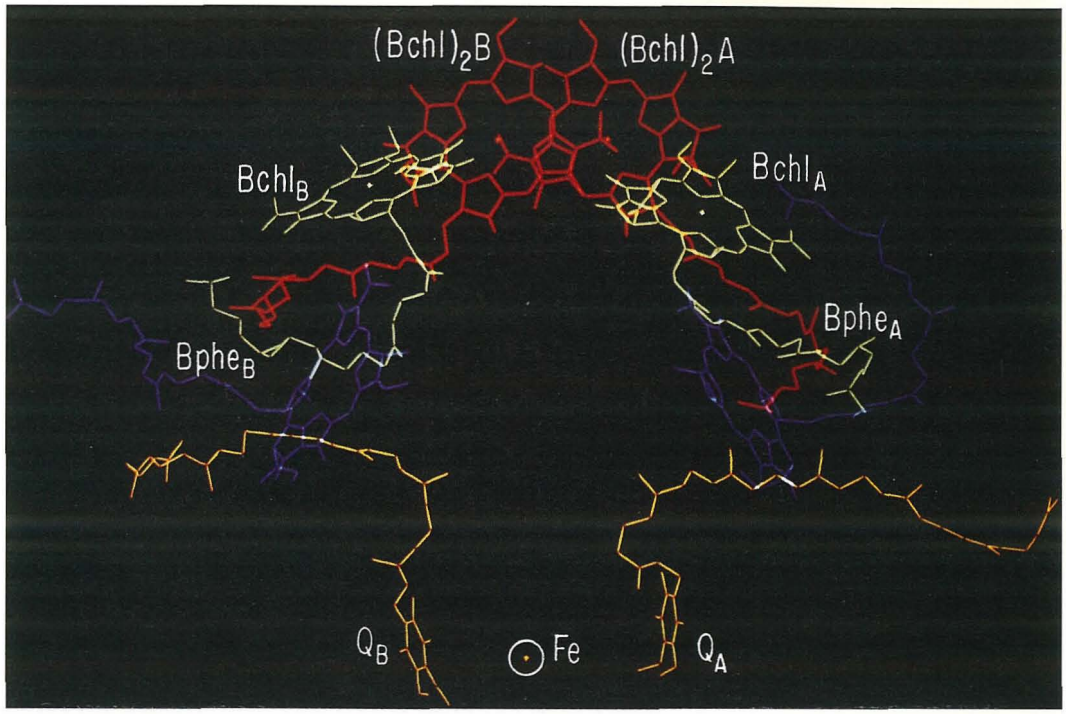

Figure 6.36
Rps. sphaeroides RC cofactors. Electron transfer proceeds preferentially along the A branch.[177] Reproduced with permission from Reference 177.

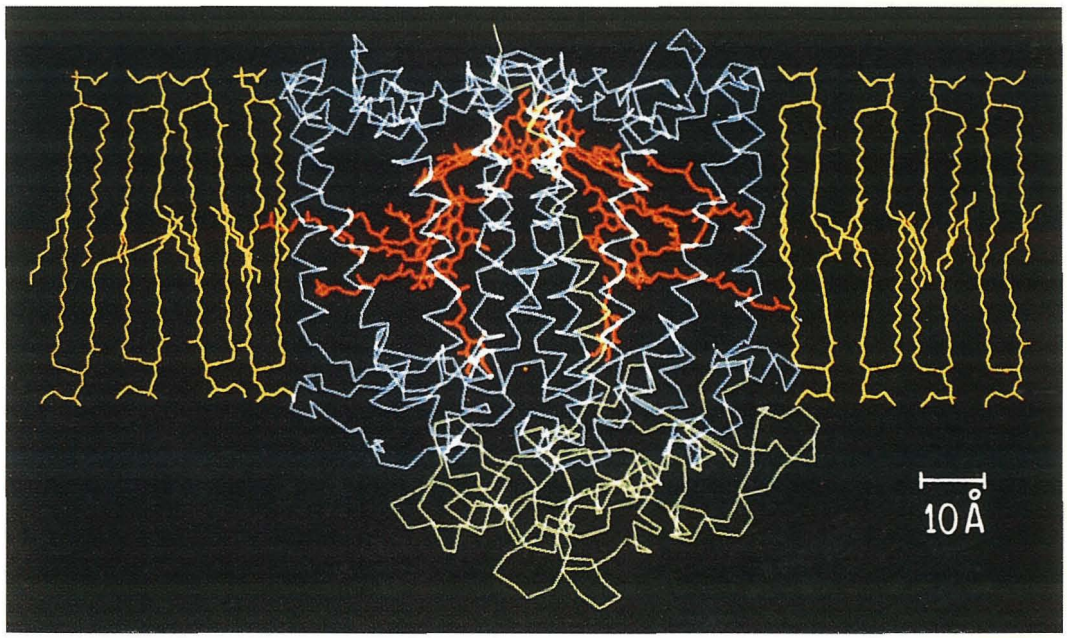

Figure 6.37
Position of the *Rps. sphaeroides* RC in the membrane bilayer. Cofactors are displayed in red, lipids in yellow, the H subunit in green, and L and M subunits in blue.[178] Reproduced with permission from Reference 178.

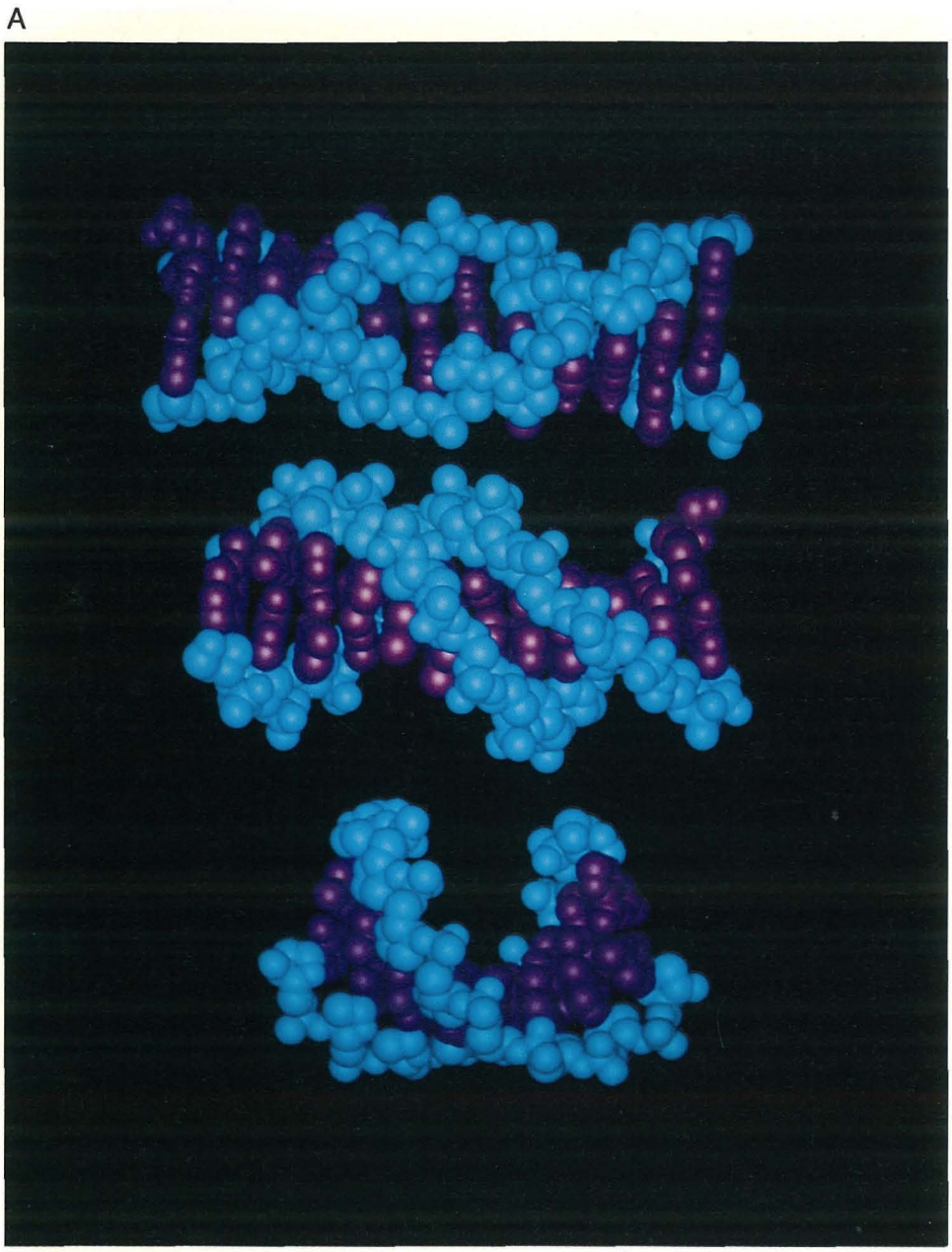

Figure 8.2
(A) Space-filling models depicting A- (left), B- (center), and Z- (right) DNA based on crystallographic data.[2–4] The sugar-phosphate backbone is shown in aqua and the base pairs in purple. This representation as well as subsequent graphics representations were obtained using the program *Macromodel*. (B) Schematic illustration of unusual conformations of DNA. (C) Space-filling models of $tRNA^{Phe}$ based on crystallographic data.[4] The sugar-phosphate backbone is shown in aqua and the bases in purple.

B

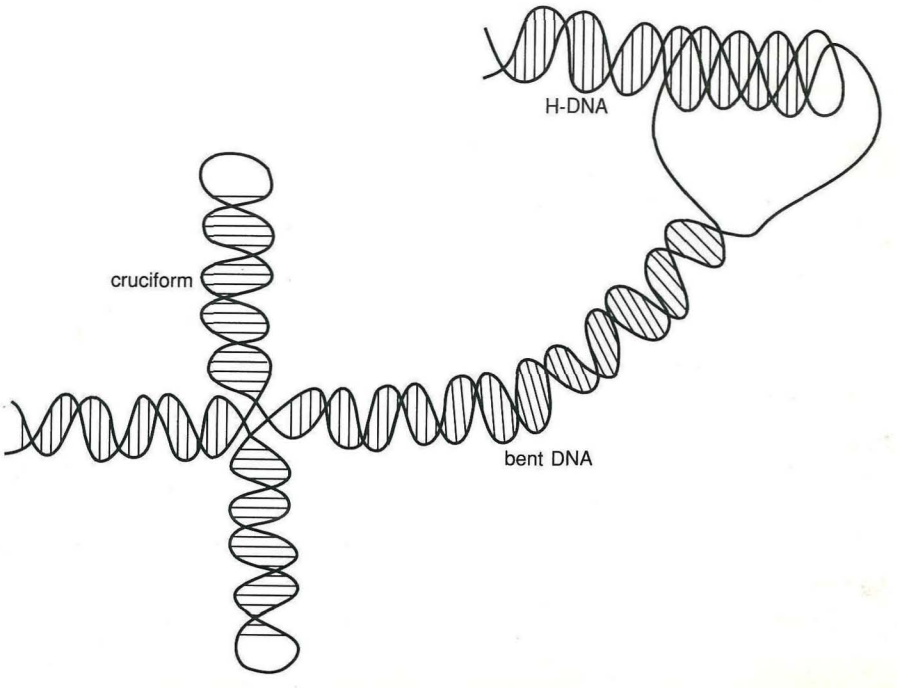

C

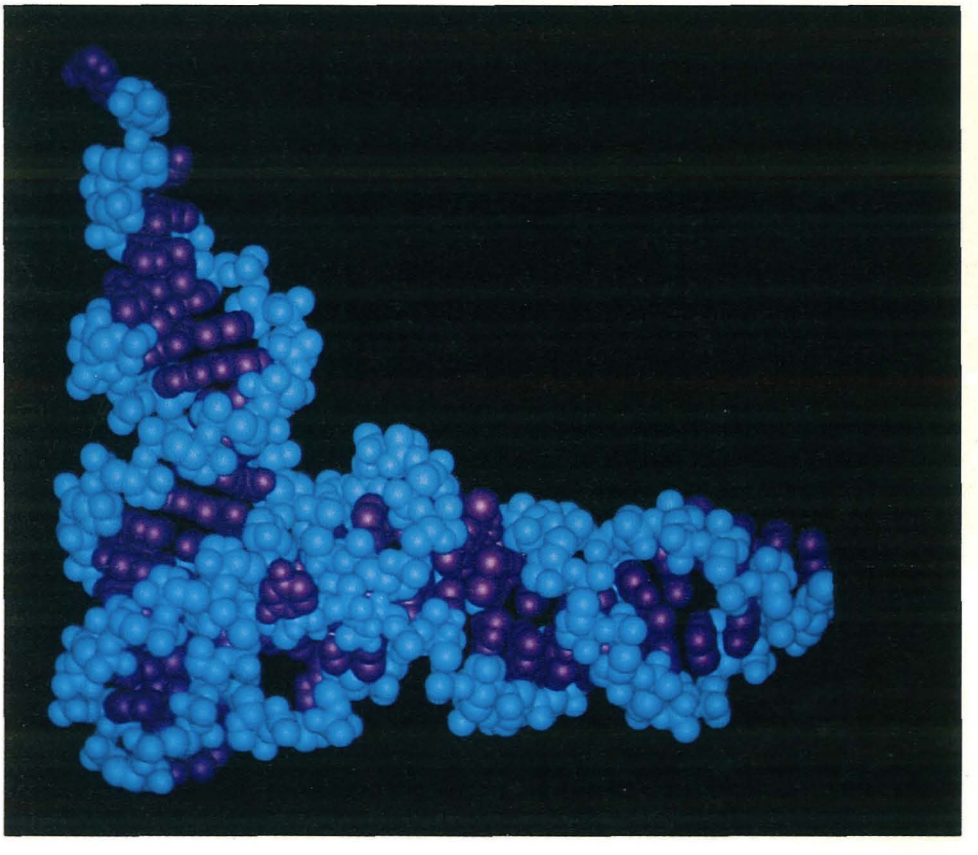

Once the hydrolysis has been performed, the cleaved amino acid still interacts with Arg-145 and with the hydrophobic pocket, whereas the amino group interacts with Glu-270. The carboxylate group of the new terminal amino acid interacts with zinc. This picture, which is a reasonable subsequent step in the catalytic mechanism, finds support from the interaction of L- and D-phenylalanine with carboxypeptidase.[131–134,138]

This mechanism, essentially based on the recent proposal by Christianson and Lipscomb,[137] underlines the role of the Zn—OH moiety in performing the nucleophilic attack much as carbonic anhydrase does. This mechanism can apply with slight changes to thermolysin[139] and other proteases. Thermolysin cleaves peptidic bonds somewhere in the peptidic chain. The mechanism could be very similar, involving zinc bound to two histidines and Glu-166 (Figure 2.31).[139] Glu-166 is monodentate. The role of Glu-270 in CPA is played by Glu-143 and the role of Arg-127 is played by His-231.

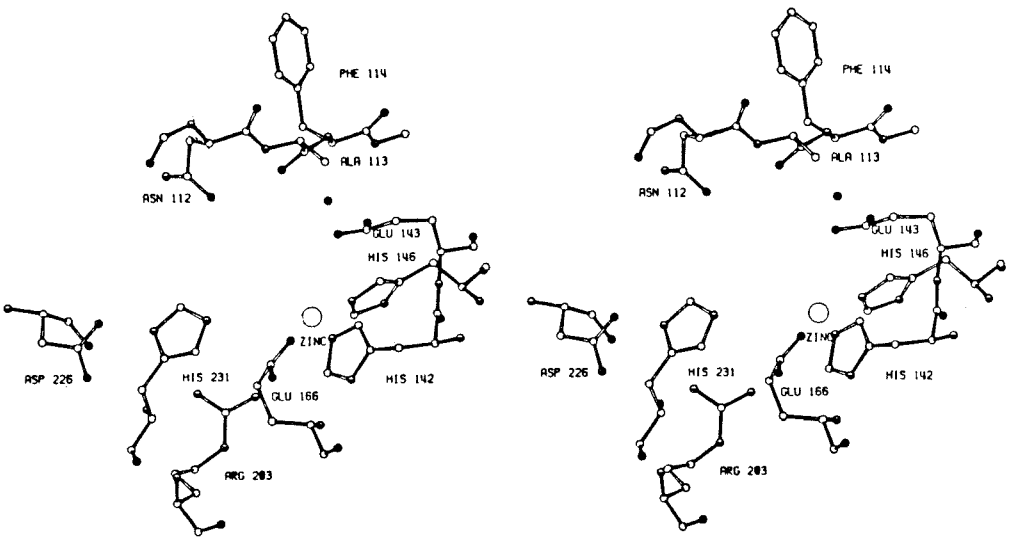

Figure 2.31
Stereo view of the active site of thermolysin.[139]

B. Ester Hydrolysis and Phosphoryl Transfer

Hydrolysis of carboxylic and phosphoric esters is also a slow process at neutral pH, and is catalyzed by acids and bases by mechanisms similar to those involved in amide and peptide hydrolysis. Metal ions are also good catalysts of both carboxylic and phosphoric ester hydrolysis, typically with rate increases much higher than those observed for hydrolysis of amides or peptides (Table

2.8). The ability of metal ions to coordinate to the carbonyl oxygen—which is higher in amides than in esters—is inversely correlated with their catalytic properties, perhaps because the main role of the metal ion is not in polarizing the carbonyl group, but in providing a metal-coordinated hydroxide as the attacking nucleophile.[108] For the hydrolysis of phosphate esters, it is difficult to draw conclusions based on experience with carboxylic esters, because, although the coordinating ability of the phosphoric oxygen may be higher, thus favoring the polarizing role of the metal, the nucleophilic attack is also likely to be easier, because the energy of the trigonal bipyramidal intermediate is probably rather low. Base-catalyzed hydrolysis of phosphate esters occurs with inversion of configuration, and this supports the existence of a trigonal bipyramidal intermediate.[140] The metal acts both as activator of substrate through binding and as Lewis acid to provide the OH moiety for the nucleophilic attack:

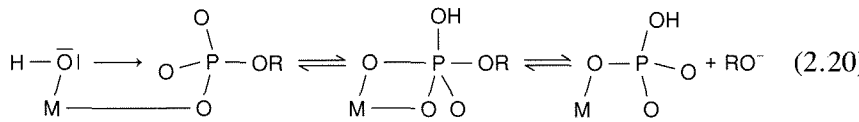

(2.20)

As with peptide hydrolysis, several enzyme systems exist that catalyze carboxylic and phosphoric ester hydrolysis without the need for a metal ion. They generally involve a serine residue as the nucleophile; in turn, serine may be activated by hydrogen-bond formation—or even proton abstraction—by other acid-base groups in the active site. The reaction proceeds to form an acyl- or phosphoryl-enzyme intermediate, which is then hydrolyzed with readdition of a proton to the serine oxygen. Mechanisms of this type have been proposed for chymotrypsin.[141] In glucose-6-phosphatase the nucleophile has been proposed to be a histidine residue.[142]

Again by analogy with peptide hydrolysis, metalloenzymes catalyzing ester hydrolysis may take advantage of additional chemical features provided by amino-acid residues present in the active-site cavity. This situation occurs with carboxypeptidase,[143] which shows esterase activity *in vitro*. Although the rate-limiting steps for carboxylic esters and peptides may differ, several features, such as the pH dependences of k_{cat} and K_m and the presence of two spectroscopically observable intermediates, point to substantially similar mechanisms. On the other hand, carboxylic ester hydrolysis catalyzed by carbonic anhydrase seems to rely on fewer additional features of the active-site cavity, perhaps only on the presence of a metal-coordinated hydroxide that can perform the nucleophilic attack on the carbonyl carbon atom.[47]

Metalloenzyme-catalyzed phosphoric ester hydrolysis can be illustrated by alkaline phosphatase, by far the most-investigated enzyme of this class. The protein is a dimer of 94 kDa containing two zinc(II) and one magnesium(II) ions per monomer, and catalyzes, rather unspecifically, the hydrolysis of a variety of phosphate monoesters as well as transphosphorylation reactions. The x-ray structure at 2.8 Å resolution obtained on a derivative in which all the native metal ions were replaced by cadmium(II) reveals three metals in each subunit,

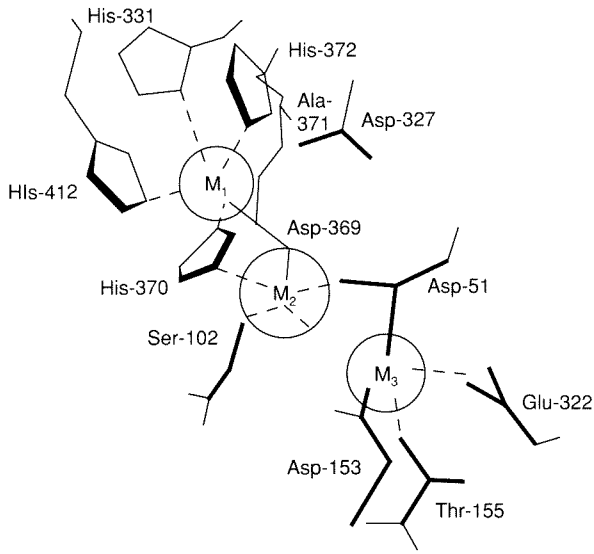

Figure 2.32
Schematic drawing of the active-site cavity of a subunit of alkaline phosphatase.[28,144,145] The catalytic metal is labeled M_1. The M_1-M_2 distance is ≃4 Å, the M_2-M_3 distance is ≃5 Å, and the M_1-M_3 distance is ≃7 Å.[144,145]

all located in a single binding region (Figure 2.32). In the native enzyme M_1 and M_2 sites are occupied by zinc and M_3 by magnesium.[144] M_1 was first reported to be coordinated to three histidine residues (His-331, 372, and 412 in Figure 2.32). Further refinement indicated that Asp-327 could be a ligand to M_1, in the place of His-372.[145] ^{1}H NMR spectroscopy of the enzyme with cobalt substituted in the M_1 site shows that there are three exchangeable protons sensing the paramagnetic metal ion.[146] They could come from three histidine NHs, or from two histidine NHs and another group containing the exchangeable proton very close to the metal ion, like an arginine. Protein ligands to M_2 are Asp-369, His-370, and Asp-51, the latter probably bridging M_2 to M_3 with the other carboxyl oxygen. M_3 is coordinated, in addition, to Asp-51, to Asp-153, to Thr-155, and to Glu-322. Several spectroscopic pieces of evidence on the native and metal-substituted derivatives indicate that M_1 is five-coordinate, but M_2 and M_3 are six-coordinate, probably with water molecules completing the coordination spheres.[28]

M_1 is essential for activity, but full catalytic efficiency is reached only when all metal ions are present. These data suggest that maximum activity is the result of fine-tuning several chemical properties of the active site as a whole, including the nature of the M_1 metal, which can be only zinc or cobalt (Table 2.4).

A further key feature of the active site is the presence of a serine residue (Ser-102), the oxygen atom of which is close to the $M_1 - M_2$ pair (especially to M_2), although not at direct binding distance according to the crystal structure. There is ample and direct evidence that Ser-102 is reversibly phosphorylated

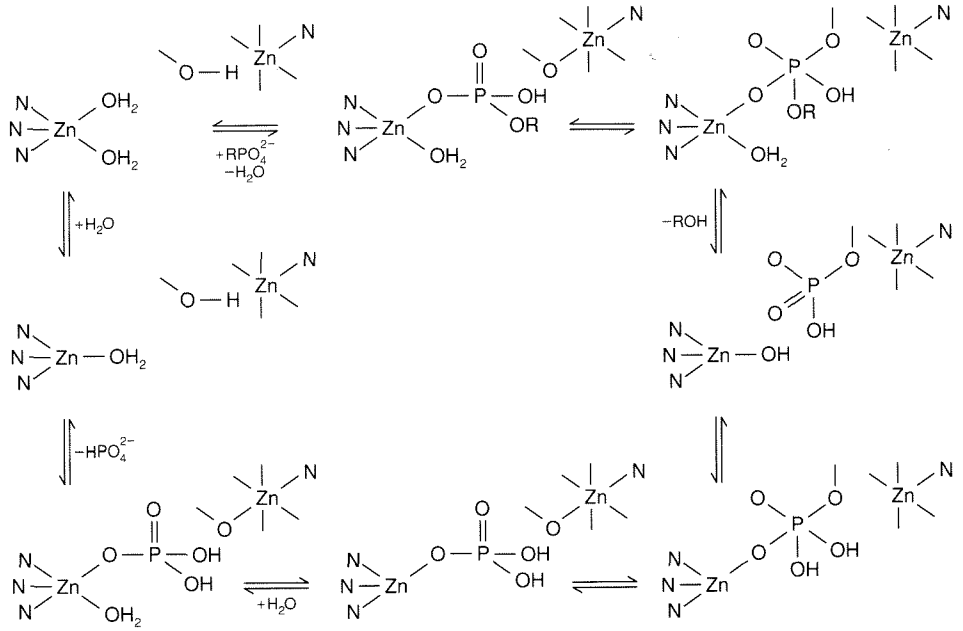

Figure 2.33
Possible catalytic cycle of AP.

during the course of the catalytic reaction, and that M_1 is able to coordinate a phosphate ion.[28]

Another crucial piece of information obtained by physico-chemical techniques is that the lability of the phosphoseryl intermediate and the catalytic activity increase with pH, depending on the state of ionization of an active-site group, which is most likely a water molecule coordinated to M_1.[147] Thus the active form of the enzyme is again a metal-hydroxide species. Furthermore, an inactive derivative with copper ions in the M_1 and M_2 sites shows evidence of magnetic coupling between the metal ions, of the magnitude expected if the two metals shared a common donor atom.[148] Likely candidates are a bridging hydroxide ion or Ser-102, which thus might be somewhat mobile relative to the position occupied in the x-ray structure, and demonstrate its potential ability to be activated for the nucleophilic attack by coordination to a metal ion. Such a mechanism would be an "inorganic" version of the type of activation postulated for chymotrypsin and other hydrolases.

A possible mechanism for alkaline phosphatase-catalyzed phosphoric ester hydrolysis could involve the following steps (Figure 2.33):

(1) Binding of the phosphate group to M_1—in the place of a water molecule—by one of the nonprotonated oxygens, and subsequent activation of the phosphorus atom for nucleophilic attack. The binding of the substrate may be strengthened by interaction with the positively charged

Arg-166 residue[149] (not shown). The steric alteration in the active site could cause movement of Ser-102 toward M_2, with deprotonation upon binding.

(2) Nucleophilic attack on phosphorus by the coordinated serine alkoxide, cleaving the ester bond and liberating the alcohol product.

(3) Formation of the phosphoseryl intermediate with cleavage of the M_1-phosphate bond, decreasing the pK_a of the second coordinated water molecule, the proton of which could be taken up by the leaving alcohol.

(4) Attack by the metal-coordinated hydroxide on the phosphoryl derivative, possibly with M_2 again polarizing the seryl oxygen, yielding a free phosphate ion coordinated to M_1. A further water molecule could aid in the liberation of phosphate via an associative mechanism.

In the presence of alcohols, alkaline phosphatase displays transphosphorylation activity, i.e., hydrolysis of the starting ester and esterification of the phosphate group with a different alcohol. This ability is easily understood if one keeps in mind that the reaction depicted above is reversible, and that a different alcohol may be involved in the formation of the ester bond. Most group-transfer reactions catalyzed by metalloenzymes are likely to proceed through the same elementary steps proposed for hydrolytic reactions.

C. Nucleophilic Addition of OH^- and H^-

Nucleophilic addition of OH^- ions as a step in enzymatic pathways is not restricted to hydrolytic processes; it often occurs in lyases, the class of enzymes catalyzing removal (or incorporation in the reverse reaction) of neutral molecules such as H_2O—but also NH_3, CO_2, etc.—from a substrate. It is outside the scope of this section to review all other mechanisms involved in lyase reactions, especially because they are not reducible to common steps and because several of them do not require the presence of a metal ion. We restrict ourselves to H_2O removal (or incorporation), a widespread feature of which seems to be the splitting of water into the constituents H^+ and OH^- ions at some step of the mechanism. As an example, the dehydration of 2-phospho-D-glycerate to phosphoenolpyruvate catalyzed by enolase, a Mg-activated enzyme,

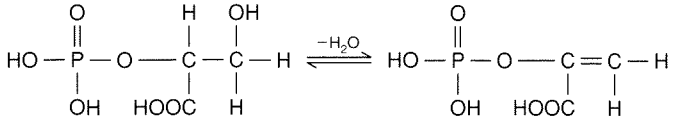

(2.21)

has been shown by kinetic isotope-effect studies[150] to proceed via fast H^+ removal from substrate followed by slow release of the product, and finally by release of OH^-. The role of a metal ion like magnesium might be to activate

the substrate by coordinating the phosphate group, rather than by providing a coordinated hydroxide for nucleophilic attack.

Other lyases, however, contain transition metal ions [often iron(II)], and their main role might well be that of lowering the pK_a of water. None of them, however, is yet known well enough to allow a detailed discussion of the molecular mechanism. A striking exception is carbonic anhydrase, which has been so extensively and successfully studied that it is ideal as a case study (Section IV).

Hydride transfer is another elementary process encountered in many enzymatic reactions. Although hydride transfer implies a redox reaction, it also involves nucleophilic attack on substrate as in the foregoing examples. Unlike OH^-, hydride ions do not exist in aqueous solutions as free ions. In biological systems hydride is always directly transferred from one organic moiety to another by simultaneous breakage and formation of covalent bonds. The activation energy for this process is much higher than, for example, that of H^+ transfer via the formation of hydrogen bonds. Moreover, unlike hydrogen-bonded species, there is no intermediate in the process that can be stabilized by the catalyst. Instead, reacting species can be destabilized in order to lower the activation energy barrier. The role of the enzyme, and of the metal ion when present, is to provide binding sites for both substrates. The enzyme achieves this both geometrically, by allowing for proper orientation of the groups, and electronically, by providing energy to overcome the activation barrier.

These general concepts can be exemplified by liver alcohol dehydrogenases (LADH), dimeric zinc enzymes of 80 kDa that catalyze the following class of reactions using the NADH/NAD^+ system as coenzyme (or, really, as cosubstrate):

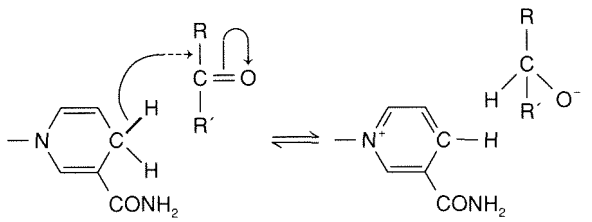

(2.22)

In particular, LADHs catalyze the reversible dehydrogenation of primary and secondary alcohols to aldehydes and ketones, respectively. Other enzymatic activities of LADHs are aldehyde dismutation and aldehyde oxidation.[151] The physiological role, although surely related to the metabolism of the above species, is not definitely settled. Much effort is being devoted to understanding the mechanism of action of this class of enzymes, which have obvious implications for the social problem of alcoholism.

Each monomer unit of LADH contains two zinc ions: one coordinated to four cysteine sulfurs, the other coordinated to two cysteine sulfurs, one histidine nitrogen, and a water molecule. The former has no apparent role in catalysis; the latter is essential for catalytic activity. The x-ray structure of the metal-depleted enzyme from horse liver has been solved at 2.4 Å resolution, and that

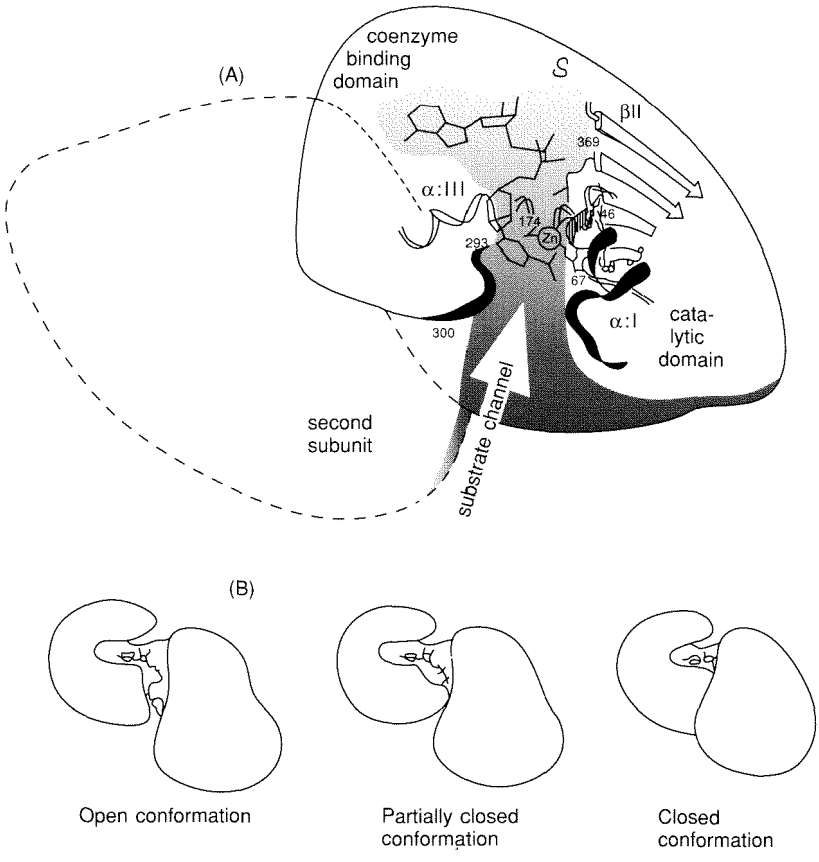

Figure 2.35
Schematic drawing of (A) the LADH dimer and (B) the domains constituting the active site of a subunit.[154]

of the holoenzyme at 2.9 Å resolution (Figure 2.34 *See color plate section, page C-6.*). Many crystal structures are also available for binary complexes with substrates, pseudosubstrates, or coenzymes, as well as for ternary complexes with coenzyme and substrates.[152] The very detailed picture emerging from such structural information has helped us understand how LADH functions. As will be evident from the following discussion, elucidation of this mechanism also reveals some important fundamental chemistry.

A key property of the enzyme, established by x-ray data, is the existence of two protein domains in each monomer that are relatively free to rotate relative to each other. The apo- and holo-enzymes exist in the so-called open form, whereas binding of NADH coenzyme induces rotation of one domain, resulting in the so-called closed form[153,154] (Figures 2.34 and 2.35). Closure brings the catalytic zinc ion into an ideal position to bind the aldehyde substrate in such a way that the reactive CH_2 group of the nicotinamide ring of NADH points toward

the carbonyl carbon (Figure 2.35). The main functions of the metal are thus to orient the substrate geometrically and to polarize the carbon-oxygen bond. Although the latter makes obvious chemical sense for the aldehyde reduction reaction, since polarization of the C=O bond facilitates nucleophilic attack of hydride at the carbonyl carbon, coordination of an alcohol to a metal is expected to decrease the alcohol's tendency to transfer hydride to NAD^+, unless the hydroxyl proton is released upon coordination.[155]

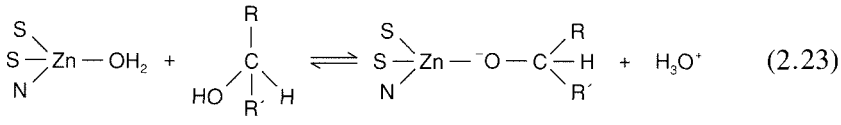

(2.23)

Formation of an alkoxide ion as an intermediate has often been questioned, because the pK_a of the alcohol would have to be reduced by about 10 units upon coordination.[156] The possibility that hydride transfer from alcohol to NAD^+ and hydroxyl proton release could occur simultaneously is attractive, but careful experiments have shown that the two steps must be kinetically separate.[157] We summarize here the key information that leads to a full, although circumstantial, rationalization of the chemical behavior of the enzyme.

(1) The activity versus pH profiles[156,158] are bell-shaped, with k_{cat} increasing with a pK_a below 7, reaching a plateau, and decreasing with a pK_a above 11, and K_m increasing with a pK_a of about 9.

(2) X-ray data show that the zinc ion is accessible to solvent in the open conformation, much less so in the closed conformation when the reduced coenzyme is bound, and inaccessible when the substrate is coordinated to the metal in the ternary complex, extruding all the water molecules from the active site.[152] None of the complexes has a coordinated water molecule as a fifth ligand when substrates or inhibitors are bound to the metal. The metal ion is always four coordinate and pseudotetrahedral. Computer graphics reveal beyond any doubt that there is no room for a fifth ligand in the active site, at least in the closed form.

(3) Many (although not all) spectroscopic data on metal-substituted derivatives and their binary and ternary complexes have also been interpreted as indicative of a four-coordinate metal.[159] Even nickel(II) and copper(II), which have little tendency to adapt to a pseudotetrahedral ligand environment, do so in LADH, the electronic structure of the latter resembling that of blue proteins (Figure 2.36).[160]

(4) The substrate binding site is actually "created" by the closure of the protein (Figure 2.34). The reactive species are thus trapped in an absolutely anhydrous environment.

The chromophoric aldehyde DACA

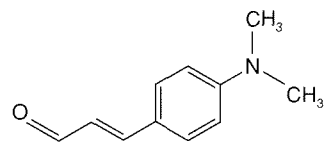

(2.24)

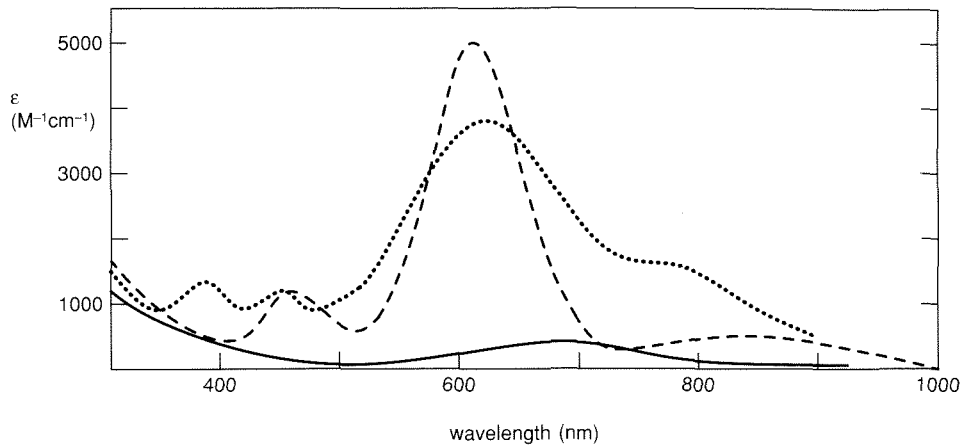

Figure 2.36
Electronic spectra of liver alcohol dehydrogenase substituted with copper at the catalytic site (· · · · ·),[160] together with the spectra of blue (stellacyanin, – – –)[161] and non-blue (superoxide dismutase, ———)[162] copper proteins.

has been extensively used as an "indicator" of the polarity of the binding site. Large red shifts of the ligand π-π^* transition upon binding indicate the polarity of the site to be much higher than in water; there is a further sizeable increase in polarity when NAD^+ instead of NADH is bound in the ternary complex.[163]

(5) The electronic spectra of the cobalt-substituted derivative are characteristically different when different anions are bound to the metal (Figure 2.37).[164] A catalytically competent ternary complex intermediate displays the electronic absorption pattern typical of anion adducts.[166]

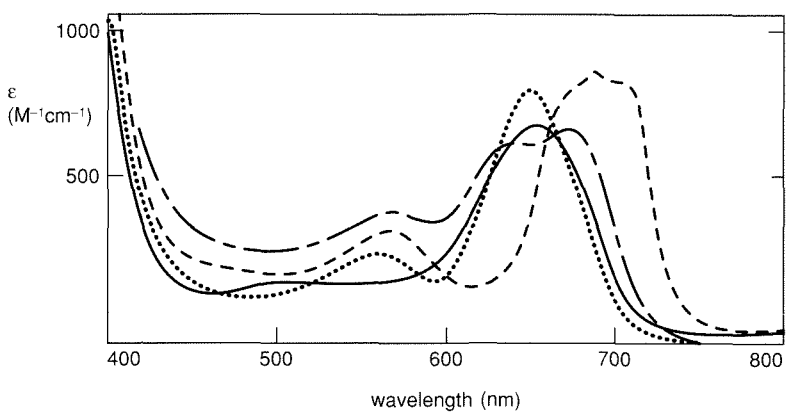

Figure 2.37
Electronic spectra of liver alcohol dehydrogenase substituted with cobalt at the catalytic site. Binary complex with NAD^+ (———);[165] ternary complex with NAD^+ and Cl^- (– – –);[165] binary complex with acetate (· · · · ·);[164] intermediate in the oxidation of benzyl alcohol with NAD^+ (— — — —).[166]

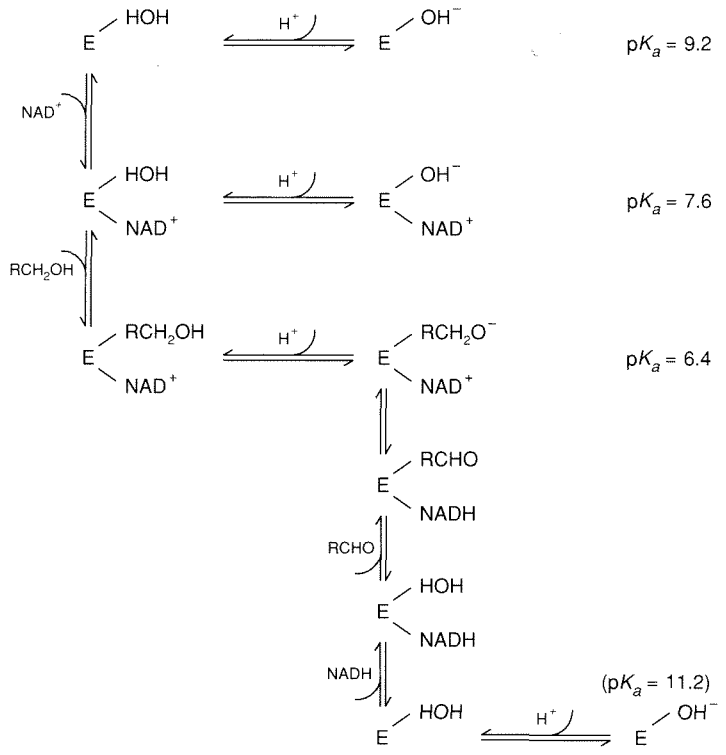

Figure 2.38
Protonation scheme for LADH and its adducts with coenzymes and substrates.[157,167]

(6) From extended kinetics measurements a protonation scheme (Figure 2.38) has been proposed that accounts for the many pK_a values observed under different conditions.[167] This scheme again requires formation of a coordinated alkoxide intermediate, but has the advantage of rationalizing in a simple way a complex pattern. In essence, the only relevant acid-base group supplied by the enzyme is the metal-coordinated water, which has a pK_a of 9.2 in the free enzyme (open form). Upon binding of NADH the pK_a increases to 11.2. Since NADH dissociation is the last and rate-limiting step of the alcohol oxidation reaction, the decrease in k_{cat} with this pK_a is accounted for by a decrease in dissociation rate of NADH from the hydroxo form. On the other hand, the pK_a of water is decreased to 7.6 upon binding of NAD^+. These rather large changes in both directions are best explained by a marked sensitivity of the coordinated water molecule to the polarity of the environment, which, with the possible exception of the unligated form that has a more or less "regular" pK_a value of 9.2, can be almost completely anhydrous and much different from that of bulk water. The nonpolar nicotinamide ring of NADH decreases the overall electrostatic interactions of the water molecule, whereas the positive charge of NAD^+ drastically increases them. In this scheme, the association rates of both coenzymes are predicted to (and, in fact, do) decrease with a pK_a of 9.2, the dissociation

rate of NAD^+ is predicted to (and does) decrease with a pK_a of 7.6, and the dissociation rate of NADH is predicted to decrease with a pK_a of 11.2 (and, indeed, it is pH-independent up to and above pH 10).

The decrease of k_{cat} at low pH depends on an ionization that in turn depends on the substrate. This pK_a must be that of the coordinated alcohol; at too low a pH, deprotonation of the coordinated alcohol becomes the rate-limiting step. The pK_a values observed for this process range from 6.4 for ethanol to 4.3 for trifluoroethanol. What is surprising for aqueous-solution chemistry—that the pK_a of a coordinated alcohol is lower than the pK_a of a coordinated water molecule—can now be explained in terms of the different polarity of the two adducts in LADH. In the binary complex with NAD^+ ($pK_a = 7.6$), the water molecule is still free to interact through H-bonding with the solvent and partially dissipate the electrostatic charge. In the ternary complex with any alcohol, the R group may prevent access of the solvent to the cavity, decreasing the dielectric constant of the medium. As a consequence, the polarity of the environment is increased. It is interesting to speculate that Nature could have chosen a stronger Lewis acid than a zinc ion coordinated to two negatively charged residues to decrease the pK_a of a coordinated alkoxide, but then the pK_a of the coordinated water would have simultaneously undergone a parallel and possibly even stronger decrease. Instead, LADH provides a self-regulating environment that is tailored to decrease the pK_a of a coordinated alcohol, once properly positioned, more than that of a coordinated water. The full catalytic cycle for the dehydrogenation reaction at pH around 7 can be summarized as follows (Figure 2.39):

(1) NAD^+ binds to the open, water-containing form of the enzyme with a maximal on-rate. The pK_a of water is decreased to 7.6, but water is still mostly unionized.

(2) A neutral alcohol molecule enters the crevice between the two domains, and coordinates the zinc ion by displacing the water molecule. The protein is still in the open form.

(3) Domain rotation brings the protein into the closed form, excluding all the residual water molecules from the active site; the combined effect of the metal positive charge and of the unshielded positive charge of the nicotinamide ring lowers the pK_a of the coordinated alcohol below 7. A proton is expelled from the cavity, possibly via a hydrogen-bond network of protein residues.

(4) Direct hydride transfer takes place from the alcohol CH to the 4-position of the properly oriented nicotinamide ring. The resulting ternary complex is an NADH-aldehyde adduct. The polarity of the active site dramatically drops.

(5) The aldehyde product leaves and is replaced by a neutral water molecule (its pK_a now being 11.2). Additional water molecules can now enter the crevice, favoring the partial opening of the structure.

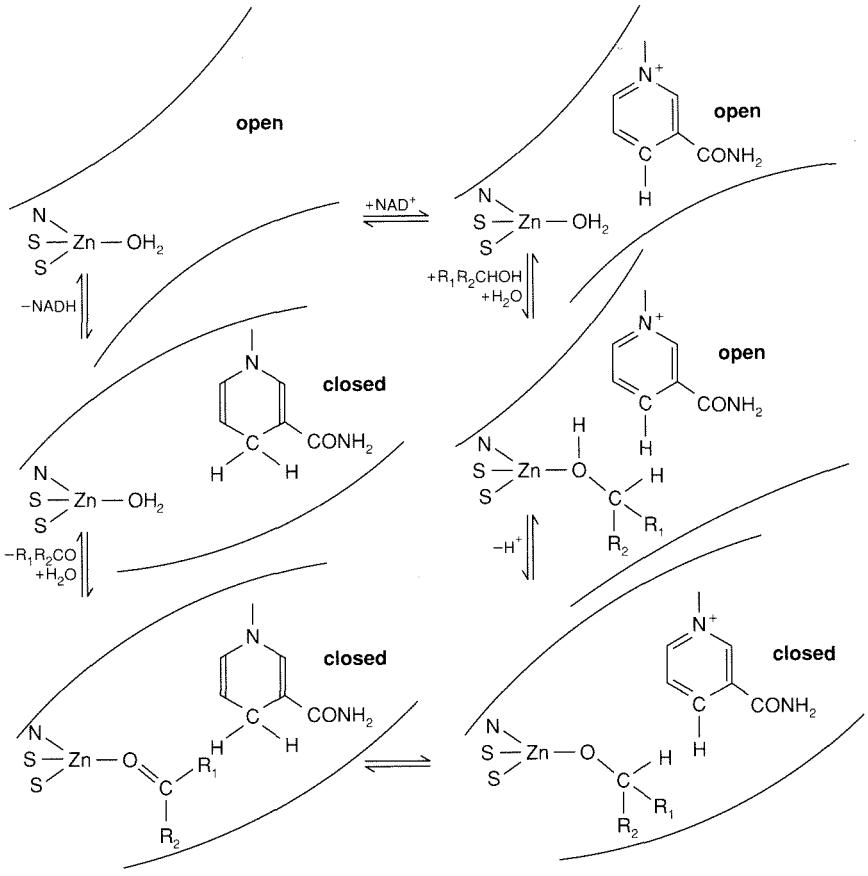

Figure 2.39
Possible catalytic cycle of LADH.

(6) The loss of contacts between the two halves of the channel favors a complete opening and then the release of NADH, whose dissociation rate is maximal and pH-independent.

D. Group Transfer and Vitamin B_{12}

1. Group transfer enzymes

The phosphodiester bond in ATP and in related molecules is a high-energy bond whose hydrolysis liberates a large quantity of energy:

$$ATP + H_2O \rightleftharpoons ADP + P_i + 30\text{-}50\ kJ\ mol^{-1} \qquad (2.25)$$

In many systems, typically the ATPases, the terminal phosphoryl group is transferred to another acidic group of the enzyme, e.g., a carboxylate group, to form another high-energy bond whose energy of hydrolysis is needed later for some

endoenergetic transformation. Therefore the first step of the reaction is the phosphoryl transfer to a group of the enzyme.

Kinases, a subset of the class of transferases, constitute a large group of enzymes that phosphorylate organic substrates:

$$ATP^{4-} + HX \rightleftharpoons ADP^{3-} + PX^{2-} + H^{+} \tag{2.26}$$

In some kinases, such as nucleoside diphosphate kinase,[168,169] an intermediate step is the phosphoryl transfer to a group belonging to the enzyme, as happens in ATPase and as was discussed in detail for alkaline phosphatase (Section V.B). In other kinases the phosphoryl transfer occurs directly from the donor to the acceptor in a ternary complex of the enzyme with the two substrates.[170] Often metal ions like magnesium or manganese are needed. These ions interact with the terminal oxygen of the ATP molecule, thus facilitating the nucleophilic attack by the acceptor. The metal ion is often associated with the enzyme. For mechanistic schemes, see the proposed mechanism of action of alkaline phosphatase, especially when a phosphoryl enzyme intermediate is involved.

2. The B_{12}-dependent enzymes

There are many enzymes that need a cobalt complex as cofactor in order to carry out vicinal 1,2 interchange:

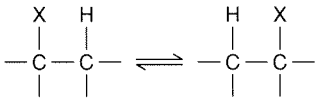

(2.27)

or

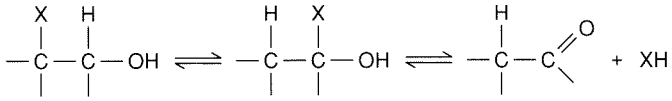

(2.28)

For the former type of reactions, X can be a group containing either C or N. Typical reactions[171] include insertion of a secondary methyl group into a main chain

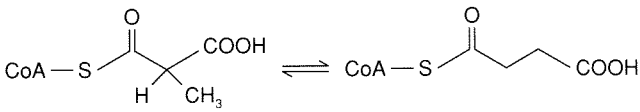

(2.29)

isomerization of an amino group from a primary to a secondary carbon

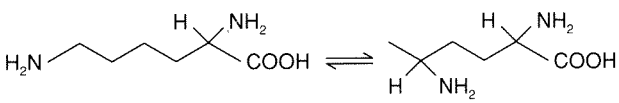

(2.30)

and deamination reactions

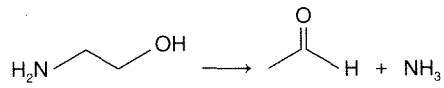

(2.31)

A list of coenzyme-B_{12}-dependent enzymes is given in Table 2.10.

Table 2.10
Some coenzyme-B_{12}-dependent enzymes.

MethylmalonylCoA mutase
Glutamate mutase
α-Methylene-glutarate mutase
Dioldehydrase
Glyceroldehydrase
Ethanoldeaminase
L-β-lysine mutase
D-α-lysine mutase
Ribonucleotide reductase
Methionine synthetase
Methane synthetase
Methyl transferase
Acetate synthetase

In coenzyme-B_{12}, cobalt is bound to a tetraazamacrocyclic ligand[172] (Figure 2.40). The cobalt atom lies approximately in the plane of the corrin ligand (shown in bold). Note that rings A and D are directly linked. The conjugation therefore extends over only 13 atoms, excluding the cobalt, and involves 14 π electrons. Complexes that possess the α-D-ribofuranose-3-phosphate and the terminal 5,6-dimethylbenzimidazole as an axial ligand are called cobalamins. The name cobamides applies to complexes that lack or have different heterocyclic groups. Finally, the upper or β position is occupied by another ligand, which may be water, OH^-, CN^-, an alkyl group, etc. The cyano derivative (ii) is vitamin B_{12}. 5′-deoxyadenosylcobalamin (i) is called coenzyme B_{12}. The cobalt atom in these complexes is a diamagnetic cobalt(III) system (d^6).

The aquo complex has a pK_a of 7.8, which compares with that of 5.7 for the aquopentaamminecobalt(III) complex at 298 K.[173] The difference has been mainly ascribed to the difference in solvation of the two complexes, although the corrin ligand bears a negative charge, which reduces the positive charge and therefore the Lewis acidity of the metal ion. The standard reduction potential between pH 2.9 and 7.8 is -0.04 V vs. SCE, featuring the conversion from aquocobalamin with bound benzimidazole (base on) to base-on cob(II)alamin.[174] The potential decreases with pH above pH 7.8 down to -0.3 V. The reduced form is five-coordinate, without the water molecule above pH 2.9, and low-spin.[175,176] The system can be further reduced at a potential of -0.85 V to

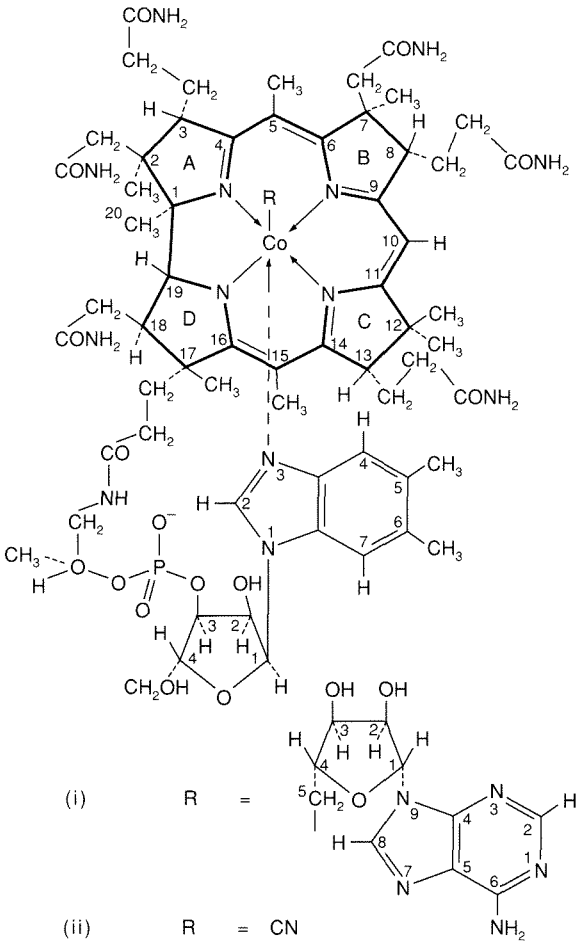

Figure 2.40
Structure of (i) coenzyme B_{12}, 5′-deoxyadenosylcobalamin, and (ii) vitamin B_{12}, cyanocobalamin.[172]

obtain cob(I)alamin, in which the metal ion is four-coordinate and low-spin (d^8). The standard reduction potential for the hexaaquocobalt(III) complex is 1.95 V, which is lowered to 0.10 for the hexaammine complex, to −0.13 for the tris-ethylenediamine complex, and to −0.80 for the hexacyanocobaltate(III) ion.[173] After reduction to cobalt(II), the model complexes are reduced to the metal.

The electronic spectrum of the metal-free corrin resembles that of metal derivatives; it seems therefore that the bands are essentially π-π^* transitions modified by the central atom and by the axial ligands.[177,178] The cob(III)alamins are red, whereas the cob(II)alamins, which are brown, show an additional band at 600 nm.[179] The latter have an EPR spectrum typical of an unpaired electron in the d_z^2 orbital with some 4s mixing: the cob(II)alamin at pH 7 has $g_{\|} = 2.004$,

$g_\perp = 2.32$, $A_\parallel(Co) = 0.0100$, $A_\perp(Co) = 0.0027\ cm^{-1}$, and $A_\parallel(N) = 0.00173\ cm^{-1}$.

Both cobalt(I) and cobalt(II)-containing cobalamins readily react with alkyl derivatives to give alkylcob(III)alamins:

$$\text{Cob(II)alamin} + CH_3I \rightarrow CH_3\text{-Cob(III)alamin} + 1/2I_2 \tag{2.32}$$

$$\text{Cob(I)alamin} + CH_3I \rightarrow CH_3\text{-Cob(III)alamin} + I^- \tag{2.33}$$

These can formally be regarded as complexes of cobalt(III) with a carbanion. These are rare examples of naturally occurring organometallic compounds. The Co—C bond in alkylcobalamins is relatively weak (bond dissociation energy $\simeq 100\ kJ\ mol^{-1}$, though higher values are reported in the literature[182,183]) and can be broken thermally (by heating the complex above 100°C)[182–184] or photochemically, even in daylight exposure.[180,181] The energy of the Co—C bond is about 17 kJ mol^{-1} greater when the transaxial base is absent.[184]

The cobalamin coenzyme is bound by the apoenzyme with no significant change in the absorption spectrum.[185] This suggests that no major change occurs in the coordination of cobalt(III). The first step of the reaction involves homolytic fission of the Co—C bond:[182–184, 186–188]

$$B\text{—}Co^{III}\text{—}R \rightarrow B\text{—}Co^{II}\cdot + R\cdot \tag{2.34}$$

where B and R are the ligands at the α and β apical positions. The 5′-deoxyadenosyl radical probably reacts with the substrate, generically indicated as SubH, to give the Sub· radical and RH. Then the rearrangement reaction proceeds along a not-well-established pathway. It is the protein-substrate binding that controls the subsequent chemistry. In the absence of protein the Co—C bond is kinetically stable; in the presence of protein and substrate the rate of labilization of the Co—C bond increases by a factor of 10^{11}–10^{12}.[182–185] By generating the radical in the coenzyme without the protein by means of photolysis or thermolysis, we enable the coenzyme to catalyze some rearrangement reactions without the protein. It may therefore be that the protein plays a major role in inducing the homolytic fission, but a relatively minor role in the subsequent steps, perhaps confined to preventing the various species from diffusing away from each other.

Studies on protein-free corrinoids and model complexes have shown that increasing the steric bulkiness around the coordinated Cα atom can cause a dramatic labilization of the Co—C bond.[189] The protein-coenzyme adduct might contain the coenzyme in a resting state and the protein in a strained state; the substrate would then switch the system into a strained coenzyme and a relaxed enzyme with little thermodynamic barrier. The strained form of the coenzyme is then in labile equilibrium with base-on cobalt(II) and the free radical.[190] This hypothesis, that conformational changes in cobalamin can switch chemical reactions on and off, is closely analogous with the known aspects of hemoglobin function.

It has been suggested that the radical formation in the coenzyme is triggered by a steric perturbation involving an enzyme-induced conformational distortion of the corrin ring toward the deoxyadenosyl group, thereby weakening the cobalt-carbon bond.[187,190–194] Structural studies of different corrinoid complexes reveal highly puckered and variable conformations of the corrin ring, attesting to its flexibility.[195] For the dimethylglyoxime models, it has been shown that increasing the size of the axial ligand B does induce Co—C bond lengthening and weakening because of conformational distortion of the equatorial ligand away from B and toward the R group.[196] It has been proposed that the flexibility of the corrin ligand is the reason why Nature does not use the porphyrin ligand in vitamin B_{12}.[197] In an alternative explanation, the weakening of the Co—C bond would be an electronic effect associated with the labilization of the Co—N bond.[198]

VI. PERSPECTIVES

Although a great deal is known about the biophysical characteristics of the various enzyme derivatives mentioned in this chapter, we are still far from a clear understanding of their mechanisms of action, especially if we take into consideration the role of each amino-acid residue inside the active-site cavity. Although we can successfully discuss why certain metal ions are used in certain biological reactions, we still do not know why nickel(II), for example, is involved in the enzymatic hydrolysis of urea.[199,200] If we are content with the explanations given in Sections III.A or V.D, we would need model compounds that are good catalysts and perform the job in several steps. This latter requirement would make the various models much more interesting, and would represent a new objective in the investigation of the structure-function relationship of catalytically active molecules. Indeed, the synthesis of large polypeptides may in principle provide such models. In this respect we need to know more about protein folding, for which emerging techniques like protein computer graphics and molecular dynamics are very promising.

Chemical modifications of proteins like the alkylation of carboxylate [124,201] or histidine [202] residues have been performed for a long time. A newer approach toward modeling the function of a protein, and understanding the role of the active site, involves cleaving part of a naturally occurring protein through enzymatic or chemical procedures, and then replacing it with a synthetic polypeptide. The use of modern techniques of molecular genetics has allowed site-directed mutagenesis to become in principle a very powerful technique for changing a single residue in a cavity. Site-directed mutagenesis is a very popular approach, and its principal limitation with respect to the synthetic polypeptide route is that only natural amino acids can be used (aside from the technical difficulties in both approaches). Small quantities of site-directed mutants have been obtained for CPA [125–127] and AP,[203] whereas the expression of CA [204,205] is now satisfactory.

Predictions of the changes in structure needed to affect the reaction pathway can nowadays be made with the aid of computers. The occurrence of the predicted change can be checked through x-ray analysis and NMR. The latter spectroscopy is today well-recognized as being able to provide structural information on small (≤20 kDa) proteins through 2- or 3-dimensional techniques.[206–208] These techniques are increasingly being applied to paramagnetic metalloproteins such as many of those discussed here.[208,209] The advantage of handling a paramagnetic metalloprotein is that we can analyze signals shifted far away from their diamagnetic positions, which correspond to protons close to the metal ion,[69] even for larger proteins. It is possible to monitor the distances between two or more protons under various conditions, such as after the addition of inhibitors or pseudosubstrates, chemical modification, or substitution of a specific amino acid.

VII. REFERENCES

1. H. Sigel and A. Sigel, eds., *Metal Ions in Biological Systems,* Dekker, **26** (1990).
2. R. K. Andrews, R. L. Blakeley, and B. Zerner, in Reference 1, **23** (1988).
3. K. Doi, B. C. Antanaitis, and P. Aisen, *Struct. Bonding* **70** (1988), 1.
4. M. M. Werst, M. C. Kennedy, H. Beinert, and B. M. Hoffman, *Biochemistry* **29** (1990), 10526, and references therein.
5. A. G. Orpen *et al.*, *J. Chem. Soc., Dalton Trans.* **S1** (1989).
6. F. H. Westheimer, *Spec. Publ. Chem. Soc.* **8** (1957), 1.
7. F. Basolo and R. G. Pearson, *Mechanisms of Inorganic Reactions,* Wiley, 2d ed., 1967.
8. L. G. Sillen and A. E. Martell, *Stability Constants of Metal-Ion Complexes,* Spec. Publ. Chem. Soc., London, **25**, 1971.
9. E. J. Billo, *Inorg. Nucl. Chem. Lett.* **11** (1975), 491.
10. I. Bertini, G. Canti, C. Luchinat, and F. Mani, *Inorg. Chem.* **20** (1981), 1670.
11. S. Burki, Ph.D. Thesis, Univ. Basel, 1977.
12. P. Wolley, *Nature* **258** (1975), 677.
13. J. T. Groves and R. R. Chambers, *J. Am. Chem. Soc.* **106** (1984), 630.
14. J. T. Groves and J. R. Olson, *Inorg. Chem.* **24** (1985), 2717.
15. L. J. Zompa, *Inorg. Chem.* **17** (1978), 2531.
16. E. Kimura, T. Koike, and K. Toriumi, *Inorg. Chem.* **27** (1988), 3687; E. Kimura *et al.*, *J. Am. Chem. Soc.* **112** (1990), 5805.
17. R. S. Brown *et al.*, *J. Am. Chem. Soc.* **104** (1982), 3188.
18. I. Bertini *et al.*, *Inorg. Chem* **29** (1990), 1460.
19. R. J. P. Williams, *Coord. Chem. Rev.* **100** (1990), 573.
20. D. W. Christianson, *Adv. Prot. Chem.* **42** (1991), 281.
21. I. Bertini, C. Luchinat, and M. S. Viezzoli, in I. Bertini *et al.*, eds., *Zinc Enzymes,* Birkhaüser, 1986, p.27.
22. D. S. Auld and B. L. Vallee, in Reference 21, p. 167.
23. G. Formicka-Kozlowska, W. Maret, and M. Zeppezauer, in Reference 21, p. 579.
24. I. Bertini and C. Luchinat, in Reference 30, p. 101.
25. I. Bertini and C. Luchinat, *Adv. Inorg. Biochem.* **6** (1984), 71.
26. H. Sigel, ed., *Metal Ions in Biological Systems,* Dekker, **12** (1981).
27. T. G. Spiro, ed., *Copper Proteins,* Wiley, 1981.
28. J. E. Coleman and P. Gettins, in Reference 21, p. 77.
29. J. E. Coleman and D. P. Giedroc, in Reference 1, **25** (1989).
30. H. Sigel, ed., *Metal Ions in Biological Systems,* Dekker, **15** (1983).
31. N. U. Meldrum and F. J. W. Roughton, *J. Physiol.* **75** (1932), 4.
32. D. Keilin and T. Mann, *Biochem. J.* **34** (1940), 1163.

33. S. Lindskog, in T. G. Spiro, ed., *Zinc Enzymes: Metal Ions in Biology,* Wiley, **5** (1983), 78; D. N. Silverman and S. Lindskog, *Acc. Chem. Res.* **21** (1988), 30.
34. J.-Y. Liang and W. N. Lipscomb, *J. Am. Chem. Soc.* **108** (1986), 5051.
35. K. M. Merz, *J. Am. Chem. Soc.* **112** (1990), 7973.
36. (a) G. Sanyal, *Ann. N. Y. Acad. Sci.* **429** (1984), 165; (b) G. Sanyal and T. H. Maren, *J. Biol. Chem.* **256** (1981), 608.
37. T. Kararli and D. N. Silverman, *J. Biol. Chem.* **260** (1985), 3484.
38. A. Liljas *et al.*, *Nature* **235** (1972), 131.
39. K. K. Kannan *et al.*, *Proc. Natl. Acad. Sci. USA,* **72** (1975), 51.
40. E. A. Eriksson *et al.*, in Reference 21, p. 317.
41. S. Lindskog in Reference 21, p. 307.
42. E. Clementi *et al.*, *FEBS Lett.* **100** (1979), 313.
43. B. P. N. Ko *et al.*, *Biochemistry* **16** (1977), 1720.
44. A. Ikai, S. Tanaka, and H. Noda, *Arch. Biochem. Biophys.* **190** (1978), 39.
45. I. Bertini, C. Luchinat, and A. Scozzafava, *Struct. Bonding* **48** (1982), 45.
46. A useful review by W. W. Cleland on pH-dependent kinetics can be found in *Methods Enzymol.,* 1987, 390.
47. Y. Pocker and S. Sarkanen, *Adv. Enzymol.* **47** (1978), 149.
48. I. Bertini and C. Luchinat, *Acc. Chem. Res.* **16** (1983), 272.
49. S. Lindskog and I. Simonsson, *Eur. J. Biochem.* **123** (1982), 29.
50. B.-H. Jonsson, H. Steiner, and S. Lindskog, *FEBS Lett.* **64** (1976), 310.
51. H. Steiner, B.-H. Jonsson, and S. Lindskog, *Eur. J. Biochem.* **59** (1975), 253.
52. D. N. Silverman *et al.*, *J. Am. Chem. Soc.* **101** (1979), 6734.
53. S. H. Koenig *et al.*, *Pure Appl. Chem.* **40** (1974), 103.
54. I. Simonsson, B.-H. Jonsson, and S. Lindskog, *Eur. J. Biochem.* **93** (1979), 4.
55. T. J. Williams and R. W. Henkens, *Biochemistry* **24** (1985), 2459.
56. I. Bertini, C. Luchinat, and M. Monnanni, in Reference 99, p. 139.
57. I. Bertini *et al.*, in Reference 21, p. 371.
58. I. Bertini *et al.*, *Inorg. Chem.* **24** (1985), 301.
59. I. Bertini *et al.*, *J. Am. Chem. Soc.* **100** (1978), 4873.
60. R. C. Rosenberg, C. A. Root, and H. B. Gray, *J. Am. Chem. Soc.* **97** (1975), 21.
61. B. Holmquist, T. A. Kaden, and B. L. Vallee, *Biochemistry* **14** (1975), 1454, and references therein.
62. M. W. Makinen and G. B. Wells, in H. Sigel, ed., *Metal Ions in Biological Systems,* Dekker, **22** (1987).
63. M. W. Makinen *et al.*, *J. Am. Chem. Soc.* **107** (1985), 5245.
64. A. E. Eriksson, Uppsala Dissertation, Faculty of Science, n. 164, 1988.
65. A. E. Eriksson, A. T. Jones, and A. Liljas, *Proteins* **4** (1989), 274.
66. A. E. Eriksson *et al.*, *Proteins* **4** (1989), 283.
67. I. Bertini *et al.*, *Inorg. Chem.*, **31** (1992), 3975.
68. P. H. Haffner and J. E. Coleman, *J. Biol. Chem.* **248** (1973), 6630.
69. I. Bertini and C. Luchinat, *NMR of Paramagnetic Molecules in Biological Systems,* Benjamin/Cummings, 1986.
70. R. D. Brown III, C. F. Brewer, and S. H. Koenig, *Biochemistry* **16** (1977), 3883.
71. I. Bertini, C. Luchinat, and M. Messori, in Reference 62, vol. 21.
72. I. Solomon, *Phys. Rev.* **99** (1955), 559.
73. I. Bertini *et al.*, *J. Magn. Reson.* **59** (1984), 213.
74. L. Banci, I. Bertini, and C. Luchinat, *Magn. Res. Rev.*, **11** (1986), 1.
75. I. Bertini *et al.*, *J. Am. Chem. Soc.*, **103** (1981), 7784.
76. T. H. Maren, A. L. Parcell, and M. N. Malik, *J. Pharmacol. Exp. Theor.* **130** (1960), 389.
77. J. E. Coleman, *J. Biol. Chem.* **243** (1968), 4574.
78. S. Lindskog, *Adv. Inorg. Biochem.* **4** (1982), 115.
79. G. Alberti *et al.*, *Biochim. Biophys. Acta* **16** (1981), 668.
80. J. I. Rogers, J. Mukherjee, and R. G. Khalifah, *Biochemistry* **26** (1987), 5672.
81. C. Luchinat, R. Monnanni, and M. Sola, *Inorg. Chim. Acta* **177** (1990), 133.
82. L. Morpurgo *et al.*, *Arch. Biochem. Biophys.* **170** (1975), 360.
83. I. Bertini and C. Luchinat, in K. D. Karlin and J. Zubieta, eds., *Biological and Inorganic Copper Chemistry*, vol. 1, Adenine Press, 1986.

84. I. Bertini *et al.*, *J. Chem. Soc., Dalton Trans.* (1978), 1269.
85. P. H. Haffner and J. E. Coleman, *J. Biol. Chem.* **250** (1975), 996.
86. I. Bertini *et al.*, *J. Inorg. Biochem.* **18** (1983), 221.
87. I. Bertini, E. Borghi, and C. Luchinat, *J. Am. Chem. Soc.* **102** (1979), 7069.
88. I. Bertini *et al.*, *J. Am. Chem. Soc.* **109** (1987), 7855.
89. P. Yeagle, Y. Lochmüller, and R. W. Henkens, *Proc. Natl. Acad. Sci. USA* **48** (1975), 1728.
90. P. J. Stein, S. T. Merrill, and R. W. Henkens, *J. Am. Chem. Soc.* **99** (1977), 3194.
91. P. S. Hubbard, *Proc. Roy. Soc. London* **291** (1966), 537.
92. A. Lanir and G. Navon, *Biochemistry* **11** (1972), 3536.
93. J. J. Led and E. Neesgard, *Biochemistry* **26** (1987), 183.
94. N. B.-H. Johnsson *et al.*, *Proc. Natl. Acad. Sci. USA* **77** (1980), 3269.
95. J. L. Evelhoch, D. F. Bocian, and J. L. Sudmeier, *Biochemistry* **20** (1981), 4951.
96. J.-Y. Liang and W. N. Lipscomb, *Proc. Natl. Acad. Sci. USA* **87** (1990), 3675.
97. K. M. Merz, *J. Mol. Biol.* **214** (1990), 799.
98. C. A. Fierke, T. L. Calderone, and J. F. Krebs, *Biochemistry* **30** (1991) 11054.
99. M. Aresta and G. Forti, eds., *Carbon Dioxide as a Source of Carbon*, Reidel, 1987.
100. M. Aresta and J. V. Schloss, eds., *Enzymatic and Model Carboxylation and Reduction Reactions for Carbon Dioxide Utilization*, Kluwer, 1990.
101. C. K. Tu and D. N. Silverman, *J. Am. Chem. Soc.* **108** (1986), 6065.
102. E. Chaffee, T. P. Dasgupta, and J. M. Harris, *J. Am. Chem. Soc.* **95** (1973), 4169.
103. J. B. Hunt, A. C. Rutenberg, and H. Taube, *J. Am. Chem. Soc.* **74** (1983), 268.
104. R. S. Brown, N. J. Curtis, and J. Huguet, *J. Am. Chem. Soc.* **103** (1981), 6953.
105. I. Tabushi and Y. Kuroda, *J. Am. Chem. Soc.* **106** (1984), 4580.
106. I. Bertini *et al.*, *Gazz. Chim. Ital.* **118** (1988), 777.
107. L. Meriwether and F. H. Westheimer, *J. Am. Chem. Soc.* **78** (1956), 5119.
108. D. A. Buckingham, D. M. Foster, and A. M. Sargeson, *J. Am. Chem. Soc.* **92** (1970), 6151.
109. M. L. Bender, R. J. Bergeron, and M. Komiyama, *The Bioorganic Chemistry of Enzymatic Catalysis*, Wiley, 1984.
110. B. Anderson *et al.*, *J. Am. Chem. Soc.* **99** (1977), 2652.
111. M. L. Bender and B. W. Turnquest, *J. Am. Chem. Soc.* **77** (1955), 4271.
112. D. L. Miller and F. H. Westheimer, *J. Am. Chem. Soc.* **88** (1966), 1514.
113. H. Kroll, *J. Am. Chem. Soc.* **74** (1952), 2036.
114. D. A. Buckingham, D. M. Foster, and A. M. Sargeson, *J. Am. Chem. Soc.* **90** (1968), 6032.
115. R. Breslow, in R. F. Gould, ed., *Bioinorganic Chemistry* (*Advances in Chemistry Series*, vol. **100**), American Chemical Society, 1971; Chapter 2.
116. A. Schepartz and R. Breslow, *J. Am. Chem. Soc.* **109** (1987), 1814.
117. J. T. Groves and R. R. Chambers, Jr., *J. Am. Chem. Soc.* **106** (1984), 630.
118. M. A. Wells and T. C. Bruice, *J. Am. Chem. Soc.* **99** (1977), 5341.
119. H. Sigel, ed., *Metal Ions in Biological Systems*, Dekker, **5** (1976).
120. N. E. Dixon and A. M. Sargeson, in Reference 33.
121. R. W. Hay, G. Wilkinson, R. D. Gillard, and J. A. McCleverty, eds., in *Comprehensive Coordination Chemistry*, Pergamon Press, 1987.
122. D. C. Rees, M. Lewis, and W. N. Lipscomb, *J. Mol. Biol.* **168** (1983), 367.
123. D. C. Rees *et al.*, in Reference 21, p. 155.
124. D. S. Auld, K. Larson, and B. L. Vallee, in Reference 21, p. 133.
125. W. J. Rutter, personal communication.
126. D. Hilvert *et al.*, *J. Am. Chem. Soc.* **108** (1986), 5298.
127. S. J. Gardell *et al.*, *J. Biol. Chem.* **262** (1987), 576.
128. D. S. Auld *et al.*, *Biochemistry,* **31** (1992), 3840; W. L. Mock and J. T. Tsay, *J. Biol. Chem.* **263** (1988), 8635.
129. G. Shoham, D. C. Rees, and W. N. Lipscomb, *Proc. Natl. Acad. Sci. USA* **81** (1984), 7767.
130. K. F. Geoghegan *et al.*, *Biochemistry* **22** (1983), 1847.
131. I. Bertini *et al.*, *J. Inorg. Biochem.* **32** (1988), 13.
132. C. Luchinat *et al.*, *J. Inorg. Biochem.* **32** (1988), 1.
133. R. Bicknell *et al.*, *Biochemistry* **27** (1988), 1050.
134. I. Bertini *et al.*, *Biochemistry* **27** (1988), 8318.
135. M. E. Sander and H. Witzel, in Reference 21, p. 207.
136. M. W. Makinen, in Reference 21, p. 215.

137. D. W. Christianson and W. N. Lipscomb, *Acc. Chem. Res.* **22** (1989), 62.
138. D. W. Christianson *et al.*, *J. Biol. Chem.* **264** (1989), 12849.
139. B. W. Matthews, *Acc. Chem. Res.* **21** (1988), 333, and references therein.
140. B. S. Cooperman, in Reference 119.
141. D. M. Blow, J. J. Birktoft, and B. S. Hartley, *Nature* **221** (1969), 337.
142. R. C. Nordlie, in P. D. Boyer, ed., *T he Enzymes*, Academic Press, 3d ed., **4** (1975), 543.
143. R. Breslow *et al.*, *Proc. Natl. Acad. Sci. USA* **80** (1983), 4585.
144. H. W. Wyckoff *et al.*, *Adv. Enzymol.* **55** (1983), 453.
145. E. E. Kim and H. W. Wyckoff, *J. Mol. Biol.* **218** (1991), 449.
146. L. Banci *et al.*, *J. Inorg. Biochem.* **30** (1987), 77.
147. P. Gettins and J. E. Coleman, *J. Biol. Chem.* **259** (1984), 11036.
148. I. Bertini *et al.*, *Inorg. Chem.* **28** (1989), 352.
149. A. Chaidaroglou *et al.*, *Biochemistry* **27** (1988), 8338.
150. E. C. Dinovo and P. D. Boyer, *J. Biol. Chem.* **246** (1971), 4586.
151. H. Dutler, A. Ambar, and J. Donatsch, in Reference 21, p. 471.
152. H. Eklund and C.-I. Bränden, in *Biological Macromolecules and Assemblies*, Wiley, 1985.
153. C.-I. Bränden *et al.*, *The Enzymes* **11** (1975), 104.
154. E. S. Cedergren-Zeppezauer, in Reference 21, p. 393.
155. H. Theorell, *Feder. Proc.* **20** (1961), 967.
156. M. W. Makinen and W. Maret, in Reference 21, p. 465.
157. J. Kvassman and G. Pettersson, *Eur. J. Biochem.* **103** (1980), 565.
158. P. F. Cook and W. W. Cleland, *Biochemistry* **20** (1981), 1805.
159. I. Bertini *et al.*, *J. Am. Chem. Soc.* **106** (1984), 1826.
160. W. Maret *et al.*, *J. Inorg. Biochem.* **12** (1980), 241.
161. H. B. Gray and E. I. Solomon, in Reference 27, p. 1.
162. J. S. Valentine and M. W. Pantoliano, in Reference 27, p. 291.
163. M. F. Dunn, A. K. H. MacGibbon, and K. Pease, in Reference 21, p. 486.
164. I. Bertini *et al.*, *Eur. Biophys. J.* **14** (1987), 431.
165. W. Maret and M. Zeppezauer, *Biochemistry* **25** (1986), 1584.
166. C. Sartorius, M. Zeppezauer, and M. F. Dunn, *Rev. Port. Quim.* **27** (1985), 256; C. Sartorius *et al.*, *Biochemistry* **26** (1987), 871.
167. G. Pettersson, in Reference 21, p. 451.
168. E. Garces and W. W. Cleland, *Biochemistry* **8** (1969), 633.
169. B. Edlund *et al.*, *Eur. J. Biochem.* **9** (1969), 451.
170. R. K. Crane, in M. Florkin and E. H. Stotz, eds., *Comprehensive Biochemistry*, Elsevier, **15** (1964), 200.
171. B. M. Babior and J. S. Krouwer, *CRC Crit. Rev. Biochem.* **6** (1979), 35.
172. C. Brink-Shoemaker *et al.*, *Proc. Roy. Soc. London, Ser. A* **278** (1964), 1.
173. B. T. Golding and P. J. Sellars, *Nature* (1983), p. 204.
174. D. Lexa and J. M. Saveant, *Acc. Chem. Res.* **16** (1983), 235.
175. R. A. Firth *et al.*, *Chem. Commun.* (1967), 1013.
176. G. N. Schrauzer and L. P. Lee, *J. Am. Chem. Soc.* **90** (1968), 6541.
177. R. A. Firth *et al.*, *Biochemistry* **6** (1968), 2178.
178. V. B. Koppenhagen and J. J. Pfiffner, *J. Biol. Chem.* **245** (1970), 5865.
179. H. A. O. Hill, in G. L. Eichhorn, ed., *Inorganic Biochemistry*, Elsevier, **2** (1973), 1067.
180. J. Halpern, *Pure. Appl. Chem.* **55** (1983), 1059.
181. J. Halpern, S. H. Kim, and T. W. Leung, *J. Am. Chem. Soc.* **106** (1984), 8317.
182. R. G. Finke and B. P. Hay, *Inorg. Chem.* **23** (1984), 3041; B. P. Hay and R. G. Finke, *Polyhedron* **4** (1988), 1469; R. G. Finke, in C. Bleasdale and B. T. Golding, eds., *Molecular Mechanisms in Bioorganic Processes*, The Royal Society of Chemistry; Cambridge, England (1990).
183. B. P. Hay and R. G. Finke, *J. Am. Chem. Soc.* **108** (1986), 4820.
184. B. P. Hay and R. G. Finke, *J. Am. Chem. Soc.* **109** (1987), 8012.
185. J. M. Pratt, *Quart. Rev.* (1984), 161.
186. J. Halpern, *Science* **227** (1985), 869.
187. B. M. Babier, *Acc. Chem. Res.* **8** (1975), 376.
188. B. T. Golding, in D. Dolphin, ed., B_{12}, Wiley, **2** (1982), 543.
189. N. Bresciani-Pahor *et al.*, *Coord. Chem. Rev.* **63** (1985), 1.
190. J. M. Pratt, *J. Mol. Cat.* **23** (1984), 187.

191. S. M. Chennaly and J. M. Pratt, *J. Chem. Soc., Dalton Trans.* (1980), 2259.
192. *Ibid.*, p. 2267.
193. *Ibid.*, p. 2274.
194. L. G. Marzilli *et al.*, *J. Am. Chem. Soc.* **101** (1979), 6754.
195. J. Glusker, in Reference 188, **1** (1982), 23.
196. G. De Alti *et al.*, *Inorg. Chim. Acta* **3** (1969), 533.
197. K. Geno and J. Halpern, *J. Am. Chem. Soc.* **109** (1987), 1238.
198. C. Mealli, M. Sabat, and L. G. Marzilli, *J. Am. Chem. Soc.* **109** (1987), 1593.
199. *Nickel and its Role in Biology*, vol. 23 of Reference 62.
200. C. T. Walsh and W. H. Orme-Johnson, *Biochemistry* **26** (1987), 4901.
201. J. F. Riordan and H. Hayashida, *Biochem. Biophys. Res. Commun.* **41** (1970), 122.
202. R. G. Khalifah, J. I. Rogers, and J. Mukherjee, in Reference 21, p. 357.
203. A. Chaidaroglou *et al.*, *Biochemistry* **27** (1988), 8338.
204. C. Forsman *et al.*, *FEBS Lett.* **229** (1988), 360; S. Lindskog *et al.*, in *Carbonic Anhydrase*, F. Botrè, G. Gros, and B. T. Storey, eds., VCH, 1991.
205. C. A. Fierke, J. F. Krebs, and R. A. Venters, in *Carbonic Anhydrase*, F. Botrè, G. Gros, and B. T. Storey, eds., VCH, 1991.
206. K. Wüthrich, *NMR in Biological Research*, Elsevier-North Holland, 1976.
207. K. Wüthrich, *NMR of Proteins and Nucleic Acids*, Wiley, 1986.
208. I. Bertini, H. Molinari, and N. Niccolai, eds., *NMR and Biomolecular Structure*, Verlag Chemie, 1991.
209. J. T. J. LeComte, R. D. Johnson, and G. N. La Mar, *Biochim. Biophys. Acta* **829** (1985), 268.
210. Recently, ^{67}Zn has been used as a relaxing probe to monitor the binding of ^{13}C-enriched cyanide to zinc in carbonic anhydrase (see Section IV.C).
211. Recent work on HCA II has improved the resolution to 1.54 Å (K. Håkan *et al.*, *J. Mol. Biol.* **227** (1993), 1192). Mutants at positions 143 (R. S. Alexander, S. K. Nair, and D. W. Christianson, *Biochemistry* **30** (1991), 11064) and 200 (J. F. Krebs *et al.*, *Biochemistry* **30** (1991), 9153; Y. Xue *et al.*, *Proteins* **15** (1993), 80) also have been characterized by x-ray methods.
212. An x-ray study of the cyanate and cyanide derivatives of the native enzyme has shown that the anions sit in the cavity without binding to the metal ion (M. Lindahl, L.A. Svensson, and A. Liljas, *Proteins* **15** (1993), 177). Since NCO^- has been shown to interact with the paramagnetic cobalt(II) center, and ^{13}C-enriched cyanide has been shown to interact with ^{67}Zn-substituted CA (see Reference 67), it appears that the structures in the solid state and solution are strikingly different.
213. Recent x-ray data on the adduct of 1,2,4-triazole with HCA II confirm H-bonding with Thr-200 (S. Mangani and A. Liljas, *J. Mol. Biol.* **232** (1993), 9).
214. An HCO_3^--complex of the His-200 mutant of HCA II has been studied by x-ray methods. The data are consistent with the coordinated oxygen being protonated and H-bonded to Thr-199 (Y. Xue *et al.*, *Proteins* **15** (1993), 80).